



ANTI-INFLAMMATORY EFFECTS OF RHEIN ANTHRAQUINONE AND CRUDE  
EXTRACTS FROM *CASSIA ALATA* LINN. IN HACAT CELLS



By

MISS Kwanchanok WADKHIEN

A Thesis Submitted in partial Fulfillment of Requirements  
for Master of Pharmacy (PHARMACEUTICAL SCIENCES)

Graduate School, Silpakorn University

Academic Year 2017

Copyright of Graduate School, Silpakorn University

ฤทธิ์ต้านการอักเสบของ rhein anthraquinone และสารสกัดจากชุมเห็ดเทศใน HaCaT  
cells



โดย  
นางสาววิญชนก วาดเขียน

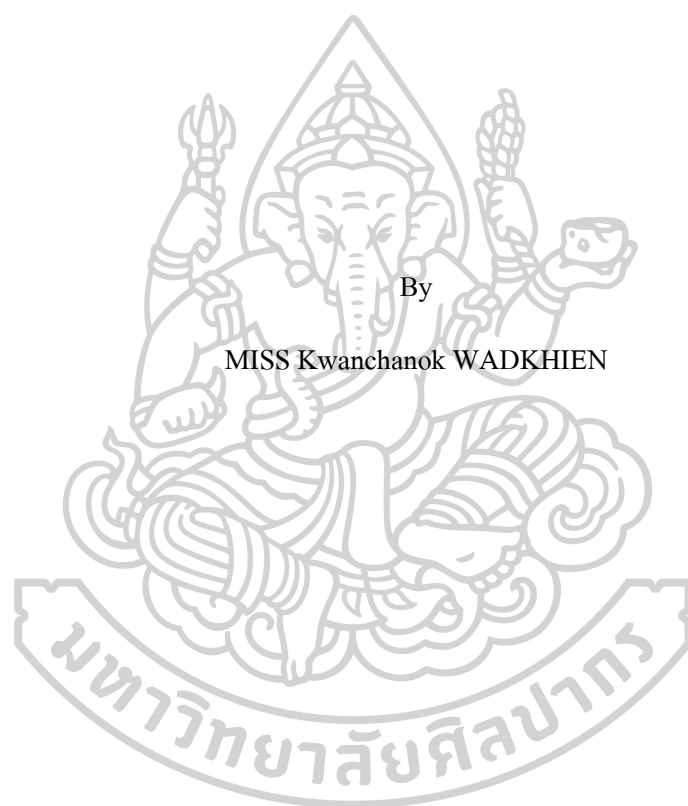
วิทยานิพนธ์นี้เป็นส่วนหนึ่งของการศึกษาตามหลักสูตรเภสัชศาสตรมหาบัณฑิต  
สาขาวิชาวิทยาการทางเภสัชศาสตร์ แผน ก แบบ ก 2 เภสัช ระดับปริญญาามหาบัณฑิต

บัณฑิตวิทยาลัย มหาวิทยาลัยศิลปากร

ปีการศึกษา 2560

ลิขสิทธิ์ของบัณฑิตวิทยาลัย มหาวิทยาลัยศิลปากร

ANTI-INFLAMMATORY EFFECTS OF RHEIN ANTHRAQUINONE AND  
CRUDE EXTRACTS FROM *CASSIA ALATA* LINN. IN HACAT CELLS



A Thesis Submitted in partial Fulfillment of Requirements  
for Master of Pharmacy (PHARMACEUTICAL SCIENCES)

Graduate School, Silpakorn University

Academic Year 2017

Copyright of Graduate School, Silpakorn University

Title ANTI-INFLAMMATORY EFFECTS OF RHEIN  
ANTHRAQUINONE AND CRUDE EXTRACTS FROM  
CASSIA ALATA LINN. IN HaCaT CELLS

By Kwanchanok WADKHIEN

Field of Study (PHARMACEUTICAL SCIENCES)

Advisor Nushjira Pongimitprasert

Pharmacy Silpakorn University in Partial Fulfillment of the Requirements  
for the Master of Pharmacy

..... Dean of graduate school  
(Assoc. Prof. Panjai Tantatsanawong, Ph.D.)

Approved by

..... Chair person  
(Associate Professor Onoomar Toyama , Ph.D.)

..... Advisor  
( Nushjira Pongimitprasert , Ph.D.)

..... Co Advisor  
(Associate Professor Chatchai Chinpaisal , Ph.D.)

..... Co Advisor  
(Assistant Professor Malai Satiraphan , Ph.D.)

..... External Examiner  
(Professor Ratee Sudsuang , Ph.D.)

56364201 : Major (PHARMACEUTICAL SCIENCES)

Keyword : CASSIA ALATA., RHEIN, HaCaT CELL, FREE RADICALS, ROS, ANTI-INFLAMMATORY

MISS KWANCHANOK WADKHIEN : ANTI-INFLAMMATORY EFFECTS OF RHEIN ANTHRAQUINONE AND CRUDE EXTRACTS FROM *CASSIA ALATA* LINN. IN HACAT CELLS THESIS ADVISOR : NUSHJIRA PONGIMITPRASERT, PH.D.

Introduction: *Cassia alata* Linn. (synonym: *Senna alata* Linn.) is a medicinal plant for which leaves have long been used as a laxative. It is included in the Thai traditional household herbal drug list for laxative and also the herbal medicine in National List of Essential Drugs (THAILAND). Furthermore, *C. alata* leaves extract has been reported to have various pharmacological activities including anti-inflammatory activities. It has been reported that rhein, an active component in *C. alata*, can inhibit inflammation via suppressing reactive oxygen species (ROS) production. ROS has been known to act as novel mediator for inflammation, leading to enhanced elaboration of cytokines such as TNF- $\alpha$  and IL-8. However, only a few research works have been done to investigate the anti-inflammatory activities on skin, especially in keratinocyte cells. Methods: A high-performance liquid chromatographic method was described for the determination of rhein anthraquinone in *C. alata* leaves extract. The anti-inflammatory effects of rhein and *C. alata* leaves extract on *tert*-Butyl hydroperoxide (*t*-BHP) induced oxidative stress in HaCaT cells were evaluated. Anti-inflammatory activities of *C. alata* leaves extract was compared with rhein standard via inhibition of ROS generation and production of TNF- $\alpha$  and IL-8. Results: Rhein anthraquinone content in *C. alata* leaves extract was 0.1225% w/w. Rhein (1-50  $\mu$ M) significantly reduced ROS generation in a concentration-dependent manner. The inhibition of ROS generation paralleled the decrease in TNF- $\alpha$  and IL-8 production. *C. alata* leaves extract exhibited stronger anti-inflammatory effects than rhein at same concentrations. Conclusion: These findings indicate that rhein and *C. alata* leaves extract may reduce inflammation of skin by decreasing TNF- $\alpha$  and IL-8 production as a result of ROS reduction. Taken together, these results indicate that *C. alata* leaves have the potential for use as an anti-inflammatory agent.

## ACKNOWLEDGEMENTS

I would like to express my sincere gratitude and appreciation to my thesis advisor, Dr. Nushjira Pongnimitprasert, for her invaluable advices, guidance, attention and encouragement throughout my study.

To my co-advisor, Assistant Professor Dr. Malai Satiraphan, I would like to thank for her guidance and meaningful advice, and for her help in making all contacts possible and successful. For Associate Professor Dr. Chatchai Chinpaisal, I would like to thank for his criticism on my thesis.

I also thank to Associate Professor Dr. Penpun Wetwitayaklung for supporting Cassia alata leaves extract and Dr. Tamaki Okabayashi from MOCID, FTM, Mahidol University, and RIMD, Osaka University for providing keratinocytes cell line (HaCaT cell).

I would like to sincerely thank all teachers, researchers and the staff in Faculty of Pharmacy, Silpakorn University, for giving me the place, equipments, knowledge and friendship.

To my laboratory brother, sister and friend, thanks for their assistance and kindness, and to my friends, I would like to thank them for their assistance and for entertaining me through the years.

To my family, I would like to thank all for their kind understanding, warmth and wonderful job in both financial and emotional support. Moreover, thank for taking care of me physically and encouraging me through all obstacles.

This thesis is partially supported by Faculty of Pharmacy, Silpakorn University.

Kwanchanok WADKHIEN

## TABLE OF CONTENTS

	Page
ABSTRACT .....	D
ACKNOWLEDGEMENTS.....	E
TABLE OF CONTENTS .....	F
LIST OF TABLES.....	I
LIST OF FIGURES .....	J
CHAPTER 1 INTRODUCTION.....	1
1.1 Statement and significance of the research problem.....	2
1.2 Objective of this research.....	3
1.3 The research hypothesis.....	3
1.4 Scope of research work.....	3
CHAPTER 2 LITERATURE REVIEWS .....	4
2.1 Cassia alata L. ....	5
2.1.1 Morphological characters of C. alata .....	5
2.1.2 Ethnopharmacological information of C. alata.....	6
2.1.3 Clinical study, pharmacological activity and toxicity of C. alata.....	8
2.1.4 Chemical constituents of C. alata .....	18
2.2 Rhein .....	24
2.2.1 Pharmacological activity of rhein .....	24
2.2.2 Rhein content in C. alata leaves extract .....	34
2.3 Reactive oxygen species (ROS).....	36

2.3.1 Antioxidant defense system.....	39
2.3.2 ROS-regulated physiological function .....	43
2.3.3 ROS-induced pathophysiology .....	49
2.3.4 Detection of ROS.....	53
2.4 Skin.....	56
2.4.1 Structure of skin.....	56
2.4.2 Function of skin .....	58
2.4.3 ROS-mediated skin inflammation.....	61
2.4.4 Antioxidant and redox balance in skin.....	63
CHAPTER 3 MATERIALS AND METHODS.....	64
3.1 Materials.....	65
3.2 Equipment .....	66
3.3 Method.....	67
3.3.1 Quantitative analysis of rhein in <i>C. alata</i> leaves extract by HPLC .....	67
3.3.2 Determination of cell viability .....	68
3.3.3 Measurement of ROS production.....	70
3.3.4 Measurement of inflammatory cytokines production by ELISA .....	70
3.3.5 Data analysis.....	72
CHAPTER 4 RESULTS AND DISCUSSION .....	73
4.1 Quantitative analysis of rhein in <i>C. alata</i> leaves extract by HPLC .....	74
4.2 Determination of cell viability.....	77
4.3 Measurement of ROS production .....	81
4.4 Measurement of inflammatory cytokines production by ELISA.....	85
CHAPTER 5 CONCLUSION .....	88



REFERENCES .....90

APPENDIX.....101

    Appendix A .....101

    Appendix B .....102

VITA .....107



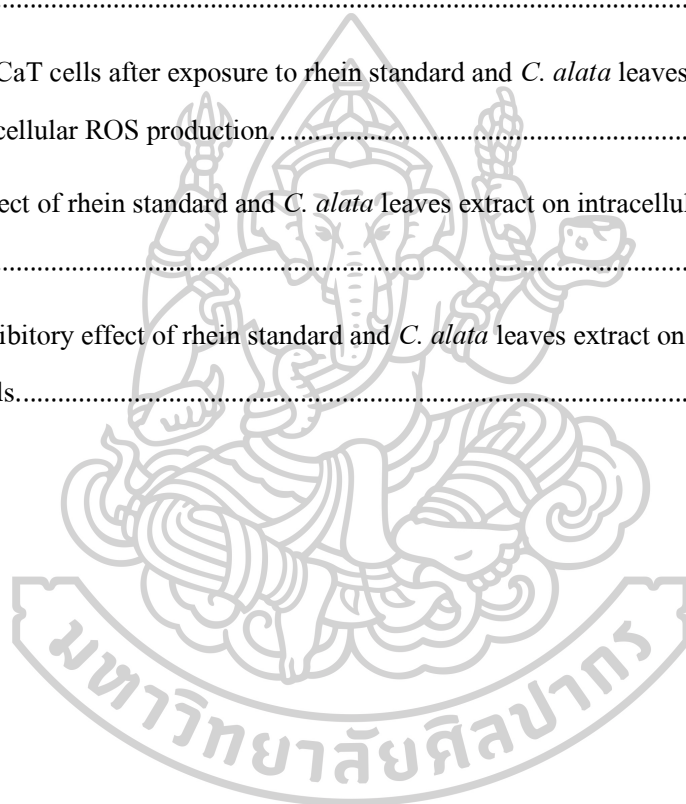
## LIST OF TABLES

	Page
Table 1 Ethnopharmacological uses of <i>C. alata</i> .....	6
Table 2 Clinical study, pharmacological activity and toxicity of <i>C. alata</i> .....	9
Table 3 The volatile oil constituents of <i>C. alata</i> .....	18
Table 4 Chemical constituents of <i>C. alata</i> .....	19
Table 5 Pharmacological activity of rhein .....	25
Table 6 Qualitative analytical methods of rhein in <i>C. alata</i> .....	34
Table 7 Quantitative analytical methods of rhein in <i>C. alata</i> .....	35
Table 8 Endogenous sources of ROS .....	37
Table 9 Antioxidant defense system.....	39
Table 10 Physiological functions of ROS .....	43
Table 11 Pathophysiological implications of altered redox regulation .....	50
Table 12 Fluorescence probes for detection ROS .....	53
Table 13 Immune components of the skin. ....	60
Table 14 Recovery of rhein in <i>C. alata</i> leaves extract.....	74
Table 15 Precision data of rhein .....	75

## LIST OF FIGURES

	Page
Figure 1 Photograph of <i>C. alata</i> .....	5
Figure 2 Chemical constituents of <i>C. alata</i> .....	22
Figure 3 Mitochondrial respiratory chain.....	38
Figure 4 Pathways of ROS formation and redox balance.....	41
Figure 5 Mechanism of action of the thioredoxin (Trx) redox system.....	42
Figure 6 Antimicrobial host defense on ROS generation by macrophages and neutrophils .....	46
Figure 7 ROS cross-talk with NO system .....	46
Figure 8 ROS-mediated thyroid hormone synthesis in thyrocytes .....	47
Figure 9 Signaling mechanisms of ROS-mediated increase in leukocyte migration .....	47
Figure 10 Regulation of HIF-1 $\alpha$ by ROS production during hypoxia .....	48
Figure 11 NOS–sGC–cGMP signal transduction pathway.....	48
Figure 12 ROS-induced MAPK signaling pathways .....	49
Figure 13 Oxidation of hydroethidine (HE) .....	54
Figure 14 Formation of fluorescent compound DCF by ROS .....	54
Figure 15 Horseradish peroxidase (HRP)-catalyzed amplex red oxidation by H <sub>2</sub> O <sub>2</sub> .....	55
Figure 16 Oxidation of dihydrorhodamine to rhodamine .....	55
Figure 17 Reaction of H <sub>2</sub> O <sub>2</sub> with pentafluorobenzenesulfonyl fluorescein .....	55
Figure 18 The cross-section of human skin.....	56
Figure 19 Structure of epidermis .....	57
Figure 20 Inflammation response in the skin .....	63
Figure 21 Structures of MTT and colored formazan product .....	69
Figure 22 Calibration curve of rhein from rhein standard solution. ....	74

Figure 23 HPLC chromatograms of <i>C. alata</i> leaves extract (lower) and rhein standard (upper) ...	75
Figure 24 UV spectra of <i>C. alata</i> leaves extract (upper) and rhein standard (lower), at retention time 10.7 minutes .....	76
Figure 25 Formazan crystals in HaCaT cells after exposure to rhein standard and <i>C. alata</i> leaves extract .....	78
Figure 26 Effect of rhein standard and <i>C. alata</i> leaves extract on cell viability in HaCaT cells using MTT.....	80
Figure 27 HaCaT cells after exposure to rhein standard and <i>C. alata</i> leaves extract on <i>t</i> -BHP induced intracellular ROS production.....	83
Figure 28 Effect of rhein standard and <i>C. alata</i> leaves extract on intracellular ROS production in HaCaT cells.....	84
Figure 29 Inhibitory effect of rhein standard and <i>C. alata</i> leaves extract on cytokines production in HaCaT cells.....	87



## CHAPTER 1

### INTRODUCTION

- 1.1 Statement and significance of the research problem
- 1.2 Objective of this research
- 1.3 The research hypothesis
- 1.4 Scope of research work



### 1.1 Statement and significance of the research problem

*Cassia alata* Linn. or Chum-het-thet, family Fabaceae, is generally known as ringworm bush, or candle bush. It is an herbal medicine that has been used in many part of the world for treatment of constipation, stomach pain [1], ringworm, scabies, pruritic, eczema, herpes and skin allergy [2]. In Thailand, *C. alata* has been approved as a laxative drug in the 2015 Thailand National List of Essential Drugs. The leaves contains anthraquinones both in aglycone and glycoside forms including rhein, aloë-emodin, chrysophanol, glycosides of rhein, emodin, physcione and sennosides A, B, C, D, while rhein is a major component [1]. It has been used in the form of herbal lotion for a variety of skin diseases such as tinea infections, insect bites, ringworms, scabies, herpes, blotch, eczema and mycosis [3]. *C. alata* leaves are also reported to possess anti-inflammatory, antimutagenic, analgesic, antidiabetic, antifungal and antimicrobial properties[2].

Skin, as the primary interface between the body and the environment, provides a first line of defense against microbial pathogens, physical and chemical insults. Keratinocytes are a major cell type of the epidermis, constituting more than 90% of epidermal cells. Keratinocytes form an effective barrier against the entry of foreign matter and infectious agents into the body and minimize moisture loss. Thus, following skin exposure to stimulus, intracellular sensors contained in the inflammasome complex in keratinocytes are activated, leading to the production of reactive oxygen species (ROS) and to processing and secretion of key pro-inflammatory cytokines. This, in turn, results in the activation of tissue-resident immune cells that induce inflammatory response [1]. Therefore, cultured keratinocytes have become a prototypic model for screening of anti-inflammatory, photo-protective, and cancer preventive substances for topical application [2].

Cellular and tissue damage caused by oxidative stress is defined by the elevated levels of free radicals or other ROS that can elicit direct or indirect damage to the body and contributes to a large number of diseases. Intracellular protective mechanisms against inflammatory stresses involve antioxidant enzymes, including superoxide dismutase (SOD), catalase (CAT) and glutathione peroxidase (GPx) in tissues. However, it appears that the various roles of enzymatic antioxidants help to protect organisms from excessive generation of oxidative stress during inflammation process, which leads to studies focusing on the role of natural products in suppressing the production of oxidation in tissues. Under normal conditions, ROS levels are controlled by the body's complex antioxidant defense system, and there is an equilibrium between ROS formation

and degradation. Overproduction of ROS or inadequate antioxidant defense disturbs this equilibrium in favor of a ROS upsurge that results in oxidative stress. Plant extracts and plant-derived antioxidant compounds may potentiate the body's antioxidant and anti-inflammatory defense mechanisms or act as antioxidants. Inflammation is a normal response to tissue injury but, if uncontrolled, leads to additional complications. At the injury site, an increase in blood vessel wall permeability followed by migration of immune cells can cause edema formation during inflammation. The released inflammatory cytokines include nitric oxide (NO), TNF- $\alpha$  (Tumor necrosis factor-alpha), interleukin-1 (IL-1), IL-6, IL-8, prostanoids, and leukotrienes [3].

At present, many of the biological activities of *C. alata* extract has been performed. However, only a few research works have been done to investigate the anti-inflammatory activities on skin, especially in cell keratinocytes. In this study, we have investigated anti-inflammatory activities of *C. alata* leaves extract compared with rhein anthraquinone as a reference.

## **1.2 Objective of this research**

- 1.2.1 To determine rhein anthraquinone content in *C. alata* leaves extract.
- 1.2.2 To investigate anti-inflammatory effect of the methanolic *C. alata* leaves extract compared to rhein anthraquinone in HaCaT cells.

## **1.3 The research hypothesis**

Rhein anthraquinone and *C. alata* leaves extract possesses anti-inflammatory activity via decreased ROS, TNF- $\alpha$  and IL-8 production.

## **1.4 Scope of research work**

Rhein anthraquinone and *C. alata* leaves extract will be evaluated for their anti-inflammatory effect, by decreasing ROS, TNF- $\alpha$  and IL-8 production in keratinocyte cell, HaCaT cells.

## CHAPTER 2

### LITERATURE REVIEWS

#### 2.1 *Cassia alata* L.

- 2.1.1 Morphological characters of *C. alata*
- 2.1.2 Ethnopharmacological information of *C. alata*
- 2.1.3 Clinical study, pharmacological activity and toxicity of *C. alata*
- 2.1.4 Chemical constituents of *C. alata*

#### 2.2 Rhein

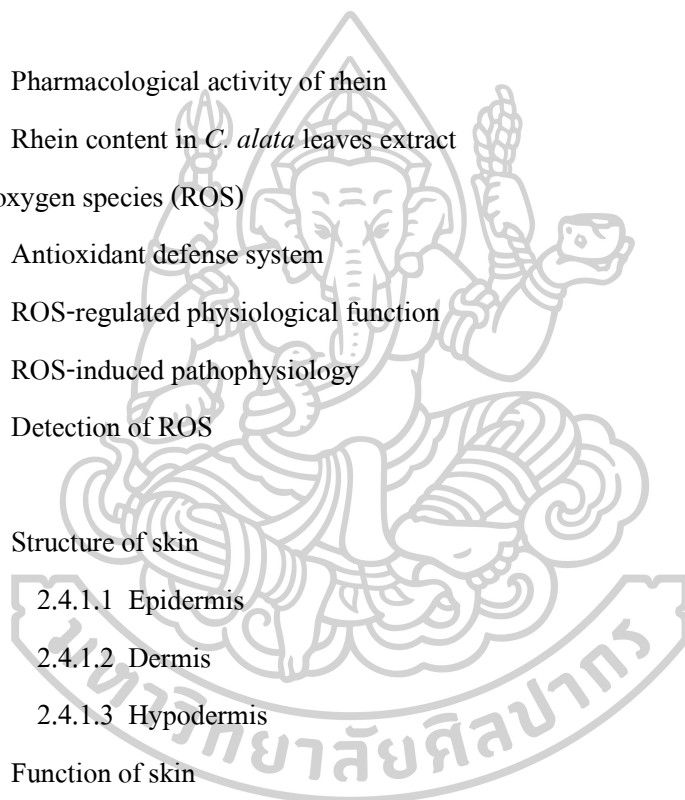
- 2.2.1 Pharmacological activity of rhein
- 2.2.2 Rhein content in *C. alata* leaves extract

#### 2.3 Reactive oxygen species (ROS)

- 2.3.1 Antioxidant defense system
- 2.3.2 ROS-regulated physiological function
- 2.3.3 ROS-induced pathophysiology
- 2.3.4 Detection of ROS

#### 2.4 Skin

- 2.4.1 Structure of skin
  - 2.4.1.1 Epidermis
  - 2.4.1.2 Dermis
  - 2.4.1.3 Hypodermis
- 2.4.2 Function of skin
- 2.4.3 ROS mediated skin inflammation
- 2.4.4 Antioxidant and redox balance in skin





## 2.1 *Cassia alata* L.

### 2.1.1 Morphological characters of *C. alata*

*Cassia alata* (L.) or *Senna alata* (L.) is native to Central America but has also been cultivated into many tropical countries. It has been generally known as candle bush and ringworm bush [4]. In Thailand, the plant is named as Chum-het-thet (central) [5], Rub-mhen-leung, Mark-ka-link-tad, Chum-hed-yai, Kee-kak (northern) [6].

*C. alata* (L.) is a shrub belonging to the Fabaceae family, subfamily Caesalpinioideae. It is an annual or biannual shrub with a nasty smell, 1–4 m tall, preferring sunny and moist areas. The leaves are yellowish-green, broad, with 5–14 leaflet pairs, the distal ones often larger and with a notched apex. Zygomorphic flowers are bright yellow, and form a generally simple erect raceme, evoking a dense golden spike or rod. They contain 7 stamens, 2 of which are much longer and a pubescent ovary [4]. The buds are rounded with 5 overlapping sepals and 5 free or less equal petals narrowed at the base [7]. The fruit is a tetragonal pod, winged on the angles, brown when ripe and containing numerous diamond-shaped brown seeds [4]. The picture of *C. alata* is shown in Figure 1.



Figure 1 Photograph of *C. alata*

Source: Thierry Hennebelle et al., “*Senna alata*,” *Fitoterapia* 80, 7 (October 2009): 385-393.

### 2.1.2 Ethnopharmacological information of *C. alata*

*C. alata* (L.) is an herbal medicine that has been used in many parts of the world for the treatment of constipation, stomach pain [8], and skin diseases such as ringworm, scabies, pruritic, eczema, herpes and skin allergy [4, 7]. In Thailand, *C. alata* has been approved as a laxative drug in the 2015 Thailand National List of Essential Drugs. The details of ethnopharmacological uses of *C. alata* are presented in Table 1.

Table 1 Ethnopharmacological uses of *C. alata*

Country	Part of use	Treatment	References
Cameroon	Leaves are boiled in water and then drunk	Fever	[9]
Nigeria	Leaves are boiled in water and then drunk	Constipation	[10]
	Leaves are boiled in water and then applied to skin	Skin diseases	[11]
	Leaves are soaked and then drunk	Antidiabetic	[12]
Malaysia	Leaves are pounded together with sulfur and then applied to skin	Ringworms, sores	[13]
Guatemala	Leaves are boiled in water and then drunk	Constipation, malaria, antidiabetic, liver diseases	[4, 14]
	Buds are boiled in water and then drunk	Thoracic pain	[14]
	Leaves are soaked and then bathed	Skin diseases, ringworm	[4]
	Leaves are soaked and then drunk	Stomach pain	
Martinique	Leaves are boiled in water and then drunk	Constipation, liver diseases, inflammation	[4]
	Leaves are pounded and then applied to skin	Skin rash, athlete's foot	
	Flowers are boiled in water and then drunk	Thoracic pain	

Table 1 Ethnopharmacological uses of *C. alata* (continued)

Country	Part of use	Treatment	References
Indonesia	Leaves are pounded and then applied to skin	Dermatitis	[15]
New Guinea	Leaves and wood	Constipation	[16]
Ghana	Leaves are soaked and then applied to skin	Herpes zoster, eczema, mycosis	[4]
	Leaves are boiled in water and then used as enema	Constipation	[17]
Fiji, Tonga and Samoa	Leaves	Ringworm	[16]
	Bark	Skin diseases, scabies, eczema	
Thailand	Leaves are pounded together with garlic and red limestone paste, then applied to skin	Ringworm, versicolor	[18]
	Leaves are pounded together with lemonade and then applied to skin	Ringworm, pityriasis versicolor	[19]
	Leaves are pounded and then cover the skin	Viral infection	
	Leaves are pounded together with water and then applied to skin	Scabies	
Sudan	Fruits are soaked and then drunk	Constipation, stomach pain, carminative, anthelmintic	[20]
	Leaves are eaten fresh	Stomach pain	
	Roots are soaked and then drunk	Jaundice	

### 2.1.3 Clinical study, pharmacological activity and toxicity of *C. alata*

In clinical study, *C. alata* is mainly used against constipation. Anthraquinone derivatives in *C. alata* have been confirmed to have stimulating laxative activity. Moreover, other studies have focused on antimicrobial activity but other properties can be of interest, such as antifungal, analgesic, antidiabetic, anti-inflammatory, anti-mutagenic and wound-healing activities. Pharmacological activity and toxicity tests of *C. alata* are presented in Table 2.



Table 2 Clinical study, pharmacological activity and toxicity of *C. alata*

Activity	Plant used	Model of study	Result	References
Antibacterial	Methanol extract of leaves	<i>In vitro</i> , zone of inhibition	Zone of inhibition (extract vs gentamycin) <ul style="list-style-type: none"> <li>- <i>Bacillus subtilis</i> (10 vs 5 mm)</li> <li>- <i>Escherichia coli</i> (10 vs 5 mm)</li> <li>- <i>Pseudomonas aeruginosa</i> (8 vs 5 mm)</li> <li>- <i>Staphylococcus aureus</i> (5 vs 5 mm)</li> </ul>	[7]
	Chloroform extract of leaves	<i>In vitro</i> , zone of inhibition	Zone of inhibition (extract vs gentamycin) <ul style="list-style-type: none"> <li>- <i>Bacillus subtilis</i> (4 vs 5 mm)</li> <li>- <i>Escherichia coli</i> (8 vs 5 mm)</li> <li>- <i>Pseudomonas aeruginosa</i> (4 vs 5 mm)</li> <li>- <i>Staphylococcus aureus</i> (6 vs 5 mm)</li> </ul>	
	Chloroform extract of leaves	<i>In vitro</i> , zone of inhibition	Zone of inhibition (extract vs gentamycin) <ul style="list-style-type: none"> <li>- <i>Escherichia coli</i> (12 vs 16 mm)</li> <li>- Methicillin resistant <i>Staph aureus</i> (MRSA) (18 vs 25 mm)</li> <li>- Methicillin susceptible strains (MSSA) (20 vs 25 mm)</li> <li>- <i>Proteus vulgaris</i> (18 vs 18 mm)</li> </ul>	[21]

Table 2 Clinical study, pharmacological activity and toxicity of *C. alata* (continued)

Activity	Plant used	Model of study	Result	References
Antibacterial	Acetone extract of roots	<i>In vitro</i> , minimal inhibitory concentrations (MICs)	<i>Bacillus cereus</i> MICs 40 µg/mL	[22]
	Methanol extract of leaves	<i>In vitro</i> , zone of inhibition	Zone of inhibition (extract vs streptomycin) <ul style="list-style-type: none"> <li>- <i>Escherichia coli</i> (8 vs 16 mm)</li> <li>- <i>Proteus mirabilis</i> (6 vs 8 mm)</li> <li>- <i>Pseudomonas aeruginosa</i> (6 vs 6 mm)</li> <li>- <i>Shigella flexneri</i> (8 vs 18 mm)</li> <li>- <i>Staphylococcus aureus</i> (10 vs 22 mm)</li> <li>- <i>Streptococcus Pyogenes</i> (12 vs 18 mm)</li> </ul>	[23]
	Methanol extract of roots	<i>In vitro</i> , zone of inhibition	Zone of inhibition (extract vs streptomycin) <ul style="list-style-type: none"> <li>- <i>Escherichia coli</i> (8 vs 16 mm)</li> <li>- <i>Proteus mirabilis</i> (6 vs 8 mm)</li> <li>- <i>Pseudomonas aeruginosa</i> (6 vs 6 mm)</li> <li>- <i>Shigella flexneri</i> (8 vs 18 mm)</li> <li>- <i>Staphylococcus aureus</i> (8 vs 22 mm)</li> <li>- <i>Streptococcus Pyogenes</i> (10 vs 18 mm)</li> </ul>	

Table 2 Clinical study, pharmacological activity and toxicity of *C. alata* (continued)

Activity	Plant used	Model of study	Result	References
Antibacterial	Methanol extract of flowers	<i>In vitro</i> , zone of inhibition	<p>Zone of inhibition (extract vs chloramphenicol)</p> <ul style="list-style-type: none"> <li>- <i>Agrobacterium tumefaciens</i> (18 vs 12 mm)</li> <li>- <i>Agrobacterium tumefaciens</i> (18 vs 12 mm)</li> <li>- <i>Bacillus cereus</i> (18 vs 16 mm)</li> <li>- <i>Bacillus coagulans</i> (20 vs 16 mm)</li> <li>- <i>Bacillus megaterium</i> (18 vs 16 mm)</li> <li>- <i>Bacillus subtilis</i> (14 vs 16 mm)</li> <li>- <i>Escherichia coli</i> (18 vs 18 mm)</li> <li>- <i>Lactobacillus casei</i> (20 vs 18 mm)</li> <li>- <i>Micrococcus luteus</i> (18 vs 16 mm)</li> <li>- <i>Micrococcus roseus</i> (18 vs 6 mm)</li> <li>- <i>Neisseria gonorrhoeae</i> (20 vs 18 mm)</li> <li>- <i>Proteus mirabilis</i> (18 vs 16 mm)</li> <li>- <i>Pseudomonas aeruginosa</i> (16 vs 24 mm)</li> <li>- <i>Salmonella typhi</i> (20 vs 16 mm)</li> <li>- <i>Salmonella typhymurium</i> (18 vs 16 mm)</li> </ul>	[24]

Table 2 Clinical study, pharmacological activity and toxicity of *C. alata* (continued)

Activity	Plant used	Model of study	Result	References
Antifungal	Aqueous extract of flower	<i>In vitro</i> , microscopic examination	Percent growth inhibition - <i>Candida albicans</i> 75 % - <i>Microsporium audouinii</i> 75 %	[25]
	Ethanol extract of leaves	<i>In vitro</i> , zone of inhibition	Zone of inhibition (extract vs clotrimazole) - <i>Microsporium caris</i> (13.00 vs 25.50 mm) - <i>Epidermophyton floccosum</i> (20.00 vs 21.50 mm) - <i>Trichophyton verrucosif</i> (20.50 vs 22.50 mm) - <i>Trichophyton mentagrophytes</i> (19.50 vs 23.00)	[26]
	Ethanol extract of leaves	<i>In vitro</i> , zone of inhibition	Zone of inhibition (extract vs clotrimazole) - <i>Candida albicans</i> (20 vs 30 mm)	[27]
	Chloroform extract of leaves	<i>In vitro</i> , zone of inhibition	Zone of inhibition (extract vs clotrimazole) - <i>Trichophyton mentagrophytes</i> (26 vs 65 mm)	



Table 2 Clinical study, pharmacological activity and toxicity of *C. alata* (continued)

Activity	Plant used	Model of study	Result	References
Antifungal	Ethanol extract of leaves	<i>In vitro</i> , zone of inhibition	<p>Zone of inhibition</p> <ul style="list-style-type: none"> <li>- <i>Aspergillus niger</i> &lt; 10 mm</li> <li>- <i>Cladosporium werneckii</i> &lt; 10 mm</li> <li>- <i>Fusarium solani</i> &lt; 10 mm</li> <li>- <i>Microsporium caris</i> &gt; 10 mm</li> <li>- <i>Microsporium gypseum</i> &gt; 10 mm</li> <li>- <i>Penicillium</i> sp. &lt; 10 mm</li> <li>- <i>Trichophyton mentagrophytes</i> &gt; 10 mm</li> <li>- <i>Trichophyton rubrum</i> &gt; 10 mm</li> </ul>	[28]
	Leaves	Clinical, topical, microscopic examination from infected skin	Infected region disappear	[29]
Anti-allergic	Hydro-alcoholic extract of leaves	<i>In vivo</i> (rat), mast cell stabilization assay	Inhibition of mast cell degranulation 75.67%	[30]
		<i>In vitro</i> , lipoxygenase assay	Half maximal inhibitory concentration (IC <sub>50</sub> ) 90.2 µg/mL	

Table 2 Clinical study, pharmacological activity and toxicity of *C. alata* (continued)

Activity	Plant used	Model of study	Result	References
Anti-lipogenic	Water extract of leaves	<i>In vivo</i> (mice), serum triglyceride and cholesterol	Decreased serum triglyceride and cholesterol	[31]
		<i>In vivo</i> (mice), liver histology analysis	Decreased triglyceride storage in liver	
		<i>In vivo</i> (mice), immunoblotting	- Reduced peroxisome proliferator activated receptor gamma (PPAR $\gamma$ ) protein expression - Elevated PPAR $\alpha$ protein expression	
Anti-diabetic	Ethyl acetate extract of leaves	<i>In vivo</i> (mice), blood glucose level	Decreased blood sugar 56.7%	[27]
		<i>In vivo</i> (mice), blood glucose level	Decrease blood sugar	
		<i>In vivo</i> (mice), serum insulin level	Reduced insulin level	
Analgesic	Methanol extract of leaves	<i>In vivo</i> (mice), serum leptin level	Reduced leptin level	[32]
		<i>In vitro</i> , $\alpha$ -glucosidase inhibition	Potent inhibited $\alpha$ -glucosidase activity (IC <sub>50</sub> = 63.75 $\mu$ g/mL)	
		<i>In vivo</i> (mice), acetic acid induced writhing test (squirm)	Percent of inhibition (extract vs mefenamic acid) 59.9% vs 78.8%	

Table 2 Clinical study, pharmacological activity and toxicity of *C. alata* (continued)

Activity	Plant used	Model of study	Result	References
Anti-mutagenic	Chloroform extract of leaves	<i>In vivo</i> (mice), count number of micronucleated polychromatic erythrocytes (MPE)	Reduced mutagenicity of tetracycline 65.8%	[27]
	Chloroform extract of leaves	<i>In vivo</i> (mice), count number of MPE	Reduced mutagenicity of mytomycin C 71%	[33]
Anti-inflammatory	Ethyl acetate extract of leaves	<i>In vivo</i> (mice), carrageenan induced paw edema test	Percent of inhibition 68.2%	[27]
	Hexane extract of leaves	<i>In vivo</i> (mice), carrageenan induced paw edema test	Percent of inhibition 65.5%	
	Heat-treated leaves extract	<i>In vivo</i> (Rat), concanavalin A induced histamine release from rat peritoneal mast cells	Percent of inhibition 98.4%	[34]
		<i>In vitro</i> , cyclooxygenase 1 and 2 (COX-1, COX-2) activity	Percent of inhibition COX-1 96.6%, COX-2 84.6%	
		<i>In vitro</i> , 5-lipoxygenase activity	Percent of inhibition 99.2%	

Table 2 Clinical study, pharmacological activity and toxicity of *C. alata* (continued)

Activity	Plant used	Model of study	Result	References
Anti-inflammatory	Ethanol extract of leaves	<i>In vitro</i> (dendritic cell), fluorescence-activated cell sorting (FACS) analysis	Inhibited TNF- $\alpha$ production	[3, 35]
	Acetone extract of roots	<i>In vitro</i> , 100 $\mu$ g/mL, DPPH assay	IC <sub>50</sub> = 29.51 $\mu$ g/mL	[22]
Anti-oxidative	Ethanol extract of leaves	<i>In vitro</i> , chemiluminescence measurements	Reduced H <sub>2</sub> O <sub>2</sub> 67%, anion superoxide 65%	[3, 35]
	Methanol extract of	<i>In vitro</i> , 100 $\mu$ g/mL, DPPH assay	IC <sub>50</sub> = 54 g/mL	[36]
Toxicity	Ethyl acetate extract of leaves	<i>In vivo</i> (mice), 150 mg extract/20 g mouse	Paralysis, screen grip loss, diarrhea, enophthalmus, hyperaemia, micturition	[27]
	Methanol extract of	<i>In vivo</i> (mice), acute toxicity	Lethal dose (LD <sub>50</sub> ) = 1459.32 mg/kg	[37]
	Hydro-ethanolic extract of leaves	<i>In vivo</i> (mice), acute toxicity	LD <sub>50</sub> = 18.5 g/kg	[38]
		<i>In vivo</i> (rat), 500 and 1000 mg/kg	No changes in alanine aminotransferase (ALT), aspartate aminotransferase (AST), alkaline phosphatase (ALP) serum level	
	Aqueous extract of leaves	<i>In vitro</i> (rat), 150 mg/kg, haematological examination	Reduced haemoglobin concentration, erythrocyte count, packed cell volume	[39]

Table 2 Clinical study, pharmacological activity and toxicity of *C. alata* (continued)

Activity	Plant used	Model of study	Result	References
Drug interaction	Aqueous extract of leaves	<p><i>In vitro</i>, 1,000 µg/mL, cytochromes P450 (CYP) inhibition assays</p> <p><i>In vivo</i> (rat), 500 µg/mL, GST inhibition assays</p>	<p>Inhibited</p> <ul style="list-style-type: none"> <li>- CYP1A2 (IC<sub>50</sub> = 28.3 µg/mL)</li> <li>- CYP3A4 (IC<sub>50</sub> = 158.8 µg/mL)</li> <li>- CYP2D6 (IC<sub>50</sub> = 165.5 µg/mL)</li> </ul> <p>Inhibited glutathione S-transferases (GSTs) IC<sub>50</sub> = 41.9 µg/mL</p>	[40]

### 2.1.4 Chemical constituents of *C. alata*

The volatile oil constituents of *C. alata* leaves were obtained by hydrodistillation using a cleverger apparatus and then subsequently analyzed by gas chromatography coupled with mass spectrometry (GC/MS). The volatile oil constituents of *C. alata* leaves are presented in Table 3 [41]. Non-volatile metabolites are presented in Table 4. Their structures are shown in Figure 2. The main reported compounds are flavonoids and anthraquinones.

Table 3 The volatile oil constituents of *C. alata*

Compounds	%	Compounds	%
1,8-cineole	39.8	tetradecanal	t
$\beta$ -caryophyllene	19.1	( <i>E</i> )-geranyl acetone	t
caryophyllene oxide	12.7	humulene epoxide II	t
germacrene D	5.5	<i>n</i> -hexadecane	t
$\alpha$ -selinene	5.4	$\beta$ -elemene	t
limonene	5.2	$\delta$ -cadinene	t
$\alpha$ -cadinol	4.2	<i>n</i> -pentadecane	t
$\alpha$ -phellandrene	3.7	$\alpha$ -terpineol	t
( <i>E</i> )-2-hexenal	3.3	Bicyclogermacrene	t
$\alpha$ -bulnesene	1.0	Benzaldehyde	t
$\alpha$ -humulene	t	( <i>E</i> )- $\beta$ -ionone	t
( <i>E</i> )- $\beta$ -farnesene	t	tricyclene	t
<i>p</i> -cymene	t		

t: Trace amount < 0.1%

Table 4 Chemical constituents of *C. alata*

Compounds	Activity	Plants parts	Identification method	References
Flavonoids	Not defined	Leaves	IR, NMR, MS	[42]
		Seeds	<sup>13</sup> C NMR, TLC	[43]
Kaempferol	Antioxidative, antiallergic, anti-inflammatory, antibacterial	Leaves	UV, HPLC, IR, NMR, LC-MS	[22, 30, 42, 44, 45]
		Roots	HPLC, LC-MS	[46]
Kaempferol-3-O-gentiobioside	Anti-inflammatory, antidiabetic antibacterial	Leaves	UV, HPLC, IR, LC-MS, <sup>1</sup> H NMR and <sup>13</sup> C NMR	[34, 44, 45]
Kaempferol-3-O-β-D-glucopyranoside	Antibacterial	Leaves	UV, IR, NMR, MS	[42, 44]
Luteolin	Antibacterial	Swigs	UV, IR, NMR, MS	[22]
Rhamnetin-3-O-(2''-O-β-D-mannopyranosyl)-β-D-allopyranoside	Not defined	Seeds	<sup>1</sup> H NMR and <sup>13</sup> C NMR, FAB-MS, TLC, IR, UV	[43]
		Leaves	UV, IR, NMR, MS	[22, 47]
Apigenin	Antibacterial	Roots	UV, IR, NMR, MS	

Table 4 Chemical constituents of *C. alata* (continued)

Compounds	Activity	Plants parts	Identification method	References	
Anthraquinones	Aloe-emodin	Leaves	UV, IR, NMR, MS	[4, 22, 33, 44, 48]	
	Aloe-emodin-8-O- $\beta$ -glucoside	Leaves	HPLC, NMR, LC-MS	[4, 45]	
	Alquinone	Roots	EI-MS, UV, IR, $^1\text{H}$ NMR	[49]	
	Emodin	Not defined	Leaves	UV, IR, NMR, MS	[22]
		Anti-inflammatory, antibacterial	Roots	HPLC, LC-MS	[46]
	Physcion	Antibacterial	Fruits	UV, IR	[4]
		Anti-inflammatory, antioxidant, anticancer, antidiabetic, anti-allergic, hepatoprotective, nephroprotective	Stems	$^1\text{H}$ NMR, IR, UV	[4, 50]
	Rhein	Antibacterial	Roots	UV, IR, NMR, MS	[22]
	Hydroxyemodin	Anti-inflammatory, antioxidant, anticancer, antidiabetic, anti-allergic, hepatoprotective, nephroprotective	Roots	HPLC, LC-MS	[46]
		Antibacterial	Leaves	HPLC, $^1\text{H}$ NMR, MS, IR, UV	[4, 30, 48]
		Fruit	UV, IR	[4]	
		Roots	UV, IR, NMR, MS	[22]	



Table 4 Chemical constituents of *C. alata* (continued)

Compounds		Activity	Plants parts	Identification method	References
Steroids	Stigmasterol	Antibacterial	Leaves	NMR, UV, IR	[33]
	$\beta$ -Sitosterol	Antibacterial	Leaves	NMR, UV, IR	
Anthrones	Alarone	Not defined	Stems	<sup>1</sup> H NMR, MS, IR, UV	[4]
Ellagitannin	2,3,7-tri-O-methylgallagic acid	Not defined	Leaves	NMR	[4]
Naphtalene	Torachryson	Not defined	Bark	<sup>1</sup> H and <sup>13</sup> C NMR, EI-MS	
Phenolic acid	Hydroxyanthracene	Laxative	Leaves	<sup>1</sup> H NMR, EI-MS, IR, UV	[4, 51]
Purine	Adenine	Antiplatelet	Leaves	<sup>1</sup> H and <sup>13</sup> C NMR, HRFAB-MS, FAB-MS, UV	[52]
Miscellaneous	<i>trans</i> -resveratrol	Antibacterial , antioxidative	Roots	UV, IR, NMR, MS	[22]

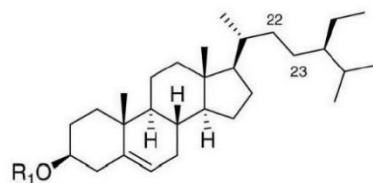


Figure 2 Chemical constituents of *C. alata*

(Stigmasterol: R<sub>1</sub>= H,  $\Delta_{22-23}$ ,  $\beta$ -Sitosterol: R<sub>1</sub>= H)

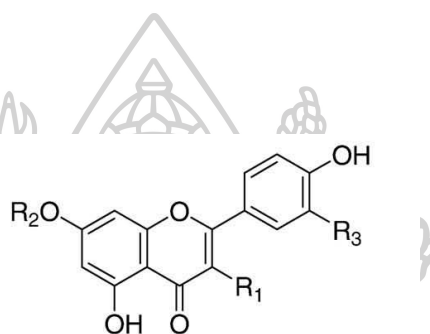


Figure 2 Chemical constituents of *C. alata* (continued)

(Chrysoeriol-7-O-(2''-O- $\beta$ -D-mannopyranosyl)- $\beta$ -D-allopyranoside: R<sub>1</sub>= H, R<sub>2</sub>=  $\beta$ -D-mannopyranosyl(1 $\rightarrow$ 6)- $\beta$ -D-allopyranoside, R<sub>3</sub>= OCH<sub>3</sub>, **Kaempferol**: R<sub>1</sub>= OH, R<sub>2</sub>= R<sub>3</sub>= H, **Kaempferol-3-O-gentiobioside**: R<sub>1</sub>= O- $\beta$ -D-glucopyranoside, R<sub>2</sub>= R<sub>3</sub>= H, **Kaempferol-3-O- $\beta$ -D-glucopyranoside**: R<sub>1</sub>= O- $\beta$ -D-glucopyranosyl(1 $\rightarrow$ 6)- $\beta$ -D-glucopyranoside, R<sub>2</sub>= H, R<sub>3</sub>= OH, **Luteolin**: R<sub>1</sub>= R<sub>2</sub>= H, R<sub>3</sub>= OH, **Rhamnetin-3-O-(2''-O- $\beta$ -D-mannopyranosyl)- $\beta$ -D-allopyranoside**: R<sub>1</sub>= O- $\beta$ -D-mannopyranosyl(1 $\rightarrow$ 6)- $\beta$ -D-allopyranoside, R<sub>2</sub>= CH<sub>3</sub>, R<sub>3</sub>= OH, **Diosmetin**: R<sub>1</sub>= R<sub>2</sub>= H, R<sub>3</sub>= OCH<sub>3</sub>, **Apigenin**: R<sub>1</sub>= R<sub>2</sub>= R<sub>3</sub>= H)

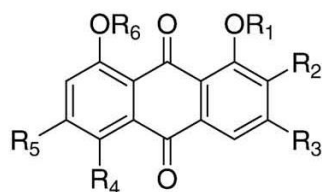
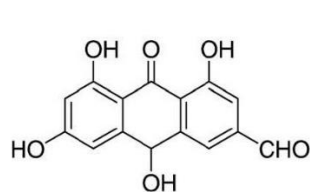
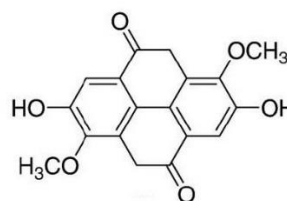


Figure 2 Chemical constituents of *C. alata* (continued)

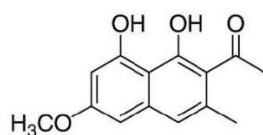
(**Aloe-emodin**: R<sub>1</sub> = R<sub>2</sub> = R<sub>4</sub> = R<sub>5</sub> = R<sub>6</sub> = H, R<sub>3</sub> = CH<sub>2</sub>OH, **Aloe-emodin-8-O-β-glucoside**: R<sub>1</sub> = R<sub>2</sub> = R<sub>4</sub> = R<sub>5</sub> = H, R<sub>3</sub> = CH<sub>2</sub>OH, R<sub>6</sub> = β-D-glucopyranoside, **Alquinone**: R<sub>1</sub> = R<sub>4</sub> = R<sub>5</sub> = R<sub>6</sub> = H, R<sub>2</sub> = OH, R<sub>3</sub> = CHO, **Emodin**: R<sub>1</sub> = R<sub>2</sub> = R<sub>4</sub> = R<sub>6</sub> = H, R<sub>3</sub> = CH<sub>3</sub>, R<sub>5</sub> = OH, **Physcion**: R<sub>1</sub> = R<sub>2</sub> = R<sub>4</sub> = R<sub>6</sub> = H, R<sub>3</sub> = CH<sub>3</sub>, R<sub>5</sub> = OCH<sub>3</sub>, **Rhein**: R<sub>1</sub> = R<sub>2</sub> = R<sub>4</sub> = R<sub>5</sub> = R<sub>6</sub> = H, R<sub>3</sub> = COOH, **Hydroxyemodin**: R<sub>1</sub> = R<sub>2</sub> = R<sub>4</sub> = R<sub>6</sub> = H, R<sub>3</sub> = CH<sub>2</sub>OH, R<sub>5</sub> = OH)



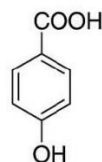
Alarone



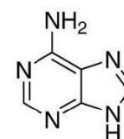
2,3,7-tri-O-methylellagic acid



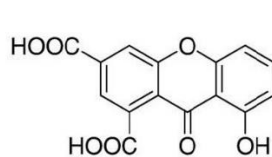
Torachryson



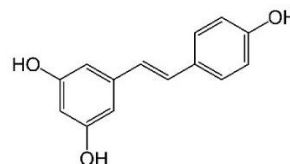
p-hydroxybenzoic acid



Adenine



Cassiaxanthone



Trans-resveratrol

Figure 2 Chemical constituents of *C. alata* (continued)

Source: Thierry Hennebelle et al., "Senna alata," **Fitoterapia** 80, 7 (October 2009): 385-393.

## 2.2 Rhein

### 2.2.1 Pharmacological activity of rhein

Rhein anthraquinone is found in medicinal plants, such as *Rheum palmatum*, *Polygonum multiflorum*, *Aloe barbadensis* [53] and *Cassia* species [54]. Rhein have been used medicinally for thousands of years diarrhea is the most common side effect as a result of stimulating laxative activity from anthraquinone derivatives. Rhein has many pharmacological activities, including hepatoprotective, nephroprotective, anti-inflammatory, antioxidant, anticancer and antidiabetic. Pharmacological activities of rhein are presented in Table 5.



Table 5 Pharmacological activity of rhein

Activity	Model of study	Result	References
Hepatoprotective	<i>In vivo</i> (rat), carbon tetrachloride/ethanol induced liver fibrosis, administering with 100 mg/kg rhein	<ul style="list-style-type: none"> <li>- Decreased serum level of ALT, hyaluronic acid, procollagen type III</li> <li>- Reduced fibrosis in liver</li> <li>- Decreased expression of alpha smooth muscle actin (<math>\alpha</math>-SMA), transforming growth factor beta 1 (TGF-<math>\beta</math>1)</li> </ul>	[55]
	<i>In vivo</i> (mice), induce by high fat diet, administering with 150 mg/kg rhein	<ul style="list-style-type: none"> <li>- Decreased serum level of ALT</li> </ul>	[56]
Nephroprotective	<i>In vivo</i> (mice), unilateral ureteral obstruction induced renal interstitial fibrosis, administering with 150 mg/kg rhein	<ul style="list-style-type: none"> <li>- Inhibited renal interstitial collagen accumulation</li> <li>- Decreased expression of <math>\alpha</math>-SMA, fibronectin, TGF-<math>\beta</math>1</li> </ul>	[57]
	<i>In vitro</i> (NRK-49F), TGF- $\beta$ 1 induced renal interstitial fibrosis	<ul style="list-style-type: none"> <li>- Decreased expression of <math>\alpha</math>-SMA, fibronectin</li> </ul>	
	<i>In vivo</i> , chronic allograft nephropathy rat model, administering with 100 mg/kg rhein	<ul style="list-style-type: none"> <li>- Reduced renal fibrosis</li> <li>- Increased expression of hepatic growth factor, bone morphogenetic protein 7</li> </ul>	[58]

Table 5 Pharmacological activity of rhein (continued)

Activity	Model of study	Result	References
Nephroprotective	<i>In vivo</i> , immunoglobulin A (IgA) nephropathy rat model, administering with 100 mg/kg rhein	<ul style="list-style-type: none"> <li>- Decreased expression of <math>\alpha</math>-SMA, fibronectin</li> <li>- Decreased volume of urinary red blood cells and urinary protein excretion</li> </ul>	[59]
	<i>In vivo</i> (rat), unilateral nephrectomy induced glomerulosclerosis	<ul style="list-style-type: none"> <li>- Decreased activity of nuclear factor kappa B (NF-kB)</li> <li>- Decreased expression of caspase-3</li> </ul>	[60]
	<i>Ex vivo</i> (renal proximal tubular of rat), high glucose and angiotensin II (AngII) induced hypertrophy of renal proximal tubular epithelial cells, incubated with 30 mg/L rhein	<ul style="list-style-type: none"> <li>- Inhibited hypertrophy of renal proximal tubular epithelial cells</li> <li>- Decreased cell size, 3H-leucine incorporation, cellular protein content</li> </ul>	[61]
Anti-inflammation	<i>In vitro</i> (human chondrocytes), induced by IL-1 $\beta$ , incubated with 10 <sup>-5</sup> M rhein	<ul style="list-style-type: none"> <li>- Increased production of aggrecan</li> <li>- Decreased production of IL-6, Stromelysin-1 (MMP-3), NO, macrophage inflammatory protein 1<math>\beta</math></li> <li>- Decreased production of prostaglandin E2 (PGE<sub>2</sub>)</li> </ul>	[62]

Table 5 Pharmacological activity of rhein (continued)

Activity	Model of study	Result	References
Anti-inflammation	<i>In vitro</i> (human osteoarthritic chondrocytes), induced by IL-1 $\beta$ , incubated with 10 <sup>-5</sup> M rhein	- Decreased production of nitrite, nitrosothiol	[63]
	<i>In vitro</i> (human osteoarthritic synovial tissue and cartilage), induced by lipopolysaccharide (LPS), incubated with 10 <sup>-6</sup> M rhein	<ul style="list-style-type: none"> <li>- Decreased production of IL-1<math>\beta</math>, NO</li> <li>- Decreased level of IL-1 receptor antagonist</li> <li>- Increased synthesis of proteoglycan</li> </ul>	[64]
	<i>In vitro</i> (human osteoarthritic synoviocytes and chondrocytes), incubated with 10 <sup>-4</sup> M rhein	<ul style="list-style-type: none"> <li>- Decreased caspase-3/7 activity</li> <li>- Increased expression of p21 and p27</li> </ul>	[65]
	<i>In vitro</i> (bovine articular chondrocytes), low oxygen tension condition and induced by IL-1 $\beta$ , incubated with 10 <sup>-5</sup> M rhein	<ul style="list-style-type: none"> <li>- Increased production of aggrecan, collagen type II</li> <li>- Decreased activity of activator protein1 (AP-1)</li> <li>- Decreased expression of matrix metalloproteinase 1 (MMP1)</li> <li>- Inhibited degradation of inhibitor kB-<math>\alpha</math> (IkB-<math>\alpha</math>) protein</li> </ul>	[66]

Table 5 Pharmacological activity of rhein (continued)

Activity	Model of study	Result	References
Anti-inflammation	<i>In vitro</i> (bovine articular chondrocytes), induced by IL-1 $\beta$ , incubated with 10 $\mu$ M rhein	<ul style="list-style-type: none"> <li>- Decreased expression of inducible nitric oxide synthase (iNOS)</li> <li>- Decreased production of NO</li> <li>- Inhibited degradation of I<math>\kappa</math>B-<math>\alpha</math>, p65</li> </ul>	[67]
	<i>In vitro</i> (rabbit articular chondrocytes), induced by recombinant human IL-1 $\alpha$ , incubated with 30 $\mu$ M rhein	<ul style="list-style-type: none"> <li>- Decreased production of sulfated glycosaminoglycan, proMMP-3</li> <li>- Decreased activity of caspase-9</li> </ul>	[68]
	<i>In vitro</i> (human umbilical vein endothelial cell), induced by LPS, incubated with 20 $\mu$ M rhein	<ul style="list-style-type: none"> <li>- Decreased expression of vascular cell adhesion molecule 1 (VCAM-1), intercellular adhesion molecule 1 (ICAM-1), E-Selectin</li> </ul>	[69]
	<i>In vivo</i> (rat), adjuvant induced arthritis, administering with 200 mg/kg rhein	<ul style="list-style-type: none"> <li>- Decreased paw swelling</li> <li>- Decreased expression of MMP-2, gp91<sup>phox</sup>, p22<sup>phox</sup>, activating transcript factor 6 (ATF6), p55Shc, phosphorylation of protein kinase B (p-Akt)</li> </ul>	[70]



Table 5 Pharmacological activity of rhein (continued)

Activity	Model of study	Result	References
Anti-inflammation	<i>In vitro</i> (monocyte-like cell line), induced by recombinant human LIGHT, incubated with 10 $\mu$ M rhein	<ul style="list-style-type: none"> <li>- Decreased production of ROS, IL-8, TNF-<math>\alpha</math>, IL-6, monocyte chemoattractant protein 1 (MCP-1)</li> <li>- Decreased expression of CCR1, CCR2, ICAM-1</li> <li>- Decreased phosphorylation of p38, mitogen activated protein kinases (MAPK), I<math>\kappa</math>B-<math>\alpha</math></li> </ul>	[71]
Antioxidant	<i>In vivo</i> (mice), induce by high fat diet, administering with 150 mg/kg rhein	- Decreased hepatic level of IL-1 $\beta$ , IL-6, IL-8, IL-12p70, TNF- $\alpha$	[56]
	<i>In vitro</i> (human umbilical vein endothelial cell), induced by hydrogen peroxide, incubated with 16 $\mu$ M rhein	- Decreased production of malondialdehyde, lactate dehydrogenase (LDH) content	[72]
	<i>In vivo</i> (rat), acetaminophen induced hepatotoxicity and nephrotoxicity, 40 mg/kg rhein	<ul style="list-style-type: none"> <li>- Decreased serum level of glutamate-pyruvate transaminase (GPT), glutamic-oxalacetic transaminase (GOT), total bilirubin, creatinine, urea nitrogen</li> <li>- Decreased production of ROS, NO, malondialdehyde</li> <li>- Histopathological damage of liver and kidney were ameliorated</li> </ul>	[73]

Table 5 Pharmacological activity of rhein (continued)

Activity	Model of study	Result	References
Anticancer	<i>In vitro</i> (human nasopharyngeal carcinoma cell), incubated with 100 $\mu$ M rhein	<ul style="list-style-type: none"> <li>- Inhibited cell invasion and migration</li> <li>- Decreased expression of MMP-9, vascular endothelial growth factor (VEGF), GRB2, SOS-1, Ras</li> </ul>	[74]
	<i>In vitro</i> (human hepatocellular carcinoma BEL-7402 cell), incubated with 200 $\mu$ M rhein	<ul style="list-style-type: none"> <li>- Inhibited cell proliferation</li> <li>- Induced cell apoptotic, cycle S-phase arrest</li> <li>- Decreased expression of c-Myc gene</li> <li>- Increased expression of caspase 3 gene</li> </ul>	[75]
	<i>In vitro</i> (human umbilical vein endothelial cell), hypoxic condition and induced by VEGF <sub>165</sub> , incubated with 100 $\mu$ M rhein	<ul style="list-style-type: none"> <li>- Inhibited cell proliferation and migration</li> <li>- Inhibited activation phosphatidylinositol 3 kinase (PI3K), p-AKT, phosphorylated extracellular signal regulated kinase (p-ERK)</li> </ul>	[76]
	<i>In vitro</i> (hormone-dependent and hormone-independent human breast adenocarcinoma cell line), hypoxic condition, incubated with 100 $\mu$ M rhein	<ul style="list-style-type: none"> <li>- Decreased cell viability, inhibited cell cycle and activity of heat shock protein 90 alpha</li> <li>- Inhibited expression of hypoxia-inducible factor 1<math>\alpha</math> (HIF-1<math>\alpha</math>), VEGF, endothelial growth factor (EGF)</li> </ul>	

Table 5 Pharmacological activity of rhein (continued)

Activity	Model of study	Result	References
Anticancer	<i>In vitro</i> (human tongue cancer cell), incubated with 100 $\mu$ M rhein	<ul style="list-style-type: none"> <li>- Decreased cell viability</li> <li>- Inhibited cell invasion and migration</li> <li>- Decreased level of MMP-2, urokinase plasminogen activator (u-PA), focal adhesion kinase (FAK), NF-kB, p65, p-AKT, p-P38, phosphorylated c-Jun N terminal kinases (p-JNK), p-ERK</li> <li>- Increased level of tissue inhibitor of metalloproteinase 1 (TIMP-1)</li> <li>- Decreased expression of MMP-9</li> </ul>	[77]
Antidiabetic	<i>In vivo</i> (diabetic mice), administering with 120 mg/kg rhein	<ul style="list-style-type: none"> <li>- Decreased level of fasting plasma glucose</li> <li>- Elevated early-phase insulin secretion</li> <li>- Improved glucose tolerance</li> </ul>	[78]
	<i>In vitro</i> (mouse pancreatic $\beta$ -cell line), hypoxic condition, incubated with 1 $\mu$ M rhein	<ul style="list-style-type: none"> <li>- Inhibited <math>\beta</math>-cell apoptosis and caspase3 activity</li> <li>- Prevented mitochondrial fragmentation</li> <li>- Inhibited expression of mitochondrial dynamin-related protein 1 (Drp1)</li> </ul>	[79]

Table 5 Pharmacological activity of rhein (continued)

Activity	Model of study	Result	References
Antidiabetic	<i>In vivo</i> (diabetic mice), administering with 120 mg/kg rhein	<ul style="list-style-type: none"> <li>- Decreased level of fasting plasma glucose</li> <li>- Inhibited <math>\beta</math>-cell apoptosis and expression of mitochondrial Drp1</li> <li>- Increased insulin secretion (induced by high glucose)</li> </ul>	[79]
	<i>In vivo</i> (diabetic mice), administering with 120 mg/kg rhein	<ul style="list-style-type: none"> <li>- Decreased serum level of plasma glucose</li> <li>- Increased insulin secretion</li> <li>- Inhibited <math>\beta</math>-cell apoptosis</li> </ul>	[80]
	<i>In vivo</i> (diabetic mice), administering with 120 mg/kg rhein	<ul style="list-style-type: none"> <li>- Decreased serum level of plasma glucose and pancreatic <math>\beta</math>-cell apoptosis</li> <li>- Elevated early-phase insulin secretion</li> </ul>	[81]
	<i>In vitro</i> , overexpression of human glucose transporter 1 (GLUT1) gene in rat mesangial cell	<ul style="list-style-type: none"> <li>- Decreased activity of glutamine fructose-6-phosphate aminotransferase (GFAT)</li> <li>- Decreased synthesis of collagen IV, fibronectin</li> </ul>	[82]
	<i>In vivo</i> (mice), induce by high fat diet, administering with 120 mg/kg rhein	<ul style="list-style-type: none"> <li>- Decreased level of fasting plasma glucose</li> </ul>	[83]

Table 5 Pharmacological activity of rhein (continued)

Activity	Model of study	Result	References
Antilipogenic	<i>In vivo</i> (mice), induce by high fat diet, administering with 120 mg/kg rhein	- Decreased serum level of total cholesterol (TC), triglyceride (TG)	[83]
	<i>In vivo</i> (mice), induce by high fat diet, administering with 150 mg/kg rhein	- Decreased serum level of TC, low density cholesterol (LDL), high density cholesterol (HDL) - Decreased liver TG	[56]
Antiallergic	<i>In vivo</i> (rat), administering with 5 mg/kg rhein	- Decreased mast cell degranulation - Inhibited lipoxigenase activity	[30]
Drug interaction	<i>In vitro</i> (rat), CYP inhibition assays	Inhibition constant ( $K_i$ ) - CYP2E1 $K_i = 10 \mu\text{m}$ - CYP2C9 $K_i = 38 \mu\text{m}$ - CYP3A $K_i = 30 \mu\text{m}$ - CYP1A2 $K_i = 62 \mu\text{m}$ - CYP2D6 $K_i = 74 \mu\text{m}$	[84]

### 2.2.2 Rhein content in *C. alata* leaves extract

*C. alata* leaves contains anthraquinones both in aglycone and glycosidic forms. The major anthraquinone in the leaves of *C. alata* is rhein. Rhein (4, 5 dihydroxyanthraquinone-2-carboxylic acid) is a lipophilic anthraquinone [53]. Different harvesting times and different drying method have an effect on the content of active compounds in *C. alata* [51]. Several analytical methods such as thin layer chromatography (TLC) and high performance liquid chromatography (HPLC) have been used for determination of rhein in *C. alata*. Qualitative and quantitative analysis of rhein in *C. alata* leaves extract are listed in Table 6, 7.

Table 6 Qualitative analytical methods of rhein in *C. alata*

Sample preparation	Method and Condition	Result	References
<p><i>C. alata</i> leaves</p> <ul style="list-style-type: none"> <li>- Crude ethanol extract: extract with 70% ethanol</li> <li>- Anthraquinone aglycone extract: decoction with water and hydrolyzed with 2 M HCL, then extract in chloroform</li> <li>- Anthraquinone glycoside extract: decoction with water and hydrolyzed with 2 M HCL, then extract in chloroform, collected aqueous layer</li> </ul>	<p>TLC</p> <ul style="list-style-type: none"> <li>- Silica gel plate (60 F<sub>254</sub>)</li> <li>- Solvent: 75:25:1 (petroleum ether : ethyl acetate : formic acid</li> <li>- Detected by spraying 10% methanolic KOH</li> </ul>	<p>Rhein containing in crude ethanol extract and anthraquinone aglycone extract</p>	<p>[5]</p>

Table 6 Qualitative analytical methods of rhein in *C. alata* (continued)

Sample preparation	Method and Condition	Result	References
<i>C. alata</i> leaves extract with 80% ethanol	TLC <ul style="list-style-type: none"> <li>- Silica gel plate (60 F<sub>254</sub>)</li> <li>- Solvent: 100:17:13 (ethyl acetate : methanol : water)</li> <li>- Detected by spraying 10% methanolic KOH</li> </ul>	Rhein containing in ethanol extract	[8]

Table 7 Quantitative analytical methods of rhein in *C. alata*

Sample preparation	Method and Condition	Result	References
<i>C. alata</i> leaves extract with methanol and 5 % HCL in methanol	HPLC <ul style="list-style-type: none"> <li>- Column: ODS-80Tm</li> <li>- Mobile phase: (70:30) methanol, 2.0 % acetic acid</li> <li>- Flow rate: 1.0 mL/min</li> <li>- Injection volume: 20 <math>\mu</math>L</li> <li>- Running time: 30 min.</li> <li>- UV detector: 254 nm</li> </ul>	- Methanol extract: rhein content 0.02 $\pm$ 0.002 %w/w - 5 % HCL in methanol extract: rhein content 0.15 $\pm$ 0.009 %w/w	[48]
<i>C. alata</i> root extract with ethanol	HPLC <ul style="list-style-type: none"> <li>- Column: C18</li> <li>- Mobile phase: (25:55:20) acetonitrile, methanol, 10 mM ammonium acetate</li> <li>- Flow rate: 0.4 mL/min</li> <li>- Injection volume: 10 <math>\mu</math>L</li> <li>- Running time: 45 min.</li> <li>- UV detector: 260 nm</li> </ul>	Rhein content 68.4 $\pm$ 1.6 ppm	[46]

### 2.3 Reactive oxygen species (ROS)

ROS are oxygen-derived small molecules, including oxygen radicals, such as superoxide anion ( $O_2^{\cdot-}$ ), hydroxyl radical ( $HO^{\cdot}$ ), peroxy ( $RO_2^{\cdot}$ ), alkoxy ( $RO^{\cdot}$ ) and non radical species that are easily converted into radicals, such as hydrogen peroxide ( $H_2O_2$ ) [85], hypochlorous (HOCl), ozone ( $O_3$ ) and singlet oxygen ( $^1O_2$ ) [86]. The generation of ROS can occur as primary function of the NADPH oxidase (NOX) or byproduct of other biological reactions such as mitochondria respiration, peroxisomes or generated by endogenous stimuli [87]. Endogenous sources of ROS production are listed in Table 8. There are multiple external triggers that induce oxidative stress. Air pollutants, tobacco smoke, radiations, alcohol and drugs, as well as xenobiotics can all contribute to oxidative stress. Infection and inflammation are common exogenous sources of ROS [88].

ROS can be both beneficial and harmful. Under normal physiological conditions, ROS are generated at low level by regulated enzymes, such as nitric oxide synthase (NOS) and NOX isoforms [89]. ROS avidly interact with a large number of molecules including proteins, lipids, carbohydrates, and nucleic acids, which may irreversibly destroy or alter the function of the target molecule [87]. Redox balance between ROS and antioxidants maintains normal condition. However, insufficient antioxidants or ROS overproduction generates oxidative stress, resulting in cellular damage. Oxidative stress has been linked to various inflammatory diseases [85].



Table 8 Endogenous sources of ROS

Sources	Reaction
Mitochondria respiratory chain	Inner mitochondrial membrane contains a series of enzyme complexes referred to as the mitochondrial respiratory chain. These include complexes I-IV. Electron leakage from complexes I and III results in reduction of molecular oxygen, thus forming $O_2^{\cdot -}$ . (Figure 3)
NADPH oxidase (NOX)	NOX is a multicomponent enzyme present in the plasma membrane and phagosomes of phagocytes. NADPH enzymes reduce molecular oxygen ( $O_2$ ) to superoxide as a primary product, and this is further converted to various ROS. (Figure 4: reaction 1) $NADPH + 2O_2 \xrightarrow{NOX} 2O_2^{\cdot -} + NADP^+ + H^+$
Xanthine oxidase (XO)	XO found on the outer surface of the plasma membrane and also in the cytoplasm. It catalyzes oxidation of hypoxanthine to xanthine and then, to uric acid during purine catabolism. (Figure 4: reaction 1) $\text{Hypoxanthine} + 2O_2 + NADPH \xrightarrow{XO} \text{Xanthine} + 2O_2^{\cdot -} + NADP^+ + H^+$ $\text{Xanthine} + 2O_2 + NADPH \xrightarrow{XO} \text{Uric acid} + 2O_2^{\cdot -} + NADP^+ + H^+$
Myeloperoxidase (MPO)	MPO is a heme enzyme localized in lysosomes of neutrophils, macrophages and monocytes. This enzyme chlorinates $H_2O_2$ to highly reactive HOCl. $H_2O_2 + Cl^- + H^+ \xrightarrow{MPO} HOCl + H_2O$
Nitric oxide synthases (NOS)	Nitric oxide synthase is a heme-containing monooxygenase that generates NO. NOS catalyze the oxidation of L-arginine to generation of L-citrulline and NO. $L\text{-arginine} + O_2 + 2H^+ \xrightarrow{NOS} L\text{-citrulline} + NO + 2H_2O$

Table 8 Endogenous sources of ROS (continued)

Sources	Reaction
Transition metals	<p>Transition metal ions such as iron (<math>\text{Fe}^{2+}</math>) and copper (Cu) generate <math>\text{HO}^\bullet</math> and <math>\text{OH}^-</math> from <math>\text{H}_2\text{O}_2</math>. (Figure 4: reaction 5)</p> <p>Haber-Weiss reaction</p> $\text{O}_2^{\bullet -} + \text{H}_2\text{O}_2 \xrightarrow{\text{Fe/Cu}} \text{OH}^- + \text{HO}^\bullet + \text{O}_2$ <p>Fenton reaction</p> $\text{Fe}^{2+} + \text{H}_2\text{O}_2 \longrightarrow \text{Fe}^{3+} + \text{OH}^- + \text{HO}^\bullet$
Lipoxygenases (LOX)	<p>LOX are a group of oxidative enzymes with a non-heme iron atom. These enzymes catalyze the insertion of oxygen into polyunsaturated fatty acids. (Figure 4: reaction 6, 7)</p> <p>Unsaturated fatty acids + <math>\text{O}_2 \xrightarrow{\text{LOX}} \text{O}_2^{\bullet -} + \text{lipid peroxyl radical}</math></p>
Cyclooxygenases (COX)	<p>COX is a bifunctional enzyme that having both COX and peroxidase activities. COX adds two <math>\text{O}_2</math> molecules to arachidonic acid (AA) by its bioxygenase activity to generate an unstable cyclic hydroperoxide, <math>\text{PGG}_2</math>. Next, it reduces <math>\text{PGG}_2</math> by its peroxidase activity to an endoperoxide, <math>\text{PGH}_2</math>. The peroxidase activity of COX generates <math>\text{NAD}^\bullet</math> and <math>\text{NADP}^\bullet</math> radicals. These radicals can eventually generate <math>\text{O}_2^{\bullet -}</math>.</p>

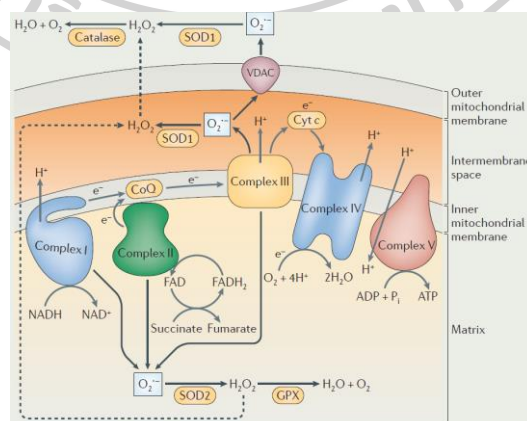


Figure 3 Mitochondrial respiratory chain

Source: A. Phillip West, Gerald S. Shadel, and Sankar Ghosh, "Mitochondria in innate immune responses," **Nature Reviews Immunology** 11, 6 (June 2011): 389-402.

### 2.3.1 Antioxidant defense system

Exposure to free radicals from a variety of sources has led organisms to develop a series of defence mechanisms. Defence mechanisms against free radical induced oxidative stress allows elimination of excess ROS. Under normal conditions, human have enzymatic antioxidant defences that include superoxide dismutase (SOD), glutathione peroxidase (GPx), catalase (CAT) [88], glutathione reductase (GR), and thioredoxin reductase (TrxR) [90]. Non-enzymatic antioxidants are represented by ascorbic acid (Vitamin C),  $\alpha$ -tocopherol (Vitamin E), glutathione (GSH), carotenoids, flavonoids [89], coenzyme Q and other antioxidants [91]. Under normal conditions, there is a balance between both the activities and the intracellular levels of these antioxidants. This balance is essential for the survival of organisms. Various pathways of antioxidant are list in Table 9.

Table 9 Antioxidant defense system

Sources	Reaction
Superoxide dismutase (SOD)	SOD are metal ion cofactor-requiring enzymes that catalyze dismutation of $O_2^{\cdot -}$ into $O_2$ and $H_2O_2$ . (Figure 4: reaction 2) $2O_2^{\cdot -} \xrightarrow{SOD} O_2 + H_2O_2$
Glutathione peroxidase (GPx) and GSH reductase (GR)	GPx converts GSH into oxidized glutathione, which also called glutathione disulfide (GSSG). During this process, reduces $H_2O_2$ to $H_2O$ and lipid hydroperoxides (ROOH) to corresponding stable alcohols. The GPX reaction is coupled to GR, which reduces oxidized GSSG to GSH (Figure 4: reaction 3,4,13) $2GSH + H_2O_2 \xrightarrow{Grx} GSSG + 2H_2O$ $2GSH + ROOH \xrightarrow{Grx} GSSG + ROH + H_2O$ $GSSG + NADPH + H^+ \xrightarrow{GR} 2GSH + NADP^+$
Catalase (CAT)	CAT dismutates $H_2O_2$ to $H_2O$ and $O_2$ $2H_2O_2 \xrightarrow{Grx} 2H_2O + O_2$

Table 9 Antioxidant defense system (continued)

Sources	Reaction
Thioredoxin (Trx) and thioredoxin reductase (TrxR)	Trx performs its antioxidant functions through peroxiredoxins (Prx), Prx uses the SH groups as reducing equivalents to reduction of H <sub>2</sub> O <sub>2</sub> . The oxidized form of Prx can be recycled back to its reduced form by Trx [92]. Oxidized Trx is reduced by TrxR at the expense of NADPH. (Figure 5)
Glutathione (GSH)	Glutathione conjugation to xenobiotic via glutathione-S-transferase (GST) results in the formation of a glutathione-S conjugate (Figure 4: reaction 17) $\text{GSH} + \text{xenobiotic} \xrightarrow{\text{GST}} \text{glutathione-S conjugate}$
Heme oxygenase-1 (HO-1)	HO-1 catalyzed the degradation of heme into carbon monoxide (CO), iron, and biliverdin. Biliverdin is rapidly converted to bilirubin by biliverdin reductase. $\text{Heme} + \text{O}_2 + \text{NADPH} \xrightarrow{\text{HO}} \text{CO} + \text{Fe}^{2+} + \text{NADP}^+ + \text{biliverdin}$
Ascorbic acid (Vitamin C)	Vitamin C is obtained from fresh fruits and vegetables. Vitamin C donates electrons to other compounds and prevents their oxidation.
$\alpha$ -tocopherol (Vitamin E)	Vitamin E is protected cell membranes from lipid peroxidation. Vitamin E scavenging lipid peroxy radicals (LOO $\cdot$ ) and itself is converted into a reactive radical. (Figure 4: reaction 8)

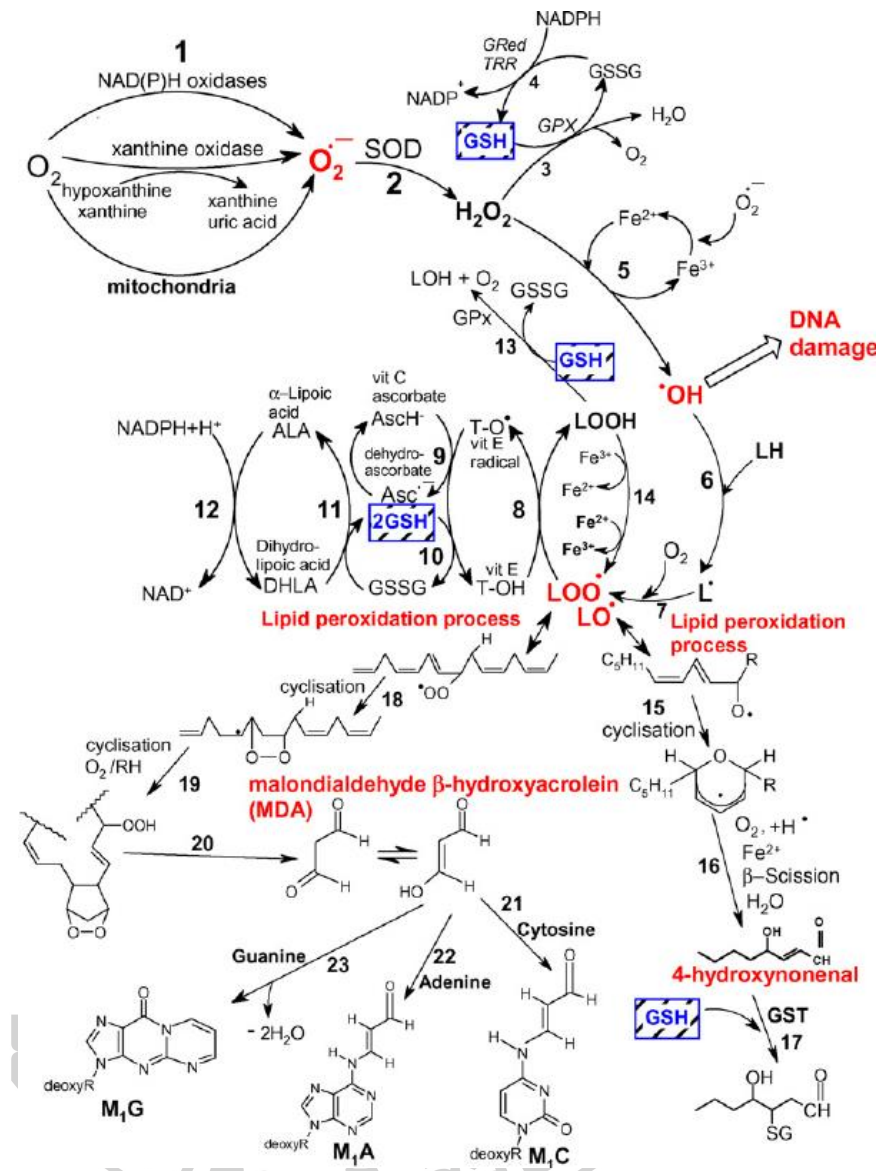


Figure 4 Pathways of ROS formation and redox balance

Reaction 1: The superoxide anion radical is formed by the process of reduction of molecular oxygen mediated by NADPH oxidases and xanthine oxidase or non-enzymatically by redox-reactive compounds such as the semi-ubiquinone compound of the mitochondrial electron transport chain.

Reaction 2: Superoxide radical is dismutated by the superoxide dismutase (SOD) to hydrogen peroxide.

Reaction 3: Hydrogen peroxide is most efficiently scavenged by the enzyme glutathione peroxidase (GPx) which requires GSH as the electron donor.

Reaction 4: The oxidized glutathione (GSSG) is reduced back to GSH by the enzyme glutathione reductase (GRed) which uses NADPH as the electron donor.

Reaction 5: Some transition metals (e.g.  $\text{Fe}^{2+}$ ,  $\text{Cu}^{+}$  and others) can breakdown hydrogen peroxide to the reactive hydroxyl radical (Fenton reaction).

Reaction 6: The hydroxyl radical can abstract an electron from polyunsaturated fatty acid (LH) to give rise to a carbon-centred lipid radical ( $\text{L}\cdot$ ).

Reaction 7: The lipid radical ( $L\bullet$ ) can further interact with molecular oxygen to give a lipid peroxy radical ( $LOO\bullet$ ). If the resulting lipid peroxy radical  $LOO\bullet$  is not reduced by antioxidants, the lipid peroxidation process occurs.

Reaction 8: The lipid peroxy radical ( $LOO\bullet$ ) is reduced within the membrane by the reduced form of Vitamin E (T-OH) resulting in the formation of a lipid hydroperoxide and a radical of Vitamin E (T-O $\bullet$ ).

Reaction 9: The regeneration of Vitamin E by Vitamin C: the Vitamin E radical (T-O $\bullet$ ) is reduced back to Vitamin E (T-OH) by ascorbic acid (the physiological form of ascorbate is ascorbate monoanion,  $AscH^-$ ) leaving behind the ascorbyl radical ( $Asc\bullet^-$ ).

Reaction 10: The regeneration of Vitamin E by GSH: the oxidized Vitamin E radical (T-O $\bullet$ ) is reduced by GSH.

Reaction 11: The oxidized glutathione (GSSG) and the ascorbyl radical ( $Asc\bullet^-$ ) are reduced back to GSH and ascorbate monoanion,  $AscH^-$ , respectively, by the dihydroliipoic acid (DHLA) which is itself converted to  $\alpha$ -lipoic acid (ALA).

Reaction 12: The regeneration of DHLA from ALA using NADPH.

Reaction 13: Lipid hydroperoxides are reduced to alcohols and dioxygen by GPx using GSH as the electron donor.

Reaction 14: Lipid hydroperoxides can react fast with  $Fe^{2+}$  to form lipid alkoxyl radicals ( $LO\bullet$ ), or much slower with  $Fe^{3+}$  to form lipid peroxy radicals ( $LOO\bullet$ ).

Reaction 15: Lipid alkoxyl radical ( $LO\bullet$ ) derived for example from arachidonic acid undergoes cyclisation reaction to form a six-membered ring hydroperoxide.

Reaction 16: Six-membered ring hydroperoxide undergoes further reactions (involving  $\beta$ -scission) to form 4-hydroxy-nonenal.

Reaction 17: 4-hydroxynonenal is rendered into an innocuous glutathyl adduct (GST, glutathione *S*-transferase).

Reaction 18: A peroxy radical located in the internal position of the fatty acid can react by cyclisation to produce a cyclic peroxide adjacent to a carbon-centred radical.

Reaction 19: This radical can then either be reduced to form a hydroperoxide (reaction not shown) or it can undergo a second cyclisation to form a bicyclic peroxide which after coupling to dioxygen and reduction yields a molecule structurally analogous to the endoperoxide.

Reaction 20: Formed compound is an intermediate product for the production of malondialdehyde.

Reactions 21: Malondialdehyde can react with DNA bases Cytosine to form adducts  $M_1C$ .

Reactions 22: Malondialdehyde can react with DNA bases Adenine to form adducts  $M_1A$ .

Reactions 23: Malondialdehyde can react with DNA bases Guanine to form adducts  $M_1G$ .

Source: Marian Valko et al., "Free radicals and antioxidants in normal physiological functions and human disease," **International Journal of Biochemistry & Cell Biology** 39, 1 (2007): 44-84.

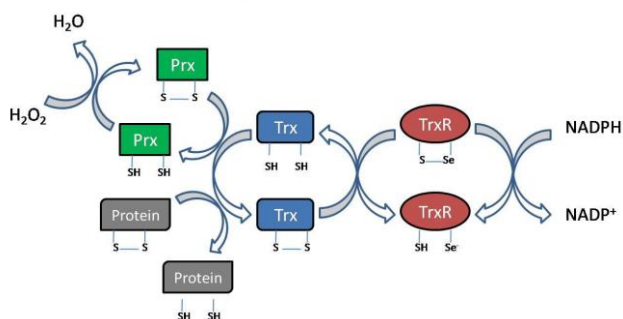


Figure 5 Mechanism of action of the thioredoxin (Trx) redox system

Source: Therese Christina Karlenius and Kathryn Fay Tonissen, "Thioredoxin and Cancer: A Role for thioredoxin in all states of tumor oxygenation," **Cancers** 2, 2 (June 2010): 209-232.

### 2.3.2 ROS-regulated physiological function

Physiological functions that involve free radical and their derivatives include regulation of production NO, regulation of cell adhesion, immune responses and vascular tone, sensing of oxygen tension and enhancing signal transduction from various membrane receptors [87]. Physiological function of ROS are shown in Table 10.

Table 10 Physiological functions of ROS

Physiological functions	Mechanism of action	References
Defense against environmental pathogens	Activated neutrophils and macrophages can produce superoxide radical and other derivatives via NADPH oxidase. When the microbial cells are engulfed into a phagosome, NADPH oxidase generates $O_2^-$ , while myeloperoxidase (MPO) generates HOCl, responsible for killing the microorganisms. (Figure 6)	[87, 89, 93, 94]
Regulation of production NO	Superoxide inactivate dimethylarginine dimethylaminohydrolase (DDAH), result in block metabolized asymmetric dimethylarginine (ADMA). The effect of ADMA is to block NO formation by NOS. (Figure 7)	[87, 95]
Biosynthesis thyroid hormones	Peroxidation reactions are important in physiological iodination of thyroid hormones, a reaction catalyzed by the thyroid peroxidase (TPO) using DUOX-derived $H_2O_2$ . $I^-$ is oxidized by the TPO- $H_2O_2$ system and is then used to iodinate tyrosyl residues in thyroglobulin (Tg), forming MIT and DIT. $H_2O_2$ is generated by the DUOX. T4 and T3 are produced by coupling of iodinated tyrosyl intermediates, which are then endocytosed, hydrolysed in lysosomes and secreted into the bloodstream (Figure 8)	[87, 96]

Table 10 Physiological functions of ROS (continued)

Physiological functions	Mechanism of action	References
Regulation of cell adhesion	Adhesion molecules are induced by ROS. During neutrophil migration, clustering of ICAM-1 activated Rac, which induces intracellular ROS generation by NOX. Increased ROS enhances the expression of P-selectin on the endothelium. In addition, ROS is activated NF-kB, which induces ICAM-1, VCAM-1, and E-selectin expression. Adhesion molecules enhances neutrophil binding on the endothelium and increases paracellular migration. (Figure 9)	[89, 94, 97]
Regulation immune response	ROS are activated T lymphocytes. Superoxide radical and hydrogen peroxide induced production of interleukin-2 (IL-2).	[89, 94]
Sensing of oxygen tension	Change in oxygen tension are sensed by changes in ROS production. Normal conditions, O <sub>2</sub> and its cofactor $\alpha$ -ketoglutarate ( $\alpha$ KG), HIF-prolyl hydroxylase 2 (HIF-PH2) hydroxylates at specific prolines proline residues in HIF-1 $\alpha$ , then hydroxylated HIF-1 $\alpha$ is ubiquitylated by the E3 ligase von Hippel-Lindau tumour-suppressor protein (VHL) and is subsequently degraded by the proteasome. Under hypoxic conditions, this process is inhibited leading to stabilization of the HIF protein. (Figure 10)	[86, 87, 89, 94]



Table 10 Physiological functions of ROS (continued)

Physiological functions	Mechanism of action	References
Regulation of vascular tone	The enzyme soluble guanylate cyclase (sGC) is activated radical. Guanylate cyclase catalyses the formation of cyclic guanosine monophosphate (cGMP), which modulates the function of protein kinases, ion channels, and regulation of smooth muscle tone and inhibition of platelet adhesion. (Figure 11)	[89, 94, 98]
Induced apoptosis	Intracellular cell damage induced Bcl-2 (a protein located in the outer membranes of mitochondria) to activate a related protein, Bax, causing mitochondria released cytochrome <i>c</i> . Cytochrome <i>c</i> binds to the protein apoptotic protease activating factor-1 (Apaf-1), followed by aggregation of these complexes to form apoptosomes which bind to and activate one of the proteases, caspase-9. Cleaved caspase-9 leads finally to digestion of structural proteins in the cytoplasm, degradation of DNA and phagocytosis of the cell.	[87, 89]
Enhance signal transduction	ROS play an important physiological role as secondary Messengers, which may act on different levels in the signal transduction cascade. Signaling of ROS may occur through activation of MAPK. MAPK activation occurs through ROS-dependent inhibition of protein tyrosine phosphatase (PTP). (Figure 12)	[87, 89]

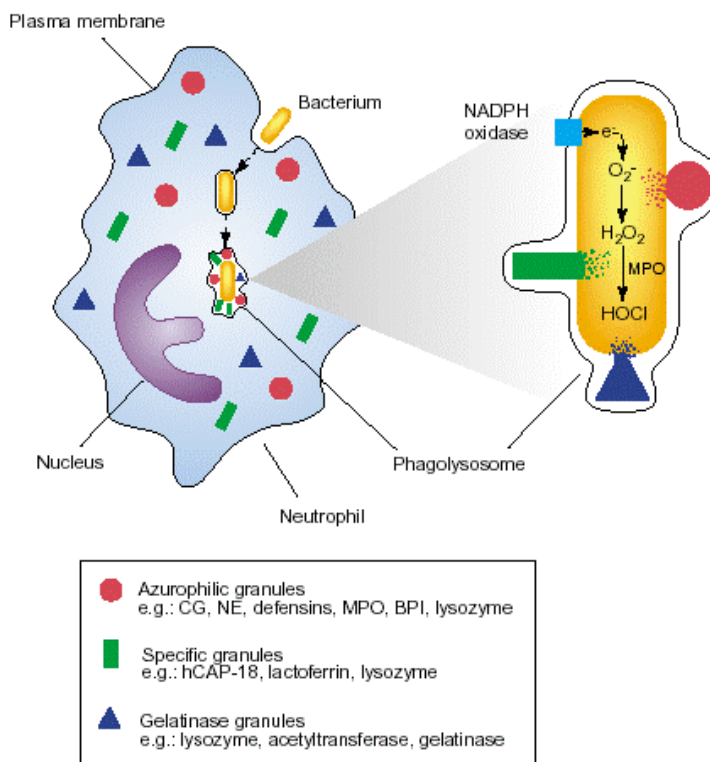


Figure 6 Antimicrobial host defense on ROS generation by macrophages and neutrophils

Source: Petra Averhoff, “Characterization of the specificity of human neutrophil elastase for *Shigella flexneri* virulence factors,” (Master degree dissertation, Humboldt-Universität zu Berlin, 2006).

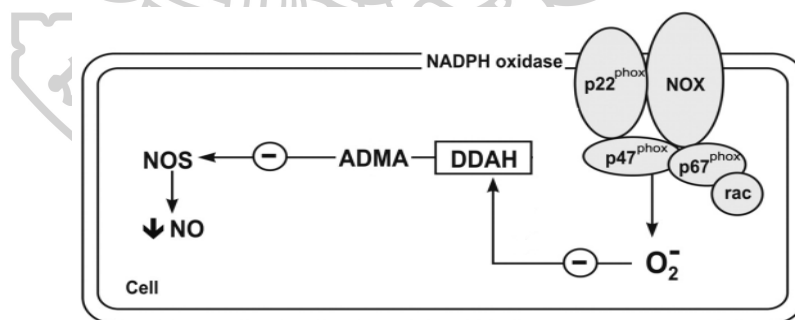


Figure 7 ROS cross-talk with NO system

Source: Fredrik Palm et al., “Dimethylarginine dimethylaminohydrolase (DDAH): expression, regulation, and function in the cardiovascular and renal systems,” **American Journal of Physiology - Heart and Circulatory Physiology** 293, 6 (December 2007): H3227-H3245.

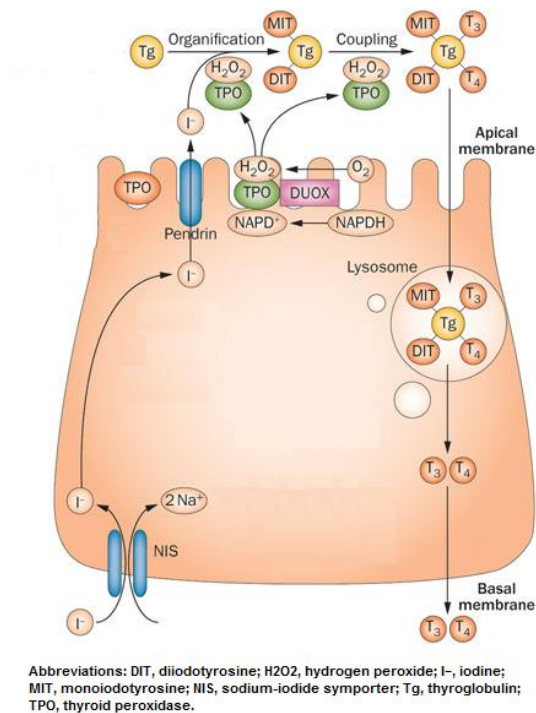


Figure 8 ROS-mediated thyroid hormone synthesis in thyrocytes

Source: Giovanni Vitale, Stefano Salvioli, and Claudio Franceschi, "Oxidative stress and the ageing endocrine system," *Nature Reviews Endocrinology* 9, 4 (April 2013): 228-240.

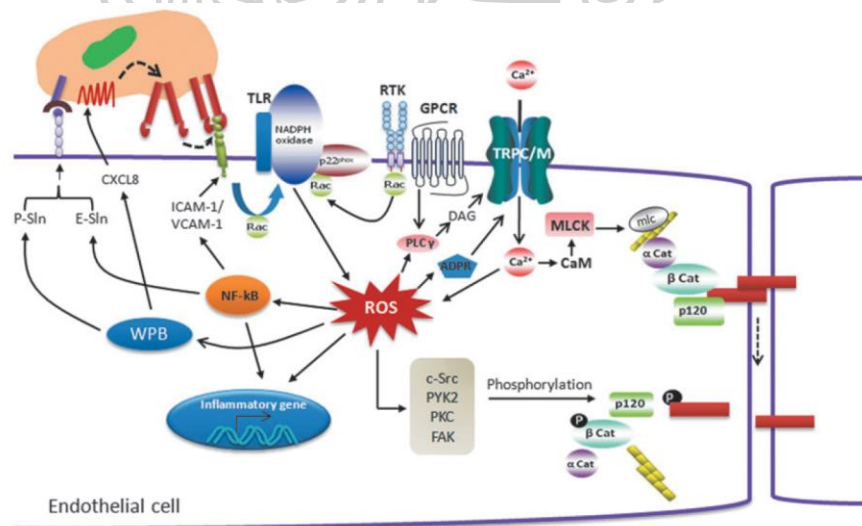


Figure 9 Signaling mechanisms of ROS-mediated increase in leukocyte migration

Source: Manish Mittal et al., "Reactive oxygen species in inflammation and tissue injury," *Antioxidants & Redox Signaling* 20, 7 (March 2014): 1126-1167.

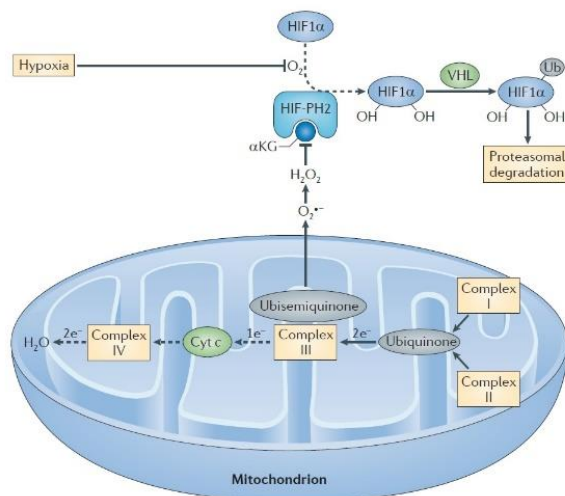


Figure 10 Regulation of HIF-1 $\alpha$  by ROS production during hypoxia

Source: Carl Nathan and Amy Cunningham-Bussel, "Beyond oxidative stress: an immunologist's guide to reactive oxygen species," *Nature Reviews Immunology* 13 (May 2013): 349-361.

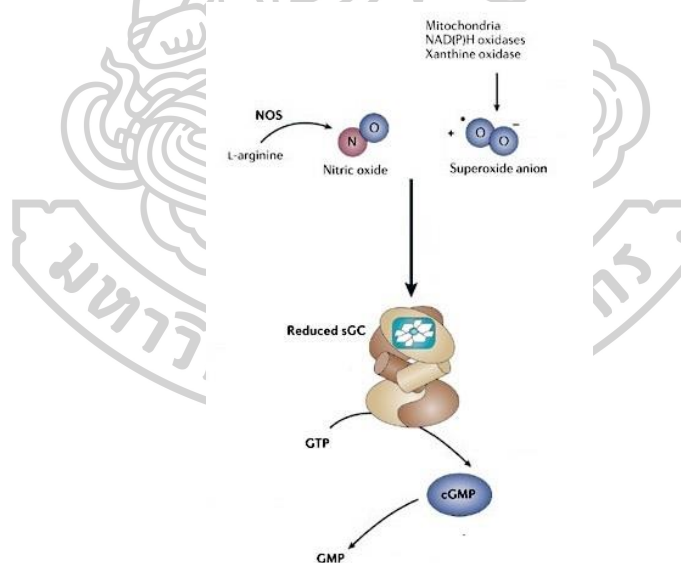


Figure 11 NOS-sGC-cGMP signal transduction pathway

Source: Oleg V. Evgenov et al., "NO-independent stimulators and activators of soluble guanylate cyclase: discovery and therapeutic potential," *Nature Reviews Drug Discovery* 5, 9 (September 2006): 755-768.

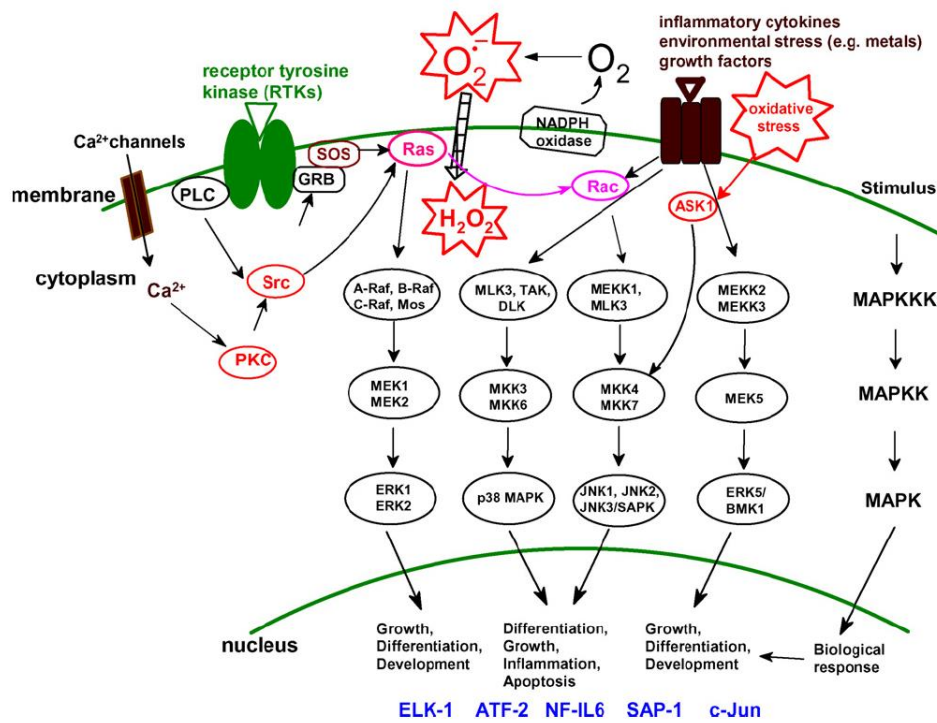


Figure 12 ROS-induced MAPK signaling pathways

Source: Marian Valko et al., "Free radicals and antioxidants in normal physiological functions and human disease," *International Journal of Biochemistry & Cell Biology* 39, 1 (2007): 44-84.

### 2.3.3 ROS-induced pathophysiology

ROS overproduction or insufficient antioxidant induced oxidative stress, resulting in cellular damage. Oxidative stress has been linked to various diseases involving cardiovascular disease, cancer, neurological disorder, diabetes, central nervous system (CVS) disorder and other diseases. Pathophysiological implications of altered redox regulation are shown in Table 11.

Table 11 Pathophysiological implications of altered redox regulation

Organ system	Diseases	Mechanism of action	References
Cardiovascular disease	Atherosclerosis	<ul style="list-style-type: none"> <li>- Superoxide production mediated endothelial dysfunction</li> <li>- Increased oxidized low-density lipoprotein (oxLDL)</li> <li>- ROS induced expression of ICAM-1</li> </ul>	[87, 89, 94, 99]
	Ischemic heart disease	<ul style="list-style-type: none"> <li>- Ischemia injury driven by ROS formation</li> </ul>	
	Hypertension	<ul style="list-style-type: none"> <li>- Vascular smooth muscle cell proliferation induced by ROS</li> <li>- Promoted oxidant production via NADH/NADPH oxidase</li> <li>- Superoxide production mediated endothelial dysfunction</li> </ul>	
	Congestive heart failure	<ul style="list-style-type: none"> <li>- Increased NO production induces cardiac dysfunction</li> <li>- Cytokine-derived ROS induced cardiac apoptosis</li> </ul>	
	Pulmonary hypertension	<ul style="list-style-type: none"> <li>- ROS activated NF-kB, MAPK and cell proliferation</li> </ul>	
Lung and airways	Pulmonary fibrosis	<ul style="list-style-type: none"> <li>- ROS induced myofibroblast differentiation and matrix synthesis</li> </ul>	[87]
	Renal hypertrophy	<ul style="list-style-type: none"> <li>- ROS activated Akt/PKB, ERK1/2</li> </ul>	

Table 11 Pathophysiological implications of altered redox regulation (continued)

Organ system	Diseases	Mechanism of action	References
Central nervous system	Alzheimer	- ROS enhanced iron induced lipid peroxidation	[87, 89, 94]
	Parkinson	- H <sub>2</sub> O <sub>2</sub> was converted to highly reactive HO <sup>•</sup> which was extremely toxic and caused damage to dopaminergic neurons - ROS enhanced iron induced lipid peroxidation	
	Demyelinating disease	- Reaction of O <sub>2</sub> <sup>•-</sup> with NO generated peroxynitrite (ONOO <sup>-</sup> ), that highly ROS and thereby damaged oligodendrites	
Endocrinology	Diabetes	- ROS activated JNK pathway in pancreatic $\beta$ -cells, which led to reduction of pancreatic and duodenal homeobox-1 (PDX-1) activity and suppression of insulin - ROS activated JNK pathway, which development of insulin resistance - ROS decreased intracellular GSH	[87, 89, 94, 100]
	Hepatocytes apoptosis	- ROS activated JNKs pathway	
	Hepatic fibrosis	- ROS induced cell proliferation and accumulation of extracellular matrix proteins	
Liver			[87]

Table 11 Pathophysiological implications of altered redox regulation (continued)

Organ system	Diseases	Mechanism of action	References
Musculoskeletal system	Rheumatoid arthritis	<ul style="list-style-type: none"> <li>- ROS damaged cellular element in cartilage and components of the extracellular matrix and reduced the sulfation of newly synthesized glycosaminoglycans</li> <li>- Decreased intracellular GSH level, impaired phosphorylation of the adaptor protein linker for T-cell activation</li> </ul>	[87, 89, 94, 101]
	Osteoporosis	<ul style="list-style-type: none"> <li>- ROS enhanced osteoclast activity through p38/MAPK activation</li> </ul>	
Cancer	Various cancer cells	<ul style="list-style-type: none"> <li>- ROS interfered the expression of a number of genes and signal transduction</li> <li>- ROS increased expression of growth factor receptor such as VEGF, EGF</li> </ul>	[89]
	Psoriasis	<ul style="list-style-type: none"> <li>- Increased iNOS expression in keratinocytes</li> </ul>	
Skin	Pyoderma gangrenosum	<ul style="list-style-type: none"> <li>- ROS activated neutrophil induce cutaneous tissue injury</li> <li>- ROS increased expression of adhesion molecules and activated NF-kB</li> </ul>	[87, 102]



### 2.3.4 Detection of ROS

ROS short lifetime makes them difficult to detect. Therefore, it is essential to develop methodologies capable of overcoming this problem. Fluorescent probes are excellent sensors of ROS due to their high sensitivity and simplicity in data collection [103]. Fluorescence probes for detection of ROS are shown in Table 12. [103-105]

Table 12 Fluorescence probes for detection ROS

Probe	ROS detected	Advantages	Disadvantages
Hydroethidine (HE) (Figure 13)	- Reacts with $O_2^{\cdot-}$ to form 2-OH-E+ - Reacts with other oxidants ( $\cdot OH$ , ONOO $^-$ ) to form E+ and dimers	Generates specific product	2-OH-E+ can only be distinguished from E+ by HPLC- based methods
2,7'-dichlorofluorescein diacetate (H <sub>2</sub> DCFDA) (Figure 14)	H <sub>2</sub> O <sub>2</sub> , HO $^\cdot$ , ROO $^\cdot$	- Cell permeable - Easy to use - Highly fluorescent	Redox-cycling
Amplex red (Figure 15)	O <sub>2</sub> $^{\cdot-}$ , H <sub>2</sub> O <sub>2</sub>	- Measuring extracellular - Highly fluorescent	Horseshoe peroxidase dependent
Dihydrorhodamine (DHR) (Figure 16)	H <sub>2</sub> O <sub>2</sub> , HOCl, ONOO $^-$	- Cell permeable - Easy to use	Redox-cycling
Pentafluorobenzenesulfonyl fluorescein (Figure 17)	O <sub>2</sub> $^{\cdot-}$ , H <sub>2</sub> O <sub>2</sub> , $\cdot OH$ , ONOO $^-$	Not dependent on peroxidase	Non specific

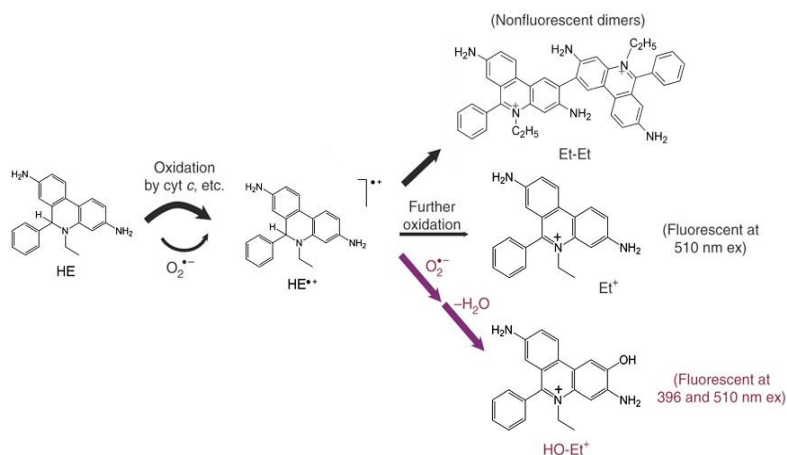


Figure 13 Oxidation of hydroethidine (HE)

Modified from: Balaraman Kalyanaraman et al., "Measuring reactive oxygen and nitrogen species with fluorescent probes: challenges and limitations," **Free Radical Biology and Medicine** 52, 1 (January 2012): 1-6.

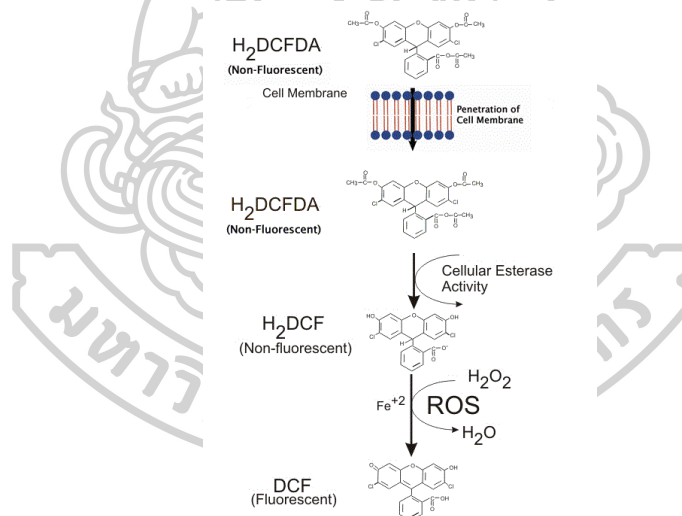


Figure 14 Formation of fluorescent compound DCF by ROS

Modified from: Balaraman Kalyanaraman et al., "Measuring reactive oxygen and nitrogen species with fluorescent probes: challenges and limitations," **Free Radical Biology and Medicine** 52, 1 (January 2012): 1-6.

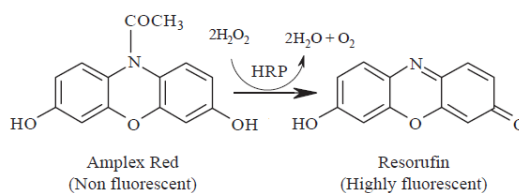


Figure 15 Horseradish peroxidase (HRP)-catalyzed amplex red oxidation by  $\text{H}_2\text{O}_2$

Source: Ana Gomes, Eduarda Fernandes, and Jose' L.F.C Lima, "Fluorescence probes used for detection of reactive oxygen species," **Journal of Biochemical and Biophysical Methods** 65: (October 2005): 45-80.

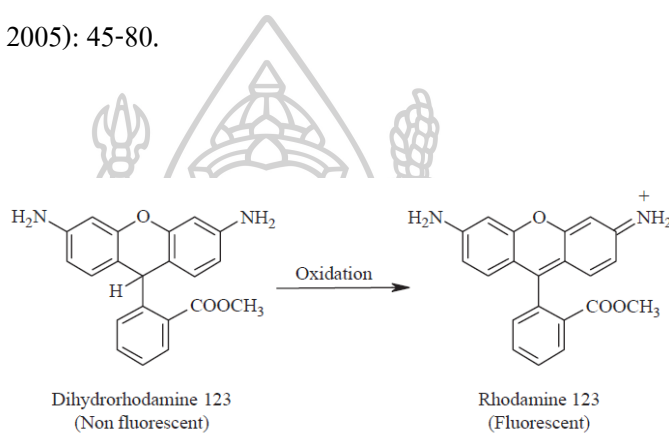


Figure 16 Oxidation of dihydrorhodamine to rhodamine

Source: Ana Gomes, Eduarda Fernandes, and Jose' L.F.C Lima, "Fluorescence probes used for detection of reactive oxygen species," **Journal of Biochemical and Biophysical Methods** 65: (October 2005): 45-80.

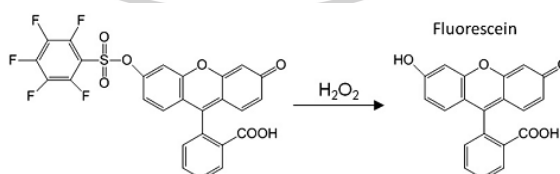


Figure 17 Reaction of  $\text{H}_2\text{O}_2$  with pentafluorobenzenesulfonyl fluorescein

Source: Ghassan J. Maghzal et al., "Detection of reactive oxygen species derived from the family of NOX NADPH oxidases," **Free Radical Biology and Medicine** 53 (September 2012): 1903-1908

## 2.4 Skin

Skin is the largest organ of the body, accounting for approximately 16% of total body weight, with a surface area of 1.8 m<sup>2</sup> [106]. Skin varies in thickness according to function and geographic location on the anatomy of the body, it is generally 1-2 mm thick [107].

### 2.4.1 Structure of skin

Skin is composed of three layers: the epidermis, the dermis, and subcutaneous tissue. The cross-section of human skin is shown in Figure 18 [107]. Hair, sebaceous, and sweat glands are regarded as derivatives of skin. Skin is a dynamic organ in a constant state of change, as cells of the outer layers are continuously shed and replaced by inner cells moving up to the surface [106].

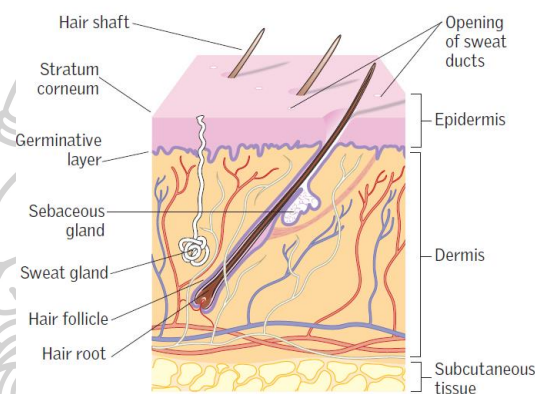


Figure 18 The cross-section of human skin

Source: Ella McLafferty, Charles Hendry, and Alistair Farley, "The integumentary system: anatomy, physiology and function of skin," **Nursing Standard** 27, 3 (September 2012): 35-42.

#### 2.4.1.1 Epidermis

The outer layer, epidermis, is stratified squamous epithelium, serving as the physical and chemical barrier between the interior body and exterior environment. The epidermis, consists of four main types of cells, most of which are keratinocytes, which function to synthesize keratin. Melanocyte cells are responsible for producing the pigment, melanin. Langerhans cells are involved in the immune response and merkel cells function in the sensation of touch. Protein bridges called desmosomes connect the keratinocytes, which are in a constant state of transition from the deeper layers to the superficial. The four separate layers of the epidermis are formed by the differing stages of keratin maturation and their movement from the stratum basale up to the stratum corneum. From

the inside layers upwards to the surface, the four layers of the epidermis are stratum basale (basal or germinativum cell layer), stratum spinosum (spinous or prickly cell layer), stratum granulosum (granular cell layer) and stratum corneum (horny layer) as shown in Figure 19. The lower three layers that constitute the living, the basal cells of the epidermis undergo proliferation cycles that provide for the renewal of the outer epidermis. In addition, the stratum lucidum is a thin layer of translucent cells seen in thick epidermis (finger tips, palms and soles) [107]. The epidermis also secretes a variety of chemokines, cytokine, growth factors, etc., for cellular communication within the epidermis as well as with dermal cells (fibroblasts, mast cells).

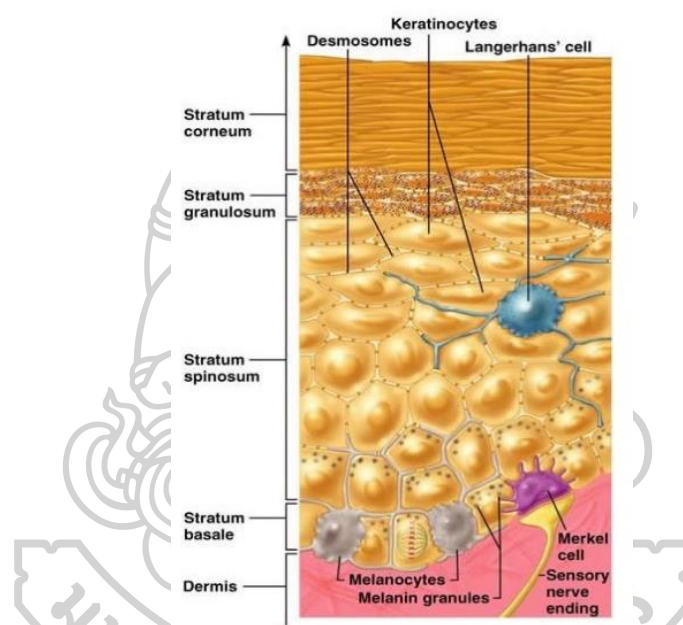


Figure 19 Structure of epidermis

Source: 2006 Pearson Education, Inc., publishing as Benjamin Cummings.

Keratinocytes are primary sensors of stressful conditions as well as participating in the immune response of the skin. Therefore cultured keratinocytes have become a prototype model for screening anti-inflammatory, photo-protective, and cancer preventive substances for topical application. The immortalized human keratinocyte cell line, HaCaT cell, presents a valuable tool for in vitro mechanistic and pharmacological assessment of cosmeceuticals or pharmaceuticals. The characteristics of the HaCaT cell line derived from spontaneously-transformed, immortal human epithelial cell culture from adult skin, which maintained normal keratinocyte morphology, epidermal differentiation capacity and remained non-tumorigenic [2].

### **2.4.1.2 Dermis**

The middle layer, the dermis, is responsible for providing nutrients and physical support to the epidermis. It is fundamentally made up of the fibrillar structural protein known as collagen. The primary cell type in the dermis are fibroblasts, which produce collagen, the extracellular structural proteins, elastin and structural proteoglycans. Other cell in dermis are immunocompetent mast cells and macrophages. Two layers comprise the dermis are thin papillary layer and thicker reticular layer. A superficial papillary dermis lies below and connects with the epidermis appears as a loose network of connective tissue. It contains the nerves and thin loosely arranged collagen fibres that nourish the epidermis. Collagen fibres make up 70% of the dermis, giving it strength and toughness. Elastin maintains normal elasticity and flexibility while proteoglycans provide viscosity and hydration [106]. Embedded within the fibrous tissue of the dermis are the dermal vasculature, lymphatics, nervous cells and fibres, sweat glands, hair roots and small quantities of striated muscle [108]. The dermis protects the body from mechanical injury, binds water, aids in thermal regulation, and includes receptors of sensory stimuli [106].

### **2.4.1.3 Hypodermis**

The subcutis or hypodermis which is made up of loose connective tissue and fat. It contains small lobes of fat cells known as lipocyte. Hypodermis performs many vital functions, including protection against external physical, chemical, and biologic assailants, as well as prevention of excess water loss from the body and a role in thermoregulation [108]. On the other hand hormone conversion takes place in this layer, converting androstenedione into estrone by aromatase. Lipocytes produce leptin, a hormone that regulates body weight by way of the hypothalamus [109].

## **2.4.2 Function of skin**

Skin has several functions, the most important of which is to form a physical barrier to the environment, against micro-organisms, ultraviolet radiation and toxic agents. As well acting as a physical barrier, skin also plays an important immunological role. It normally contains all the elements of cellular immunity, with the exception of B cells [107]. Immune components of the skin are shown in Table 13. Melanocytes, located in the basal layer, and melanin have important roles in the skin's barrier function by preventing damage by UV radiation. Melanin absorbs UV radiation, thus protecting the cell's nuclei from DNA damage [106].

Skin is also provided with an abundant blood supply, which aids in thermoregulation for body temperature to remain constant to maintain homeostasis. When the skin is reacted to external stimuli such as cold, heat, pain, touch and pressure, the receptors in the skin monitor temperature and transmit impulses to hypothalamus, is the region that controls body temperature, thirst, hunger and other homeostatic systems. Thermoregulatory mechanisms occurring in the skin include insulation, sweating and control of blood flow. The body is insulated by subcutaneous adipose tissue, which is found under the dermis. Eccrine sweat glands are stimulated to produce sweat when the core temperature rises above 37°C. Sweat, in turn, cools the body through the process of evaporation.

Vitamin D is synthesized by the skin as a consequence of the exposure of the skin to UV light. Vitamin D is necessary for controlling the amount of calcium and phosphorus that is absorbed through the small intestine and mobilized from the bone [107].

Other function of skin includes sensation, allowing and limiting the inward and outward passage of water, electrolytes and various substances, which helps to maintain the elasticity of the skin and has a role in the body's fluid and electrolyte balance [106, 107].

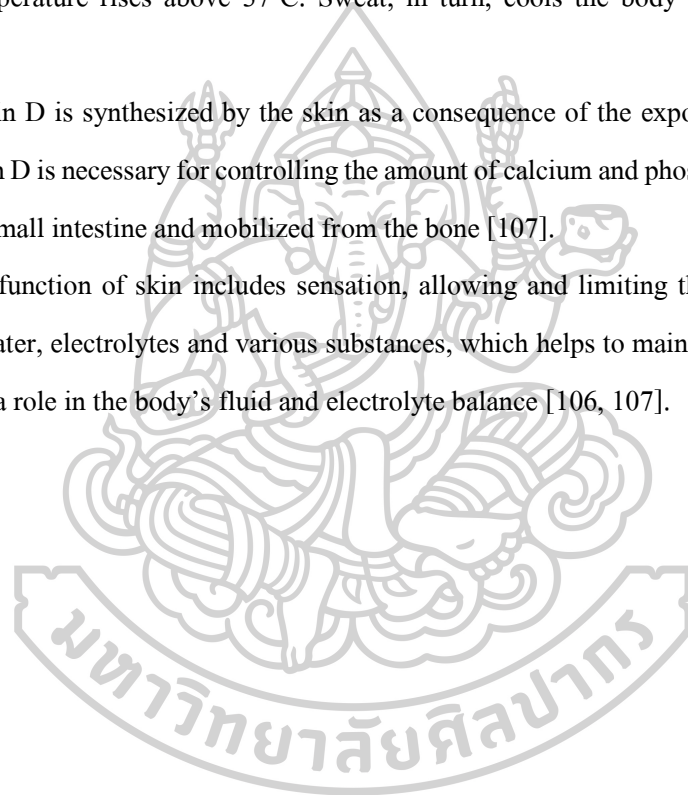


Table 13 Immune components of the skin.

Defense type	Component	Immune action
Structural	Skin	Impenetrable physical barrier to most external organisms
	Blood and lymphatic vessels	Provision of transport network for cellular defense
Cellular	Langerhans cells	Antigen presentation
	T lymphocytes	Facilitate immune reactions. Self-regulating through the action of T suppressor cells
	Mast cells	Facilitate inflammatory skin reactions
	Keratinocytes	Secrete inflammatory cytokines; have ability to express surface immune reactive molecules.
Systemic	Cytokines	Cell mediation chemicals produced by components of the cellular defense system.
	Eicosanoids	Non-specific inflammatory mediators produced by mast cells, macrophages and keratinocytes.
	Adhesion molecules	Increase the number of cellular defense facilitators in an area by binding to T cells.
	Complement cascade	Activation of this initiates a host of destructive mechanisms, including opsonization, lysis, chemotaxis and mast cell degranulation.
Immunogenetic	Major histocompatibility complex (MHC)	Enables immunological recognition of antigens.



### 2.4.3 ROS-mediated skin inflammation

The primary function of skin is to form a physical and chemical barrier to the external environment, against injurious insults. Harmful stimuli such as micro-organisms, ultraviolet radiation, toxic agents or irritants evoke a complex response known as inflammation. Inflammation is an essential response in the protection against injurious insults. The five classical signs of acute inflammation are pain, heat, redness, swelling, and functional loss. These signs can be explained by the different phases that the inflammatory response generally follows dilation of capillaries to increase blood flow, vasopermeabilization, leukocyte recruitment elimination of pathogens or injurious stimuli and resolution of inflammation [85]. At the molecular level, stimuli triggers generated ROS through the oxidative burst in infiltrating leukocytes at the site of inflammation [110].

Cytokines are key modulators of inflammation, participating in acute and chronic inflammation. Key pro-inflammatory cytokines include IL-1, IL-6 and TNF- $\alpha$  and pro-inflammatory chemokine, IL-8. TNF- $\alpha$  is the prototypic member of the TNF superfamily of type II transmembrane proteins with diverse functions in cell differentiation, inflammation, immunity and apoptosis. TNF- $\alpha$  is primarily secreted from activated macrophages, although it may be secreted by other cell types including monocytes, T cells, mast cells, natural killer cells (NK cells), keratinocytes, fibroblasts and neurons. It is a potent inflammatory mediator that is central to the inflammatory action of the innate immune system, including induction of cytokine production, activation or expression of adhesion molecules, and growth stimulation. Indeed, it has been shown to be one of the most important and pleiotropic cytokines mediating inflammatory and immune responses [111]. IL-8, also known as CXCL8, is one of the most widely studied chemokines and is a critical inflammatory mediator. IL-8 is a member of the CXC primary inflammatory cytokine produced by many cells such as monocytes/macrophages, T cells, neutrophils, endothelial cells, keratinocytes, fibroblasts and melanocytes. In many cell types, the synthesis of IL-8 is strongly stimulated by lipopolysaccharides, IL-1 and TNF- $\alpha$ . However, ionizing radiation, phytohemagglutinin, concanavalin A, double-stranded RNA, phorbol esters, and viruses may also function as inducers of IL-8 expression [112]. The main role of IL-8 in inflammation is in the recruitment of neutrophils, although it is responsible for the chemotactic

migration and activation of monocytes, lymphocytes, basophils, and eosinophils at sites of inflammation [111].

Inflammation in the skin results in the appearance of macrophages and other leucocytes. As a result of oxidative stress stimulated ROS generation during the pathogenesis of skin inflammation, ROS can cause DNA strand break as well as lipid peroxidation, membrane and protein damage [113] and a number of signaling pathways are activated. Inflammation response in skin is shown in Figure 20. ROS enhances the phosphorylation of inhibitor of NF- $\kappa$ B (I $\kappa$ B), led to the ubiquitylation of I $\kappa$ B and its subsequent degradation by the proteasome. NF- $\kappa$ B is then released and translocates to the nucleus to initiate transcription [86]. TNF- $\alpha$ , IL-1, IL-6, IL-8, and iNOS, which coordinate inflammatory responses [102]. ROS drive activation of MAPKs, the most important of which are ERK, JNK, and p38 kinases. ERK and JNK are important in recruiting c-Fos and c-Jun to the nucleus where they activate the transcription factor AP-1, which subsequently regulates genes in the pathogenesis of inflammation (such as iNOS, COX-2), whereas activation of p38 is important in the transcriptional activation of NF- $\kappa$ B and AP-1 [110].

Oxidative stress leads directly to keratinocyte activation, with release of IL-1 and TNF- $\alpha$ . Secretion of IL-1 and TNF- $\alpha$  results in activation of endothelial cells, production of the surface leucocyte adhesion ligands ICAM-1, E-selectin and VCAM-1 [114]. IL-1 induces mast cells to express prostaglandins. Prostaglandins and histamine released from the mast cells can induce vasodilation, which assists leucocytes entering to the site of inflammation [113]. IL-8 and IL-6 are concomitantly secreted by keratinocytes [112]. IL-8 assists leucocytes, primarily neutrophils, from surrounding blood vessels in migration into the inflammation region, while IL-6 can trigger the activation of monocytes and other infiltrating leucocytes to secrete cytokines and chemokines [113].

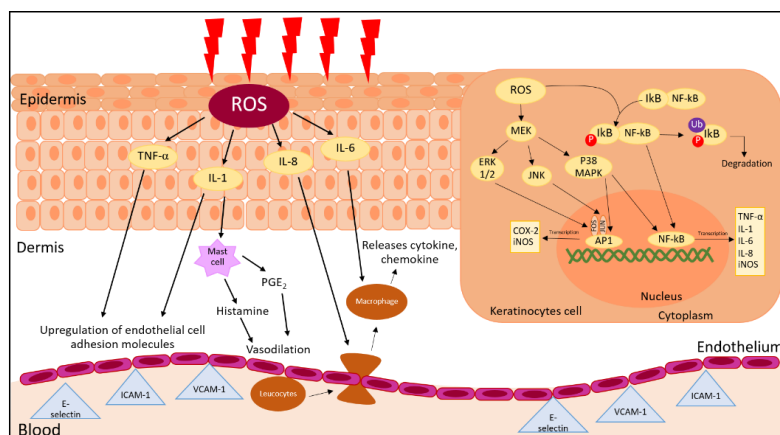


Figure 20 Inflammation response in the skin

#### 2.4.4 Antioxidant and redox balance in skin

Free radicals are formed in skin following exposure to environmental stimuli and immune reactions. Under physiological conditions, ROS buildup in the skin is limited by numerous antioxidant defense systems, including both non-enzymatic and enzymatic antioxidants, thereby maintaining physiological homeostasis. The antioxidant defense system in skin is mainly comprised of the abundantly expressed antioxidant enzymes SOD, catalase, GPx and Prx. SOD catalyzes the conversion of  $O_2^{\cdot -}$  radicals into  $H_2O_2$  using NADPH as a cofactor. Excessive amounts of  $H_2O_2$  are harmful to cells and their rapid scavenging by either catalase, Prx or by GPx and the glutathione system that reduces the  $H_2O_2$  to oxygen and water. Besides the classical ROS-detoxifying enzymes, the heme oxygenase (HO) system also exhibits potent antioxidant functions. HO enzymes catalyze the degradation of heme into CO, iron, and biliverdin. Biliverdin is rapidly converted to bilirubin by biliverdin reductase. Both biliverdin and bilirubin are strong antioxidants. Ferrous iron ( $Fe^{2+}$ ) is released during heme degradation. It can participate in ROS-generating Fenton reaction, leading to cellular damage. Ferritin is a ubiquitous iron-binding protein that can accommodate iron atoms. In contrast, non-enzymatic antioxidants molecules include GSH, vitamin E and vitamin C. GSH and vitamin C are soluble antioxidants, whereas vitamin E is membrane-bound and capable of intercepting free radical-mediated chain reactions [110]. Furthermore, the efficiency of the dietary non-enzymatic antioxidants depends on bioavailability as well as conversion into the active form upon ingestion and antioxidant enzymes may therefore confer more efficient protection against acute oxidative and inflammatory stress [85].

## CHAPTER 3

### MATERIALS AND METHODS

#### 3.1 Materials

#### 3.2 Equipment

#### 3.3 Method

##### 3.3.1 Quantitative analysis of rhein in *C. alata* leaves extract by HPLC

###### 3.3.1.1 Standard preparation

###### 3.3.1.2 Sample preparation

###### 3.3.1.3 Method validation

###### 3.3.1.3.1 Calibration curve

###### 3.3.1.3.2 Accuracy

###### 3.3.1.3.3 Precision

###### 3.3.1.3.4 Specificity

###### 3.3.1.4 Determination of rhein content

##### 3.3.2 Determination of cell viability

###### 3.3.2.1 Rhein standard preparation

###### 3.3.2.2 *C. alata* leaves extract preparation

###### 3.3.2.3 Cell viability determination

##### 3.3.3 Measurement of ROS production

##### 3.3.4 Measurement of inflammatory cytokines production by ELISA

###### 3.3.4.1 ELISA for TNF- $\alpha$

###### 3.3.4.2 ELISA for IL-8

##### 3.3.5 Data analysis

### 3.1 Materials

- 3.1.1 0.05% Trypsin-EDTA (1X) (Lot. No.1300240, Gibco)
- 3.1.2 0.05% Trypsin-EDTA (1X) (Lot. No.CP15-1034, Capricorn scientific)
- 3.1.3 0.25% Trypsin-EDTA (1X) (Lot. No.1546270, Lot. No.1606137, Gibco)
- 3.1.4 2,7'-dichlorofluorescein diacetate (Lot. No. 869447, Invitrogen)
- 3.1.5 Acetic acid HPLC grade (Lot. No. K45094483 345, Merck)
- 3.1.6 Amphotericin B solution tissue culture grade (Lot. No. 3085C249, Amresco)
- 3.1.7 Bovine Serum Albumin fraction V (Lot. No. K00115-0193, GE healthcare)
- 3.1.8 Dimethyl sulfoxide (Lot. No. 1307ACG2013, Bio basic)
- 3.1.9 Dimethyl sulfoxide (Lot. No. I7010-15, Vivantis)
- 3.1.10 Dulbecco's Modified Eagle Medium 1X (Lot. No. 1439934, Gibco)
- 3.1.11 Dulbecco's Modified Eagle Medium powder (Lot. No. 1606694, Gibco)
- 3.1.12 Dulbecco's Phosphate Buffered Saline 10X (Lot. No.CP14-1205, Capricorn scientific)
- 3.1.13 Dulbecco's Phosphate Buffered Saline 1X (Lot. No.1508021, Gibco)
- 3.1.14 *C. alata* leaves extract from Associate Professor Dr. Penpun Wetwitayaklung from Silpakorn University
- 3.1.15 Ethanol (Lot. No. K45094483 345, Merck)
- 3.1.16 Fetal Bovine Serum (Lot. No. A15112-1066, GE healthcare)
- 3.1.17 Fetal Bovine Serum (Lot. No.41Q1337K, Gibco)
- 3.1.18 HaCaT cells from Dr. Tamaki Okabayashi from MOCID, FTM, Mahidol University, and RIMD, Osaka University
- 3.1.19 Hank's Balanced Salt Solution 1X (Lot. No.1491037, Lot. No.1606163, Gibco)
- 3.1.20 Hank's Balanced Salt Solution 1X (Lot. No.H00912-2718, PAA Laboratories)
- 3.1.21 Hank's Balanced Salt Solution 1X (Lot. No.CP13-1021, Capricorn scientific)
- 3.1.22 Human TNF- $\alpha$  Screening set (Lot. No. 1720163A, Thermo scientific)
- 3.1.23 Human IL-8 Screening set (Lot. No. LH119932, Thermo scientific)
- 3.1.24 Hydrochloric acid, 1.0 N (Lot. No.14010201, RCI Labscan)
- 3.1.25 Methanol HPLC grade (Lot. No.04030189, Labscan)
- 3.1.26 MTT (Lot. No. 1210DU33563, Bio basic)

- 3.1.27 Penicillin-Streptomycin (Lot. No.1546632, Lot. No. 1582954, Lot. No. 1665608, Lot. No. 1697545, Gibco)
- 3.1.28 Phosphate Buffered Saline 10X (Lot. No.1535896, Gibco)
- 3.1.29 Rhein (Lot. No. SLBC4285V, Sigma)
- 3.1.30 Sodium hydrogen carbonate (Lot. No.13030055, RCI Labscan)
- 3.1.31 Sodium hydroxide, 1.0 N (Lot. No.14010433, RCI Labscan)
- 3.1.32 Sucrose analytical grade (Lot. No. AF701056, Ajax Finechem)
- 3.1.33 *tert*-Butyl hydroperoxide (Lot. No.BCBC4509, Sigma-Aldrich)
- 3.1.34 Tween 20 biotech grade (Lot. No. E7009-15, Vivantis)

### 3.2 Equipment

- 3.2.1 เครื่องอบใบหุ้มเห็ดเทศ
- 3.2.2 Grinder (LG-500A, Baixin, China)
- 3.2.3 หม้ออังไอน้ำ
- 3.2.4 Whatman filter paper no.1
- 3.2.5 Analytical balance (Model CP224S, Sartorius, Germany)
- 3.2.6 High performance liquid chromatography (HPLC) Model 1100 series (Agilent, Germany) consists of the following
  - 3.2.6.1 Degasser (G1322A, Agilent, Germany)
  - 3.2.6.2 Liquid chromatography pump (G1311A, Agilent, Germany)
  - 3.2.6.3 Autosample (G1313A, Agilent, Germany)
  - 3.2.6.4 Diode array detector (G1315B, Agilent, Germany)
  - 3.2.6.5 Software chrom quest (Agilent, Germany)
  - 3.2.6.6 Main injection (G1328B, Agilent, Germany)
- 3.2.7 HPLC column (Zorbax Eclipse Plus C18 4.6 x 250 mm, Agilent Technologies, USA)
- 3.2.8 Transsonic cleaning baths (890/H, ELMA, Germany)
- 3.2.9 Laboratory CO<sub>2</sub> incubators (Hera cell 240, Heraeus, Germany)
- 3.2.10 Biological safety cabinets class II (HS12, Heraeus, Germany)
- 3.2.11 Multispeed refrigerated centrifuge (PK121R, ALC, UK)
- 3.2.12 Fusion microplate analyzer (A153601, Packard Bioscience, CT, USA)

- 3.2.13 Microscope (T-DH, Nikon, Japan)
- 3.2.14 pH Tester (PH-30A, Clean Instruments, USA)
- 3.2.15 Lab dancer (336500, IKA, Malaysia)
- 3.2.16 Vacuum pump (TC-501v, Sparmax, Taiwan)
- 3.2.17 Reusable bottle top filter size 47mm, 500 mL (DS0320-5045, Thermo scientific, USA)

### 3.3 Method

#### 3.3.1 Quantitative analysis of rhein in *C. alata* leaves extract by HPLC

Separation was achieved isocratically on a C18 column (Zorbax Eclipse Plus C18 4.6 x 250 mm). The mobile phase consisted of methanol and 0.5% acetic acid in the ratio 70:30, v/v and was pumped at flow rate of 1 mL/min. The total running time was 30 minutes and injection volume was 20  $\mu$ L. The quantitative wavelength was set at 254 nm. The experiments were run in triplicate. (This method modified from reference [48].)

##### 3.3.1.1 Standard preparation

Standard solution of rhein was prepared in methanol at various concentrations of 2.5, 5, 10, 15, 20, 25, 35  $\mu$ g/mL. All solutions were filtered prior to analysis through 0.45  $\mu$ m nylon syringe filter.

##### 3.3.1.2 Sample preparation

0.1 g of *C. alata* leaves extract was accurately weighed and dissolved in methanol, and adjusted to 10 mL in a volumetric flask. All solutions were filtered prior to analysis through 0.45  $\mu$ m nylon syringe filter.

##### 3.3.1.3 Method validation

###### 3.3.1.3.1 Calibration curve

The average peak area of standard solution were reported and used for rhein quantification. The linearity of peak area response versus concentration of rhein was studied in the concentration ranges of 2.5-35  $\mu$ g/mL.

### 3.3.1.3.2 Accuracy

0.1 g of *C. alata* leaves extract was accurately weighed and dissolved in methanol, and adjusted to 10 mL in a volumetric flask. 200 µL extract portions were fortified with 12, 15 and 18 µL of rhein standard solution, and adjusted to 10 mL in volumetric flask. All solutions were filtered prior to analysis through 0.45 µm nylon syringe filter. The amount of each analysis was determined in triplicate, then percentage recoveries were calculated as follows.

$$\% \text{ recovery} = \frac{(\text{Conc. of total rhein in rhein added extract} - \text{Conc. of rhein in non rhein added extract})}{(\text{Conc. of rhein added in the extract})} \times 100$$

### 3.3.1.3.3 Precision

Precision of method was obtained by calculating the relative standard deviation (RSD) from repeated injections of solution. The intra-day precision was determined by six replicate injections, while the inter-day precision was determined by six injections on different two days.

### 3.3.1.3.4 Specificity

The specificity was tested by HPLC chromatograms recorded for rhein standard and *C. alata* leaves extract. Retention time and uv spectra of rhein peak have been compared.

### 3.3.1.4 Determination of rhein content

0.1 g of *C. alata* leaves extract was accurately weighed and dissolved in methanol, and adjusted to 10 mL in a volumetric flask. All solutions were filtered prior to analysis through 0.45 µm nylon syringe filter. The percentage of rhein was calculated from calibration curve.

## 3.3.2 Determination of cell viability

### 3.3.2.1 Rhein standard preparation

Rhein was dissolved in 0.1M sodium hydroxide (NaOH) and diluted with hank's balanced salt solution (HBSS) at various concentration of 1, 25, 50, 75, 100 µM. All solutions were freshly prepared and protected from light.

### 3.3.2.2 *C. alata* leaves extract preparation

*C. alata* leaves extract was dissolved in 10 µL dimethyl sulfoxide (DMSO) and adjusted with HBSS to 10 mL. (Final concentration = 0.1%DMSO)



### 3.3.2.3 Cell viability determination

Cell viability was determined by MTT (3-(4,5-dimethylthiazol-2-yl)-2,5-diphenyl tetrazolium bromide) colorimetric assay. The concept of method was to detect the absorbance of formazan (dark purple), which was produced from the reduction of MTT (yellow) by mitochondrial succinate dehydrogenase within viable cells. Briefly, MTT solution was freshly prepared in phosphate buffered saline (PBS) solution to final concentration 0.5 mg/mL and protected from light. Finally the insoluble formazan was solubilized with DMSO, and the absorbance was measured at the wavelength of 550 nm in microplate reader [115, 116].

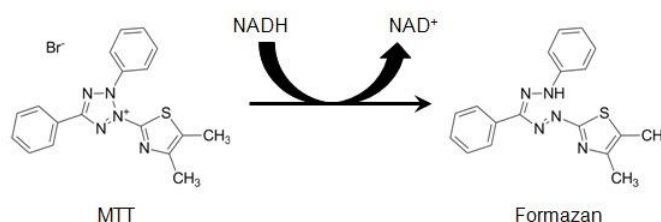


Figure 21 Structures of MTT and colored formazan product

Source: Terry L. Riss et al, "Cell Viability Assays," **In Assay Guidance Manual**, (2016): 262-291.

HaCaT cells were seeded in 96-well flat bottom plate at  $2.5 \times 10^4$  cells/well and incubated in 5% CO<sub>2</sub> incubator at 37°C for 48 hours. After 48 hours incubation, cells were treated with 200  $\mu$ L 1, 25, 50, 75, 100  $\mu$ M rhein or 0.01%, 0.05%, 0.1%, 0.3% *C. alata* leaves extract for 1 hour. Then, 100  $\mu$ L of MTT solution was added in each well. After incubation at 37°C for 4 hours, supernatant was discarded and 100  $\mu$ L DMSO was added for dissolving formazan crystals. Cell viability was determined by measuring the absorbance at the wavelength 550 nm using a microplate reader. Experimental data were analyzed as percentage of cell viability and compared with Dulbecco's modified eagle medium (DMEM) as control. The percentage of cell viability was calculated as follows:

$$\% \text{ cell viability} = \frac{(A_{550} \text{ sample} - A_{550} \text{ Blank})}{(A_{550} \text{ control} - A_{550} \text{ Blank})} \times 100$$

### 3.3.3 Measurement of ROS production

HaCaT cells were seeded in 96-well flat bottom plate at  $2.5 \times 10^4$  cells/well and incubated in 5% CO<sub>2</sub> incubator at 37°C for 48 hours. After 48 hours incubation, cells were treated with 200 µL of 1, 25, 50 µM rhein or 0.01% *C. alata* leaves extract for 1 hour. Then, 200 µL of 1mM *t*-BHP (*tert*-Butyl hydroperoxide) was added in each well to induce oxidative stress. After incubation at 37°C for 1 hour, supernatant was discarded and 100 µL of 20 mM H<sub>2</sub>DCFDA was added. Reactions were incubated at 37°C for 30 minutes. ROS production was detected by fluorescence microscopy at excitation wavelength 485 nm and emission wavelength 535 nm. Experiment data were analyzed as percentage of ROS production and compared with cell control.

### 3.3.4 Measurement of inflammatory cytokines production by ELISA

This assay employs the quantitative sandwich enzyme immunoassay technique. A sandwich immunoassay is a method using two antibodies, which bind to different sites on the antigen or ligand. A monoclonal antibody, which is highly specific for the antigen, has been pre coated onto a microplate. The antigen is then added, where it is bound by the immobilized antibody. After washing any unbound antigen, followed by addition of a second antibody referred to as the detection antibody. The detection antibody binds the antigen. As a result, the antigen is 'sandwiched' between the two antibodies. The antibody binding affinity for the antigen is usually the main determinant of immunoassay sensitivity. As the antigen concentration increases, the amount of detection antibody increases, leading to a higher measured response. The standard curve of a sandwich-binding assay has a positive slope. To quantify the extent of binding, the antibody is linked to the biotin and that can be recognized by the streptavidin-HRP complex. In the last step, peroxidase substrate is added to the reaction that forms a colorimetric readout as the detection signal. The signal generated is proportional to the amount of target antigen present in the sample [117].

HaCaT cells were seeded in 24-well flat bottom plate at  $10^5$  cells/well and incubated in 5% CO<sub>2</sub> incubator at 37°C for 72 hours. After 96 hours incubation, cells were treated with 500 µL of 1, 25, 50 µM rhein or 0.01% *C. alata* leaves extract for 1 hour, followed by 500 µL of 1mM *t*-BHP (*tert*-Butyl hydroperoxide). After exposure to *t*-BHP for 1 hour, the supernatant was collected and store at -80 °C. TNF- $\alpha$  and IL-8 levels were measured in the supernatant samples by ELISA.

#### **3.3.4.1 ELISA for TNF- $\alpha$**

ELISA plate was coated by 100  $\mu$ L of coating antibody and incubated overnight at room temperature. Surface space of plate was blocked by 300  $\mu$ L of blocking buffer and incubated for 1 hour at room temperature. 100  $\mu$ L of sample or TNF- $\alpha$  standards (15.625, 31.25, 62.5, 125, 250, 500, 1,000 pg/mL) was added and incubated for 1 hour at room temperature. Plate was washed three times by adding 300  $\mu$ L washing buffer. Human TNF- $\alpha$  was captured again by adding 100  $\mu$ L detection antibody and incubated for 1 hour at room temperature. Plate was washed three times by adding 300  $\mu$ L washing buffer. Then, 100  $\mu$ L Streptavidin-HRP was added and incubated for 30 minutes at room temperature. Plate was washed three times by adding 300  $\mu$ L washing buffer. The reaction was initiated by adding 100  $\mu$ L substrate solution into each well and incubated in the dark for 20 minutes at room temperature. Stop the reaction by adding 100  $\mu$ L stop solution. Measure the absorbance at wavelength 450 nm. The standard curve was used to determine human TNF- $\alpha$  amount in a sample. The standard curve was generated by plotting the average absorbance on vertical (Y) axis vs human TNF- $\alpha$  concentration (pg/mL) on the horizontal axis. Human TNF- $\alpha$  secretion was analyzed as human TNF- $\alpha$  concentration and compared with cell control.

#### **3.3.4.2 ELISA for IL-8**

ELISA plate was coated by 100  $\mu$ L of coating antibody and incubated overnight at room temperature. Surface space of plate was blocked by 300  $\mu$ L of blocking buffer and incubated for 1 hour at room temperature. 100  $\mu$ L of sample or IL-8 standard (31.25, 62.5, 125, 250, 500 pg/mL) was added and incubated for 1 hour at room temperature. Plate was washed three times by adding 300  $\mu$ L washing buffer. Human IL-8 was captured again by adding 100  $\mu$ L detection antibody and incubated for 1 hour at room temperature. Plate was washed three times by adding 300  $\mu$ L washing buffer. Then, 100  $\mu$ L Streptavidin-HRP was added and incubated for 30 minutes at room temperature. Plate was again washed three times by adding 300  $\mu$ L washing buffer. The reaction was initiated by adding 100  $\mu$ L substrate solution in to each well and incubated in the dark for 20 minutes at room temperature. Stop the reaction by adding 100  $\mu$ L stop solution. Measure the absorbance at wavelength 450 nm. The standard curve was used to determine human IL-8 amount in a sample. The standard curve was generated by plotting the average absorbance on vertical (Y) axis vs human IL-8 concentration (pg/mL) on the horizontal axis. Human IL-8 secretion was analyzed as human IL-8 concentration and compared with cell control.

### 3.3.5 Data analysis

Experiments were performed in triplicate manner. The results were shown as mean  $\pm$  SD. Differences between groups were analyzed by using one-way ANOVA. Significance was accepted at p-value  $<0.05$ ,  $0.01$ ,  $0.001$ .



## CHAPTER 4

### RESULTS AND DISCUSSION

#### 4.1 Quantitative analysis of rhein in *C. alata* leaves extract by HPLC

##### 4.1.1 Method validation

###### 4.1.1.1 Calibration curve

###### 4.1.1.2 Accuracy

###### 4.1.1.3 Precision

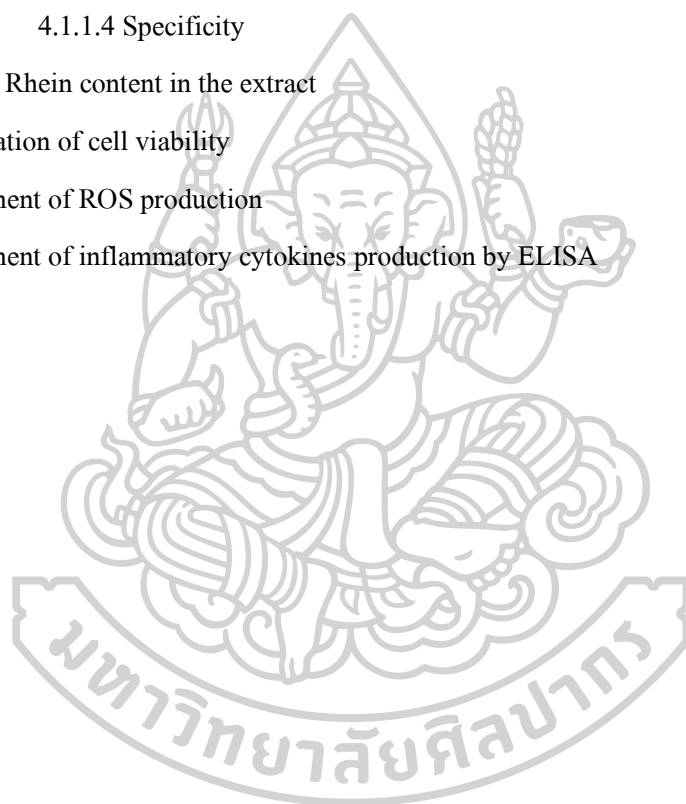
###### 4.1.1.4 Specificity

##### 4.1.2 Rhein content in the extract

#### 4.2 Determination of cell viability

#### 4.3 Measurement of ROS production

#### 4.4 Measurement of inflammatory cytokines production by ELISA



## 4.1 Quantitative analysis of rhein in *C. alata* leaves extract by HPLC

### 4.1.1 Method validation

#### 4.1.1.1 Calibration curve

The linearity of peak area response versus concentration of rhein was studied in the range of 2.5-35  $\mu\text{g/mL}$ . The calibration equation ( $y=64.509x+34.997$ ), with the correlation coefficient ( $R^2$ ) 0.9981, demonstrated the linearity of the method. (Figure 22)

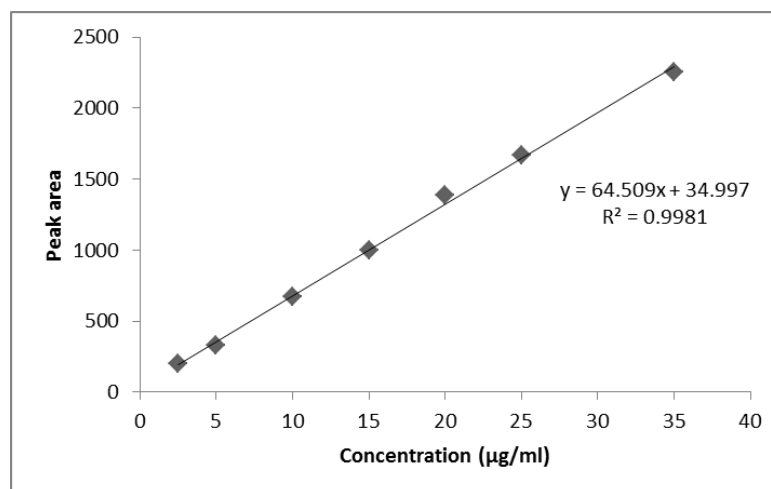


Figure 22 Calibration curve of rhein from rhein standard solution.

#### 4.1.1.2 Accuracy

The recovery results were within the acceptable criteria (90-110%). The results suggested good accuracy of the HPLC method. (Table 14)

Table 14 Recovery of rhein in *C. alata* leaves extract

Concentration of rhein added in the extract ( $\mu\text{g/mL}$ )	Calculated concentration* ( $\mu\text{g/mL}$ ) $\pm$ SD (n=3)	% Recovery
12	11.24 $\pm$ 0.28	93.69
15	13.89 $\pm$ 0.15	92.60
18	16.80 $\pm$ 0.39	93.35

\* Calculated concentration = Conc.of total rhein in rhein added extract-Conc.of rhein in non rhein added extract

#### 4.1.1.3 Precision

The %RSD for inter-day and intra-day were shown in Table 15. The results showed that %RSD is less than 2.0%, indicating that the method was sufficiently precised.

Table 15 Precision data of rhein

	%RSD	
	Intra-day (n=6)	Inter-day (n=6)
Rhein	1.87	1.95
<i>C. alata</i> leaves extract	1.94	1.68

#### 4.1.1.4 Specificity

Rhein was eluted at retention time of 10.7 minutes in the chromatograms as shown in Figure 23. The obtained chromatograms of the extract showed no interference to rhein peak. UV spectra of *C. alata* leaves extract and rhein standard have been compared. (Figure 24)

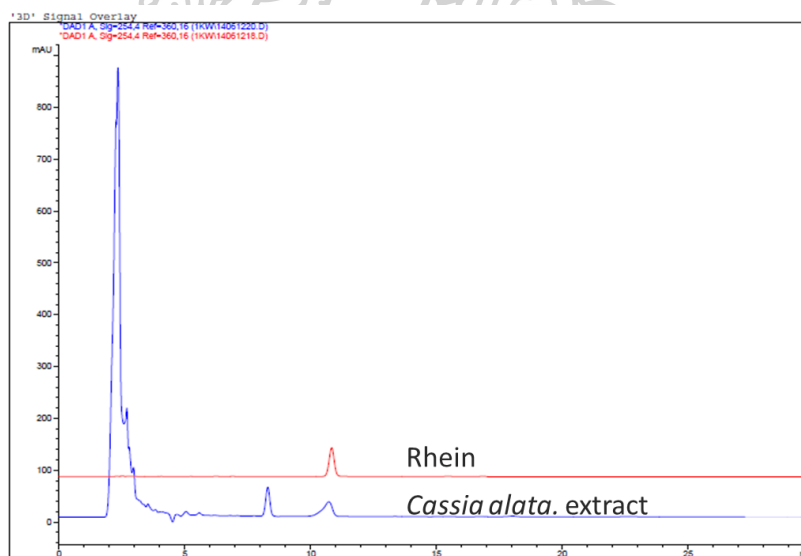


Figure 23 HPLC chromatograms of *C. alata* leaves extract (lower) and rhein standard (upper)

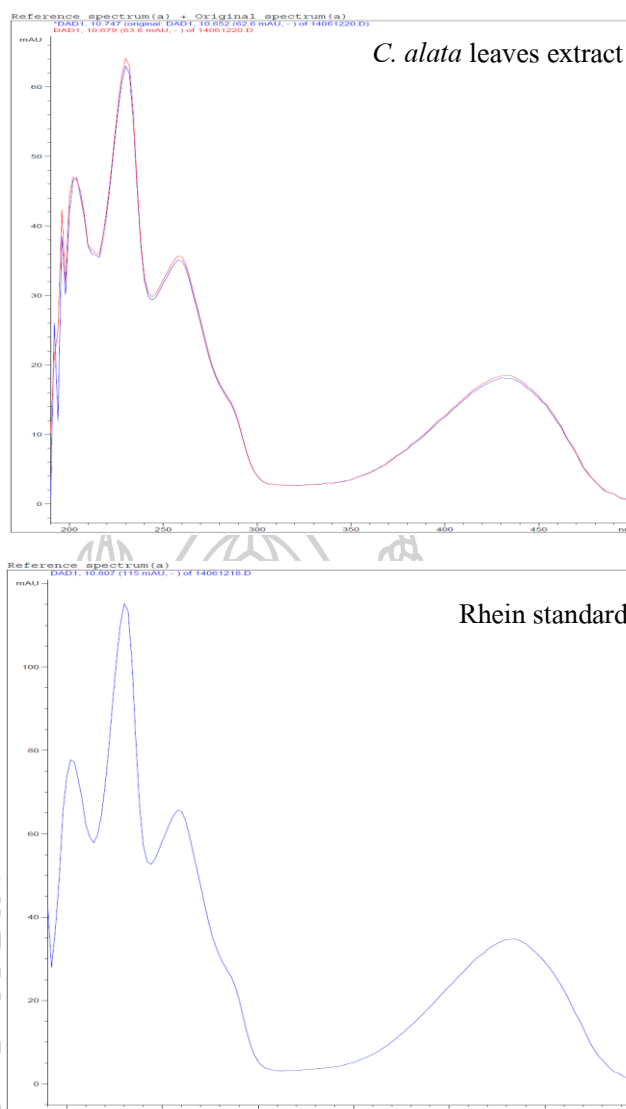


Figure 24 UV spectra of *C. alata* leaves extract (upper) and rhein standard (lower), at retention time 10.7 minutes

#### 4.1.2 Rhein content in the extract

The percentage of rhein content in the extract of *C. alata* leaves determined by HPLC was  $0.1225 \pm 0.0001$  %w/w, calculated from the calibration curve.

The previous studies used analytical method such as TLC and HPLC to determine rhein anthraquinone content in *C. alata* leaves extract [5, 8, 46, 48]. It has been determined in the range of 0.02-0.15% w/w. Our studies have determined content of rhein by HPLC. The rhein content in methanolic extracts of *C. alata* leaves was conform to the previous studies.



#### 4.2 Determination of cell viability

To ensure cell viability during whole experiments, HaCaT cells were treated with various concentrations of rhein standard (1-100  $\mu\text{M}$ ) and *C. alata* leaves extract (0.01-0.3%w/v) in order to find the concentration which more than 80% of cell survived. Following rhein standard and *C. alata* leaves extract incubation, cell viability were determined with MTT.

After incubation of HaCaT cells with rhein standard and *C. alata* leaves extract, the cells were photographed before dissolving formazan crystals with dimethyl sulfoxide (DMSO) under the microscope. The results are shown in Figure 25

Cell viability of control is expressed as 100% cell viability. Cell viabilities after incubation with 1, 25, 50, 75 and 100  $\mu\text{M}$  rhein standards were  $97.78\pm 9.33$ ,  $93.58\pm 7.67$ ,  $92.57\pm 6.87$ ,  $75.92\pm 6.11$  and  $62.79\pm 6.70$ , respectively (Figure 26A). Cell viabilities after incubation with 0.01, 0.05, 0.1 and 0.3%w/v *C. alata* leaves extract were  $92.86\pm 8.29$ ,  $76.17\pm 8.86$ ,  $65.60\pm 9.02$  and  $42.88\pm 9.39$ , respectively (Figure 26B). The result showed that rhein standard at 1-50  $\mu\text{M}$  and *C. alata* leaves extract at 0.01%w/v had no effect on HaCaT cell viability. Therefore, rhein standard 1-50  $\mu\text{M}$  and *C. alata* leaves extract 0.01%w/v were used for the cell treatment in the subsequent experiment.



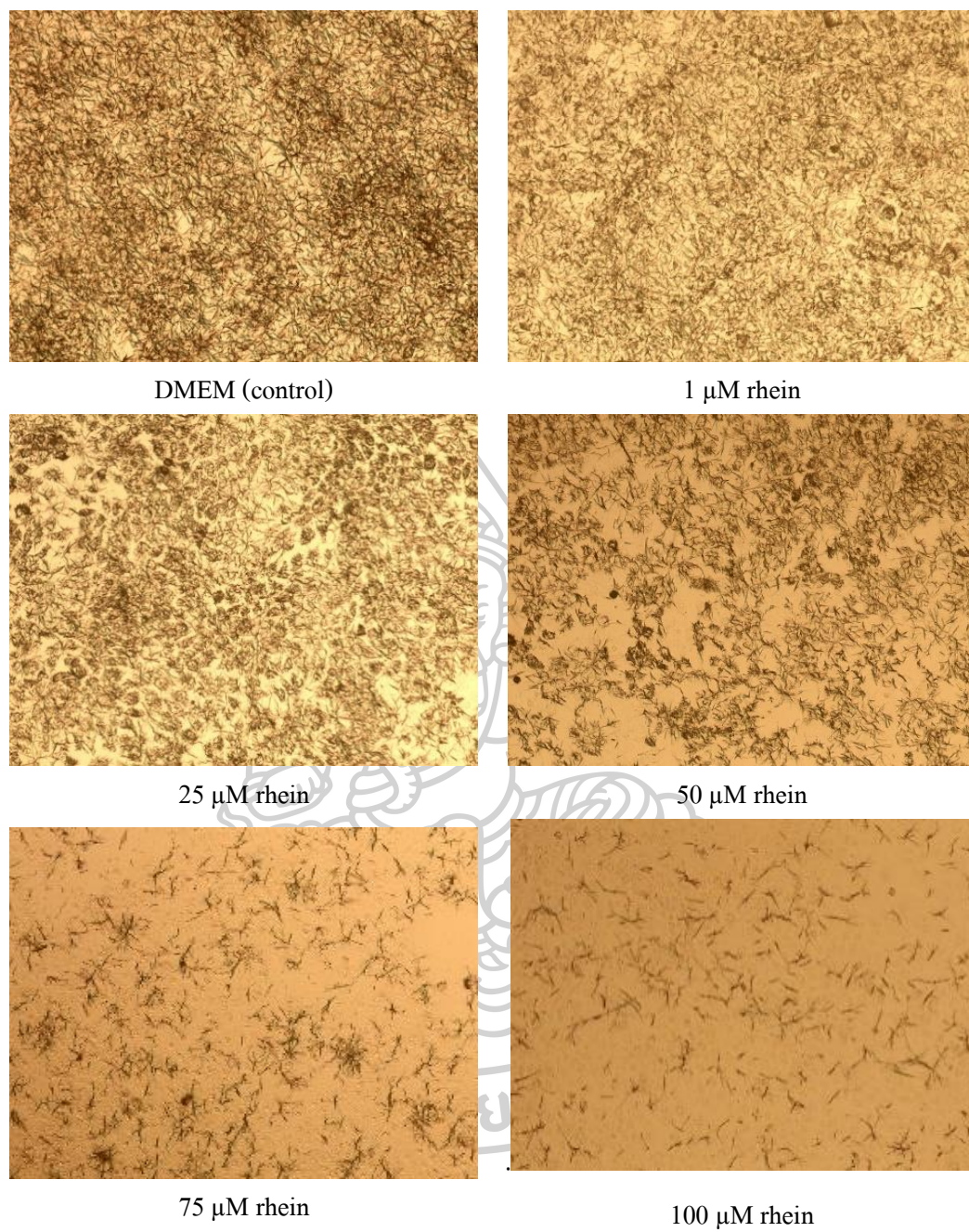


Figure 25 Formazan crystals in HaCaT cells after exposure to rhein standard and *C. alata* leaves extract.

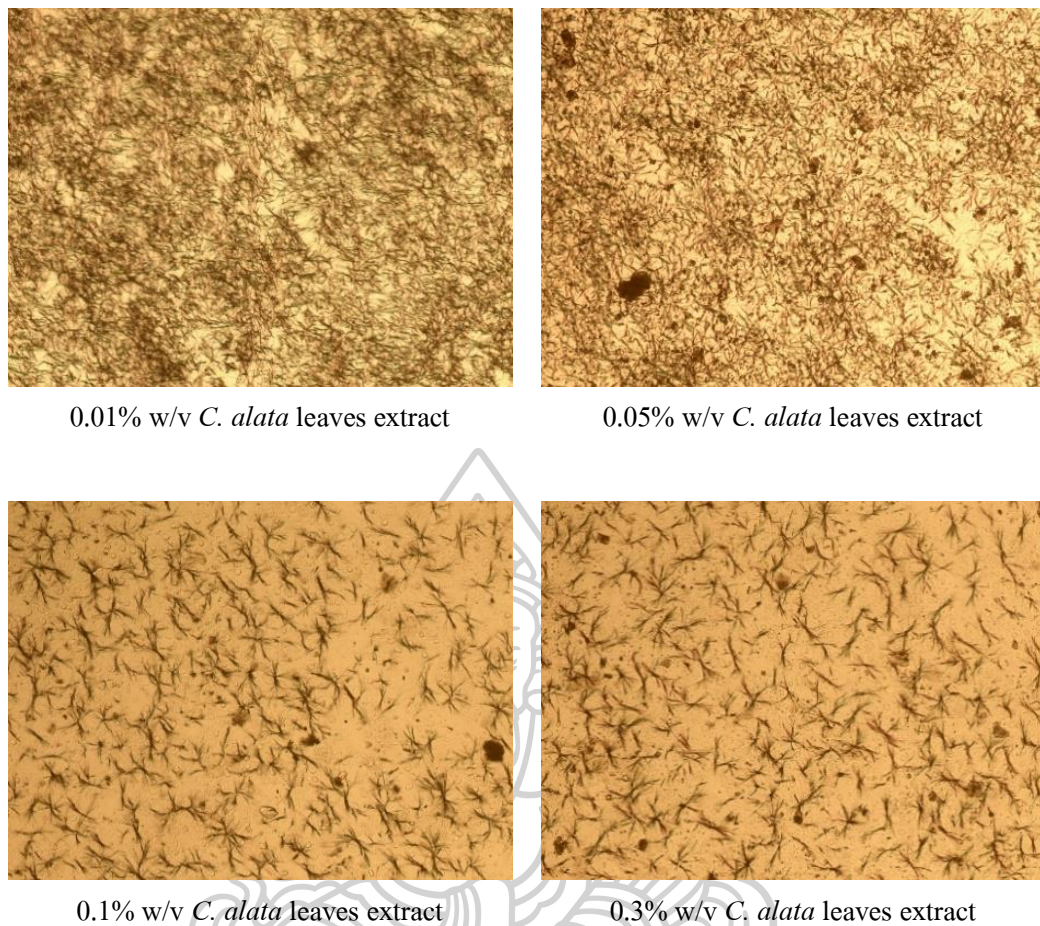


Figure 25 Formazan crystals in HaCaT cells after exposure to rhein standard and *C. alata* leaves extract. (continued)



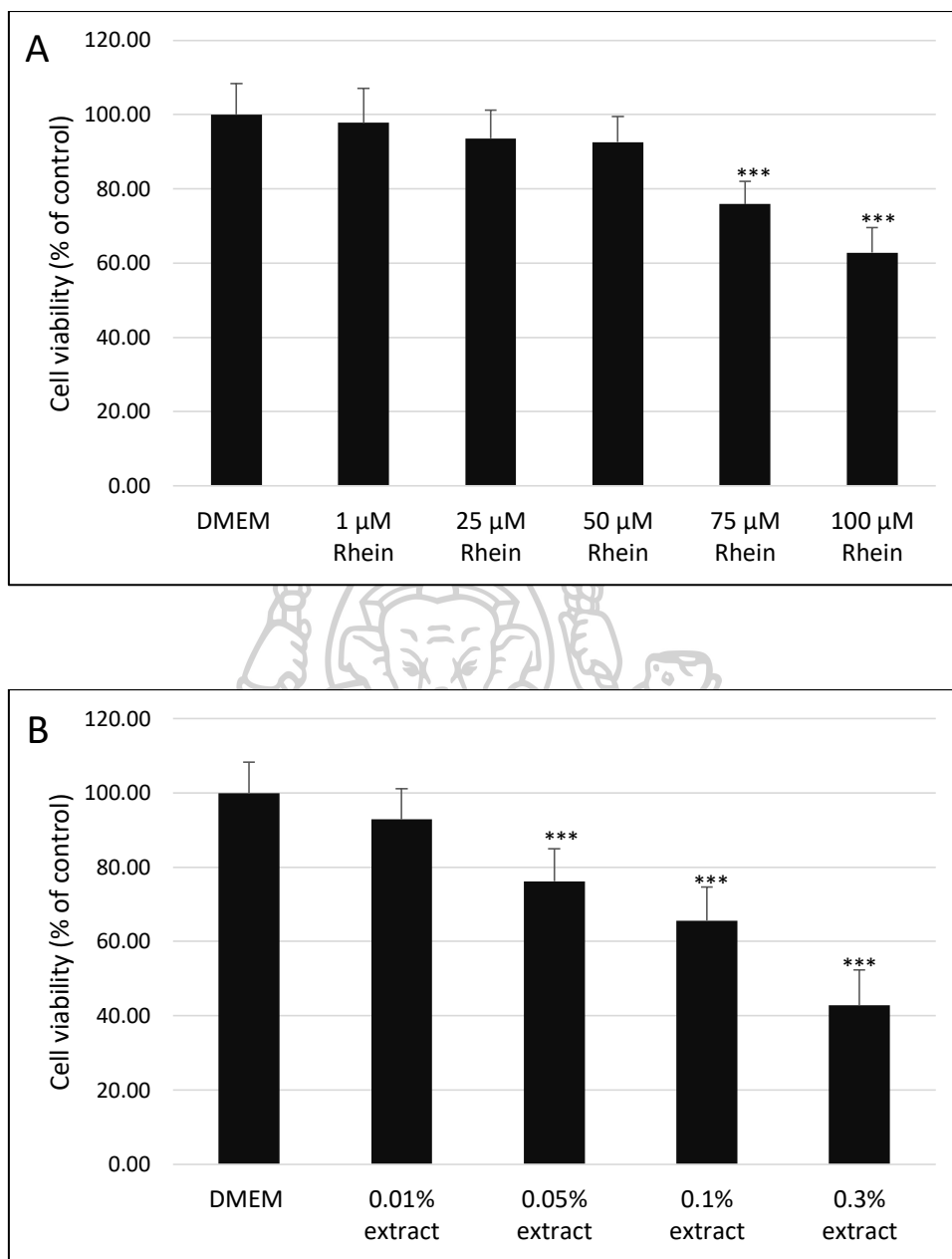


Figure 26 Effect of rhein standard and *C. alata* leaves extract on cell viability in HaCaT cells using MTT.

HaCaT cells were treated with various concentrations of rhein standard (A) and *C. alata* leaves extract (B). Data are expressed as mean±SD (n=3). \*\*\* $p \leq 0.001$  compared to the DMEM control group.

### 4.3 Measurement of ROS production

In this experiment we used *t*-BHP to induced oxidative stress. *t*-BHP is an organic hydroperoxidant that can be metabolized to free radical intermediates, which can subsequently initiate lipid peroxidation, affect cell integrity, and form covalent bonds with cellular molecules resulting in cell injury. These phenomena are similar to the oxidative stress occurring in the cell [118].

To determine effect of rhein standard and *C. alata* leaves extract on intracellular ROS production. HaCaT cells were treated with various concentrations of rhein standard (1-50 $\mu$ M) and *C. alata* leaves extract (0.01 %w/v), then exposed to *t*-BHP to induced ROS production. ROS production were investigated by H<sub>2</sub>DCFDA fluorescence probe.

The morphology of HaCaT cells (Figure 27) are observes under the microscope. HaCaT cell with DMEM solution treatment showed polygonal-shaped, adherent cells growing as a confluent monolayer. Cells treated with *t*-BHP had a morphological change, shrink into spherical shape. Cells treated with rhein standard (1, 25, 50 $\mu$ M) and *C. alata* leaves extract (0.01 %w/v), displayed only moderate morphological changed.

Experiment data were analyzed as percentage of ROS production and compared with control cells. The production of ROS in control group is expressed as 100%. ROS production significantly increases after exposure to *t*-BHP (202.97 $\pm$ 18.63) (Figure 28). HaCaT cells were pre-incubated with 1, 25 and 50  $\mu$ M rhein standard prior to treatment with 1 mM *t*-BHP. ROS production after exposure to *t*-BHP were 158.23 $\pm$ 23.72, 136.83 $\pm$ 15.07 and 116.00 $\pm$ 23.08, respectively (Figure 28A). ROS production after pre-incubation with 0.01 %w/v *C. alata* leaves extract and exposure to *t*-BHP were 91.33 $\pm$ 3.43 (Figure 28B).

ROS has been known to act as novel mediator for inflammation. ROS production induced by *t*-BHP is significantly increased, signifying inflammation state in the cells. Pre-treatment with rhein standard and *C. alata* leaves extract effectively inhibited *t*-BHP induced ROS production in a concentration-dependent manner. Similar results with rhein were reported for monocyte cell line that rhein can decreased ROS production [71]. Moreover, rhein can protect the  $\beta$ -cells against hyperglycemia-induced cell apoptosis through suppressing ROS production [79] and against acetaminophen-induced hepatic and renal toxicity [73].

As mentioned above, percentage of rhein content in the extract of *C. alata* leaves determined by HPLC was  $0.1225 \pm 0.0001$  %w/w. In 0.01 %w/v *C. alata* leaves extract, rhein content was equivalent to 0.43  $\mu$ M. A decrease in ROS production of 55% was observed when cells were treated with 0.01 %w/v *C. alata* leaves extract, while pre-treatment with 1, 25 and 50  $\mu$ M rhein standard resulted in decreases in ROS production of 25%, 36%, 41%, respectively. *C. alata* leaves extract exhibited stronger anti-inflammatory effects than the rhein standard. This may be due to other compounds, such as kaempferol [22, 42, 45], aloe-emodin [22] and emodin [22, 71] in the extract, that also have anti-inflammatory effects.



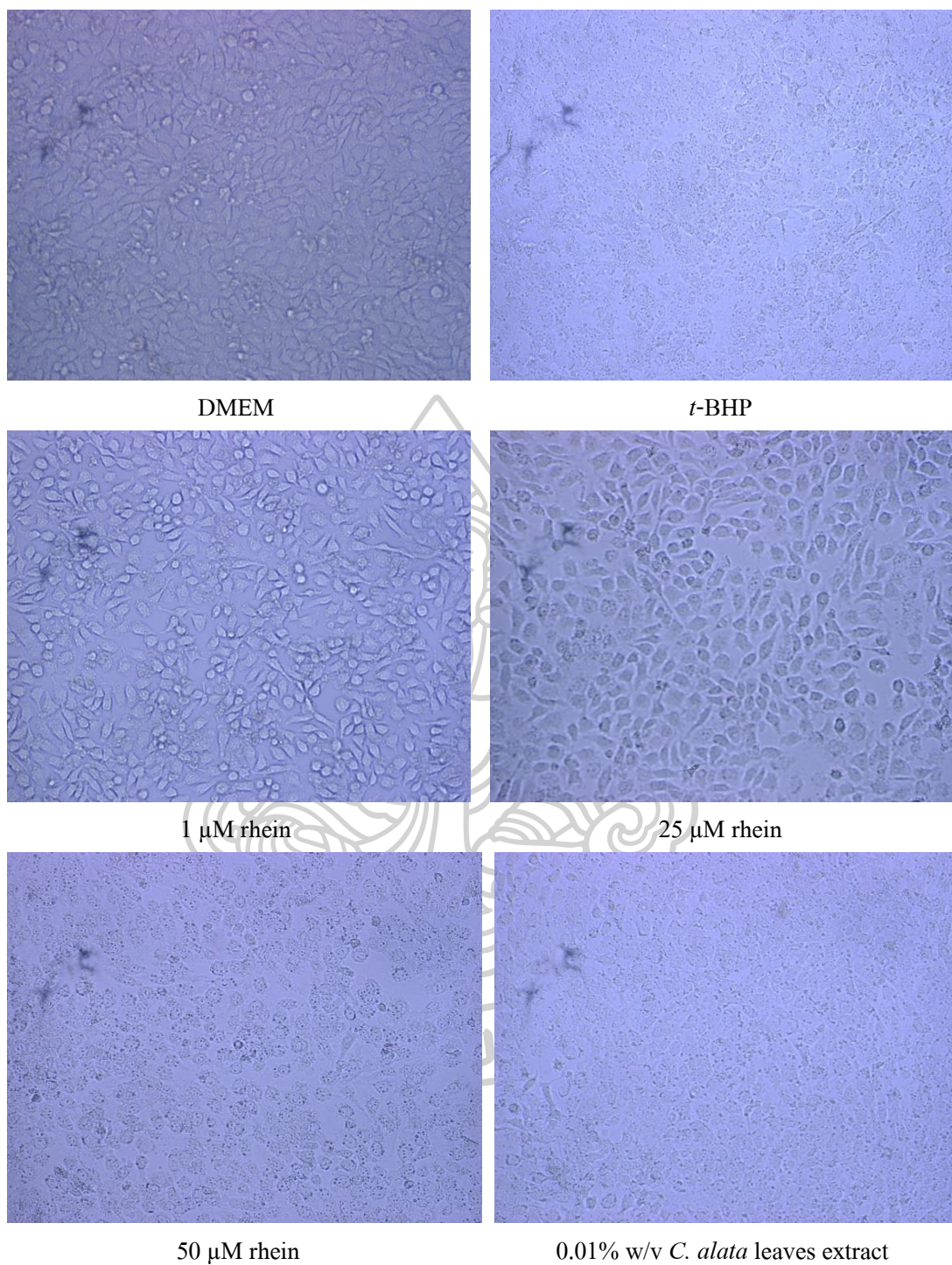


Figure 27 HaCaT cells after exposure to rhein standard and *C. alata* leaves extract on *t*-BHP induced intracellular ROS production.

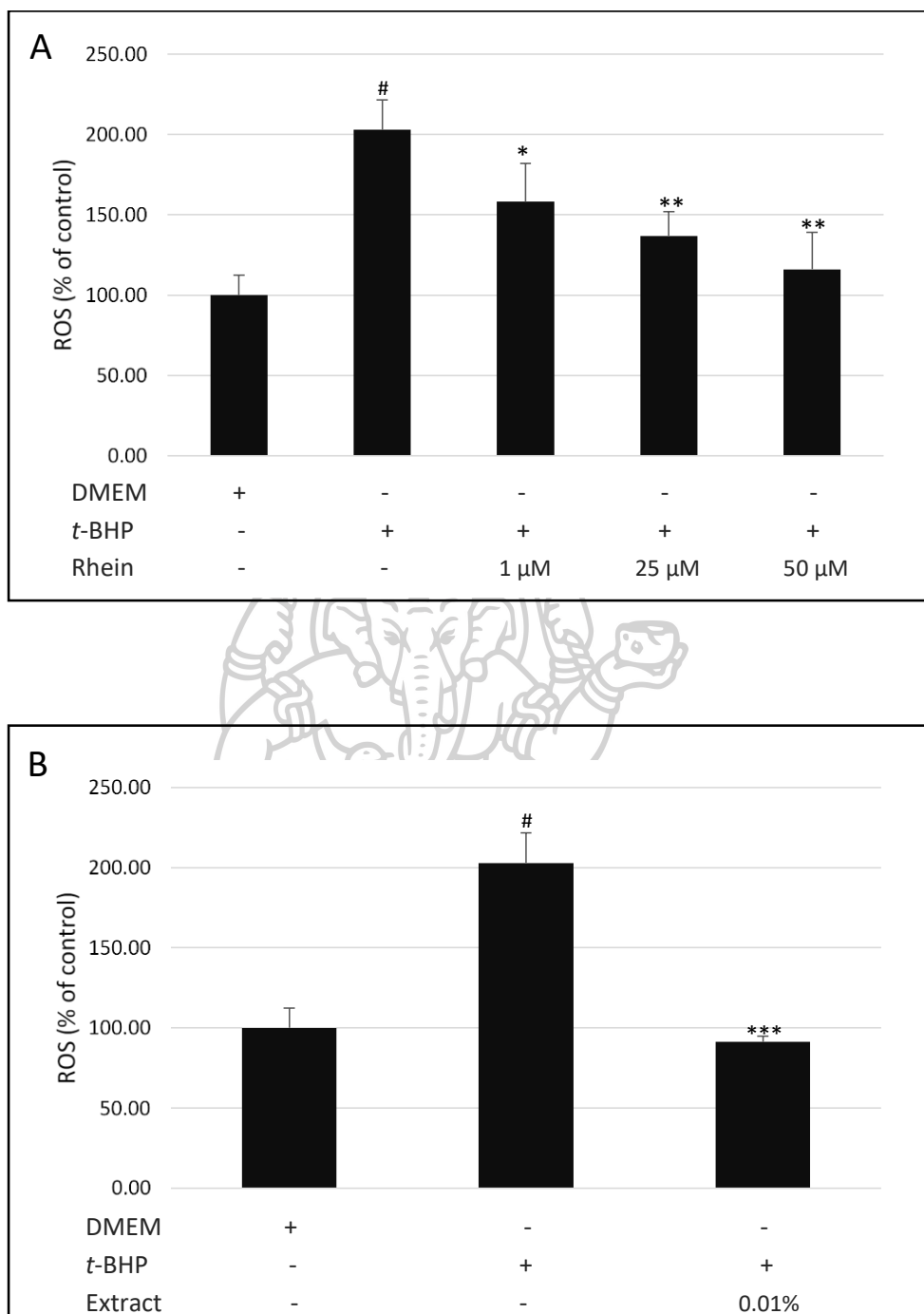


Figure 28 Effect of rhein standard and *C. alata* leaves extract on intracellular ROS production in HaCaT cells.

ROS production in various concentrations of rhein standard (A) and *C. alata* leaves extract (B). Data are expressed as mean  $\pm$  SD (n=3). # $p \leq 0.001$  compare to DMEM, \* $p \leq 0.05$ , \*\* $p \leq 0.01$ , \*\*\* $p \leq 0.001$  compared to *t*-BHP treated group.



#### 4.4 Measurement of inflammatory cytokines production by ELISA

ROS induces inflammation by stimulate the production of pro-inflammatory cytokines. TNF- $\alpha$  and IL-8 are pro-inflammatory cytokines which appear to be major mediators in skin inflammation [111, 112]. Previous studies have revealed that *C. alata* leaves extract effectively inhibited ROS and TNF- $\alpha$  production in monocyte cells [3]. Rhein is a major compound in *C. alata*. [8] and has been shown to have anti-inflammatory activity [56, 62-64, 69-71]. Rhein treatment inhibited in LIGHT-induced IL-8, MCP-1, TNF- $\alpha$  and IL-6 production in monocyte cell [71].

In order to determine the role of ROS induced TNF- $\alpha$  and IL-8 production. HaCaT cells were treated with rhein standard and *C. alata* leaves extract, and cells were then stimulated with 1 mM *t*-BHP. The cell-free supernatants were then collected, after which the cytokines/chemokines were assayed using ELISA kits for TNF- $\alpha$  and IL-8.

As shown in Figure 29A, the amount of TNF- $\alpha$  secretion of control cell was 160.33 $\pm$ 16.95 pg/mL and TNF- $\alpha$  secretion significantly increase after expose to *t*-BHP (731.44 $\pm$ 95.95 pg/mL). The amount of TNF- $\alpha$  secretion of cells treated with 1, 25 and 50  $\mu$ M rhein standard prior to treatment with 1 mM *t*-BHP were 123.50 $\pm$ 15.61, 118.39 $\pm$ 15.22 and 108.10 $\pm$ 10.13 pg/mL, respectively. The amount of TNF- $\alpha$  secretion of cells treated with 0.01 %w/v *C. alata* leaves extract and exposure to *t*-BHP were 91.25 $\pm$ 12.56 pg/mL.

As shown in Figure 29B, the amount of IL-8 secretion of control cells was 436.36 $\pm$ 48.65 pg/mL and IL-8 secretion was significantly increased after exposure to *t*-BHP (1,313.39 $\pm$ 219.61 pg/mL). HaCaT cells were pre-incubated with 1, 25 and 50  $\mu$ M rhein standard prior to treatment with 1 mM *t*-BHP. The amount of IL-8 after expose to *t*-BHP were 777.60 $\pm$ 61.04, 706.73 $\pm$ 80.10 and 673.11 $\pm$ 61.46 pg/mL, respectively. The amount of IL-8 secretion of cells treated with 0.01 %w/v *C. alata* leaves extract and exposure to *t*-BHP were 504.99 $\pm$ 148.54 pg/mL.

TNF- $\alpha$  and IL-8 production in *t*-BHP induced HaCaT cell were elevated significantly from control, that could represent the inflammation state in the cells. Pre-treatment with rhein could diminish TNF- $\alpha$  and IL-8 production of *t*-BHP treated cells. We previously reported that *t*-BHP induced ROS production were reduced by rhein standard and *C. alata* leaves extract. Taken together, these results suggest that ROS plays a significant role in *t*-BHP induced TNF- $\alpha$  and IL-8 production. Thus, blocking ROS production inhibits *t*-BHP induced TNF- $\alpha$  and IL-8

production. Moreover, *C. alata* leaves extract exhibited stronger anti-inflammatory effects than rhein standard. *t*-BHP induced TNF- $\alpha$  production was inhibited by 87% when cells were treated with 0.01 %w/v *C. alata* leaves extract (0.43  $\mu$ M rhein content), while 83%, 84%, 85% inhibition were seen with 1, 25 and 50  $\mu$ M rhein standard, respectively. The results obtained from IL-8 production were also similar. 0.01 %w/v *C. alata* leaves extract inhibited *t*-BHP-induced IL-8 production of 62% while 1, 25 and 50  $\mu$ M rhein standard resulted in 41%, 46%, 49% inhibition, respectively. This may be due to other compounds, such as flavonoids [22, 42, 45] and other anthraquinones [22, 71] in the extract, that also have anti-inflammatory effects.



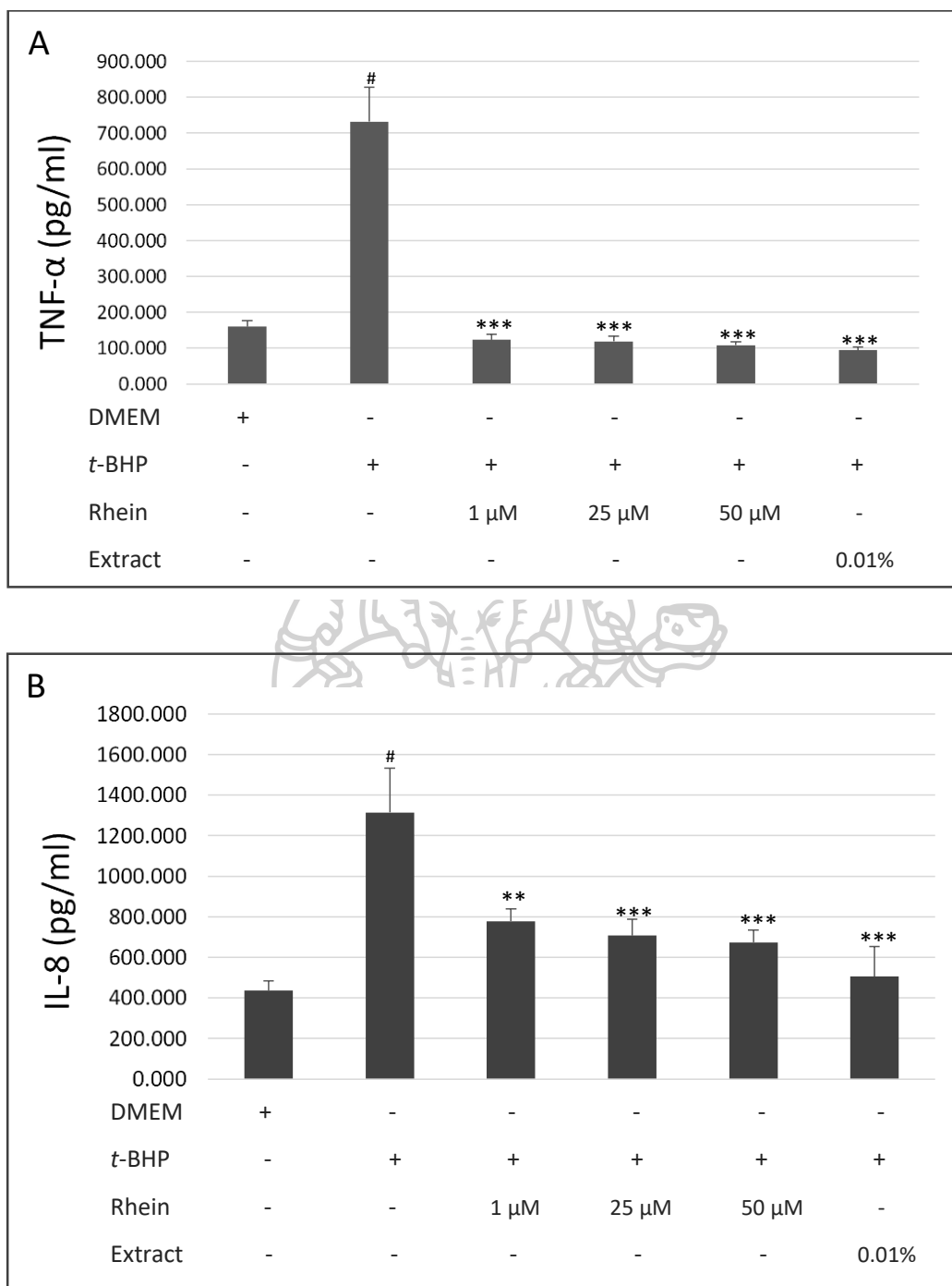


Figure 29 Inhibitory effect of rhein standard and *C. alata* leaves extract on cytokines production in HaCaT cells.

TNF- $\alpha$  (A) and IL-8 (B). Data are expressed as mean $\pm$ SD (n=3). #p  $\leq$  0.05 compare to control, \*p  $\leq$  0.05, \*\*p  $\leq$  0.01, \*\*\*p  $\leq$  0.001 compared to t-BHP treated group.

## CHAPTER 5

### CONCLUSION

Human epidermal keratinocytes are located on the outer skin surface. Keratinocytes are always exposed to external stimuli which consequently induce ROS generation in cells [119]. Since ROS play a crucial role in inflammation, they serve as a target for inflammation therapy [85]. *Cassia alata* Linn. is widely distributed in the tropical countries. Many countries used *C. alata* leaves for treatment of skin diseases such as ringworm, eczema, pruritic, itching, scabies and other related disease [120]. *C. alata* leaves are used in preparation of herbal formulations such as herbal tea, extracts, tincture, herbal soaps and shampoos for dermatological skin diseases [35]. *C. alata* leaves extract is composed of rhein anthraquinone which have been reported for their anti-inflammatory activity [121].

The purpose of this research was to determine rhein anthraquinone content in *C. alata* leaves extract and investigate anti-inflammatory activities of rhein and *C. alata* leaves extract on *t*-BHP induced inflammation in the human keratinocytes, HaCaT cell.

The previous studies used analytical method such as TLC and HPLC to determine rhein anthraquinone content in *C. alata* leaves extract [5, 8, 46, 48]. Our studies have determined content of rhein by HPLC. The study revealed that the rhein content in methanolic extracts of *C. alata* leaves is  $0.1225 \pm 0.0001$  %w/w.

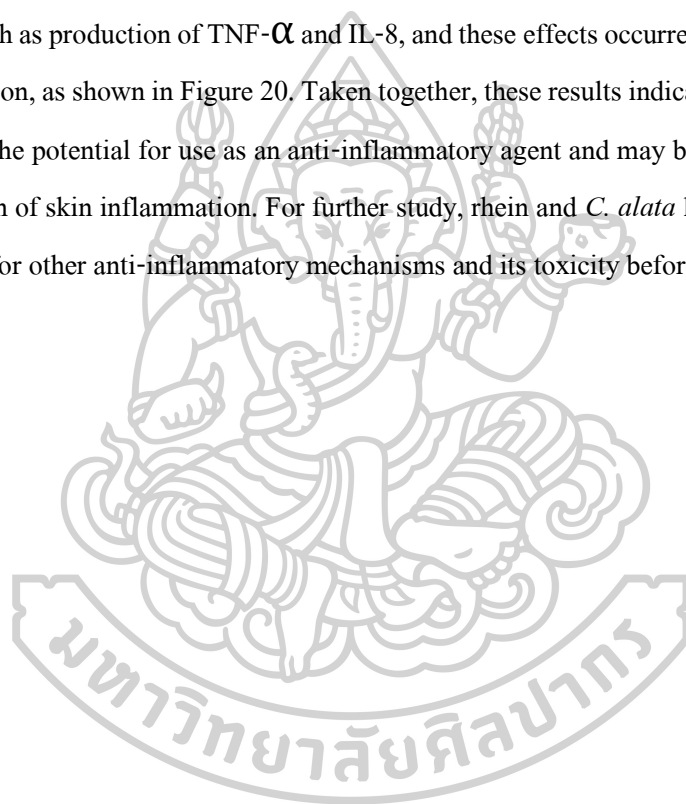
It has been known that rhein decrease ROS, IL-8 and TNF- $\alpha$  production in monocytes [71]. *C. alata* leaves extract has been shown to reduce production of TNF- $\alpha$ , H<sub>2</sub>O<sub>2</sub> and O<sub>2</sub><sup>-</sup> in monocytes [35]. In this study, we investigated effect of rhein standard and *C. alata* leaves extract in HaCaT cell on intracellular ROS production by H<sub>2</sub>DCFDA fluorescence probe. We found that ROS production induced by *t*-BHP was significantly increased compared to control cell. Pre-treatment with rhein standard or *C. alata* leaves extract could diminish ROS production.

Previous studies have revealed the roles of TNF- $\alpha$  and IL-8 as pro-inflammatory cytokines. Consistent with other inflammatory diseases, pro-inflammatory cytokines, including TNF- $\alpha$  and IL-8, appear to be major mediators in skin inflammation [111, 112]. Therefore, in the current study, the levels of TNF- $\alpha$  and IL-8 in the human keratinocytes were investigated by ELISA. The results illustrated that *t*-BHP induced TNF- $\alpha$  and IL-8 production, representing the

inflammation state in the cells. Pre-treatment with rhein and *C. alata* leaves extract could diminish TNF- $\alpha$  and IL-8 production of *t*-BHP-treated cells.

*C. alata* leaves extract exhibited stronger inhibition of ROS production than rhein standard. The same result was obtained concerning inhibition of *t*-BHP-induced TNF- $\alpha$  and IL-8 production. This may be due to other compounds such as kaempferol [22, 42, 45], aloe-emodin [22] and emodin [22, 71] in the extract that also have anti-inflammatory effects.

In summary, rhein and *C. alata* leaves extract inhibited *t*-BHP-induced inflammatory responses such as production of TNF- $\alpha$  and IL-8, and these effects occurred via the suppression of ROS production, as shown in Figure 20. Taken together, these results indicated that *C. alata* leaves extract have the potential for use as an anti-inflammatory agent and may be particularly useful for the prevention of skin inflammation. For further study, rhein and *C. alata* leaves extract should be investigated for other anti-inflammatory mechanisms and its toxicity before further development.



## REFERENCES

1. Nestle, Frank O. et al. (2009). "Skin immune sentinels in health and disease." **Nature reviews. Immunology** 9, 10 (October): 679-691.
2. Pastore, Saveria. et al. (2011). "Differential modulation of stress-inflammation responses by plant polyphenols in cultured normal human keratinocytes and immortalized HaCaT cells." **Journal of Dermatological Science** 63, 2 (August): 104-114.
3. Sagnia, Bertrand. et al. (2014). "Antioxidant and anti-inflammatory activities of extracts from *Cassia alata*, *Eleusine indica*, *Eremomastax speciosa*, *Carica papaya* and *Polyscias fulva* medicinal plants collected in cameroon." **PLoS ONE** 9, 8 (August): 1-10.
4. Hennebelle, Thierry. et al. (2009). "*Senna alata*." **Fitoterapia** 80, 7 (October 1): 385-393.
5. Mansuang Wuthi-udomlert, Pavena Kupittayanant, and Wandee Gritsanapan. (2010). "In vitro evaluation of antifungal activity of anthraquinone derivatives of *Senna alata*." **Journal of Health Research** 24, 3: 117-122.
6. The Botanical Organization Ministry of Natural Resource and Environment Thailand. (2011). **Medical plant database**. Accessed 8 april 2016. Available from <http://www.qsbg.org/Database/plantdb/mdp/medicinal-specimen.asp?id=571>
7. Idu, Macdonald., S.E. Omonigho, and Clara Leyibo Igeleke. (2007). "Preliminary investigation on the phytochemistry and antimicrobial activity of *Senna alata* L. flower." **Pakistan Journal of Biological Sciences** 10, 5 (March): 806-809.
8. Wandee Gritsanapan, and Peeranuch Mangmeesri. (2009). "Standardized *Senna alata*. leaf extract." **Journal of Health Research** 23, 2 (January): 59-64.
9. Jiofack, T. et al. (2010). "Ethnobotanical uses of medicinal plants of two ethnoecological regions of Cameroon." **International Journal of Medicine and Medical Sciences** 2, 3: 60-79.
10. Ezuruike, Udoamaka F., and Jose M. Prieto. (2014). "The use of plants in the traditional management of diabetes in Nigeria: Pharmacological and toxicological considerations." **Journal of Ethnopharmacology** 155, 2 (September): 857-924.
11. Ajibesin, Kola' K. et al. (2008). "Ethnobotanical survey of Akwa Ibom State of Nigeria." **Journal of Ethnopharmacology** 115, 3 (February 12): 387-408.

12. Abo, K. A., A. A. Fred-Jaiyesimi, and A. E. A. Jaiyesimi. (2008). "Ethnobotanical studies of medicinal plants used in the management of diabetes mellitus in South Western Nigeria." **Journal of Ethnopharmacology** 115, 1 (January 4): 67-71.
13. Ong, H. C., and J. Norzalina. (1999). "Malay herbal medicine in Gemencheh, Negri Sembilan, Malaysia." **Fitoterapia** 70, 1 (February 1): 10-14.
14. Longuefosse, Jean-Louis., and Emmanuel Nossin. (1996). "Medical ethnobotany survey in Martinique." **Journal of Ethnopharmacology** 53, 3 (September 1): 117-142.
15. Roosita, Katrin. et al. (2008). "Medicinal plants used by the villagers of a Sundanese community in West Java, Indonesia." **Journal of Ethnopharmacology** 115, 1 (January 4): 72-81.
16. World Health Organization. (1998). **Medicinal plants in the south pacific**. Manila: WHO Regional Office for the Western Pacific.
17. Komlaga, Gustav. et al. (2015). "Medicinal plants and finished marketed herbal products used in the treatment of malaria in the Ashanti region, Ghana." **Journal of Ethnopharmacology** 172, 22 (August): 333-346.
18. คณะกรรมการคุ้มครองและส่งเสริมภูมิปัญญาการแพทย์แผนไทย. (2552). ตำราอ้างอิงยาสมุนไพร เล่ม ๑ เฉลิมพระเกียรติพระบาทสมเด็จพระเจ้าอยู่หัว เนื่องในมหามงคลสมัยที่ทรงครองสิริราชสมบัติครบ ๖๐ ปี. กรุงเทพมหานคร: บริษัทอมรินทร์พริ้นติ้งแอนด์พับลิชชิ่ง จำกัด (มหาชน).
19. Oratai Neamsuvan. et al. (2015). "A survey of herbal formulas for skin diseases from Thailand's three southern border provinces." **Journal of Herbal Medicine** 5, 4 (December 1): 190-198.
20. Suleiman, Mohamed Hammad Adam. (2015). "An ethnobotanical survey of medicinal plants used by communities of Northern Kordofan region, Sudan." **Journal of Ethnopharmacology** 176, 24 (December 24): 232-242.
21. Pesewu, George A., Ronald R. Cutler, and David P. Humber. (2008). "Antibacterial activity of plants used in traditional medicines of Ghana with particular reference to MRSA." **Journal of Ethnopharmacology** 116, 1 (February 28): 102-111.
22. Trinop Promgool, Orasa Pancharoen, and Suwanna Deachathail. (2014). "Antibacterial and antioxidative compounds from *Cassia alata* Linn." **Songklanakarin Journal of Science and Technology** 36, 4: 459-463.

23. Doughari, J.H., and B Okafor. (2007). "Antimicrobial Activity of *Senna alata* Linn." **East and Central African Journal of Pharmaceutical Sciences** 10, 1: 17-21.
24. Khan, M. R., M. Kihara, and A. D. Omoloso. (2001). "Antimicrobial activity of *Cassia alata*." **Fitoterapia** 72, 5 (June 1): 561-564.
25. Abubacker, Maghdu Nainamohamed. , Renuka Ramanathan, and Thiruppathi Senthil Kumar. (2008). "In vitro antifungal activity of *Cassia alata* Linn. flower extract." **Natural Product Radiance** 7, 1: 6-9.
26. Sule, W.F. et al. (2010). "In vitro antifungal activity of *Senna alata* Linn. crude leaf extract." **Research Journal of Biological Sciences** 5, 3: 275-284.
27. Villasenor, I. M. et al. (2002). "Bioactivity studies on *Cassia alata* Linn. leaf extracts." **Phytotherapy Research** 16 supplement 1 (March): S93-96.
28. Ibrahim, Darah., and Halim Osman. (1995). "Antimicrobial activity of *Cassia alata* from Malaysia." **Journal of Ethnopharmacology** 45, 3 (March 1): 151-156.
29. Damodaran, S., and S. Venkataraman. (1994). "A study on the therapeutic efficacy of *Cassia alata* Linn. leaf extract against Pityriasis versicolor." **Journal of Ethnopharmacology** 42, 1 (March 1): 19-23.
30. Singh, Baljinder. et al. (2012). "The hydroalcoholic extract of *Cassia alata* (Linn.) leaves and its major compound rhein exhibits antiallergic activity via mast cell stabilization and lipoxygenase inhibition." **Journal of Ethnopharmacology** 141, 1 (May 7): 469-473.
31. Jarinyaporn Naowaboot, and Supaporn Wannasiri. (2016). "Anti-lipogenic effect of *Senna alata* leaf extract in high-fat diet-induced obese mice." **Asian Pacific Journal of Tropical Biomedicine** 6, 3 (March 1): 232-238.
32. Varghese, George Kadakasseril., Lekshmi Vijaya Bose, and Solomon Habtemariam. (2013). "Antidiabetic components of *Cassia alata* leaves: Identification through  $\alpha$ -glucosidase inhibition studies." **Pharmaceutical Biology** 51, 3 (March 1): 345-349.
33. Jofilena, Joy G., Consolacion Ragasa, and John A. Rideout. (2000). "An antimicrobial and antimutagenic anthraquinone from *Cassia alata*." **ACGC Chemical Research Communications** 10: 15-20.
34. Moriyama, Hiroyoshi. et al. (2003). "Antiinflammatory activity of heat-treated *Cassia alata* leaf extract and its flavonoid glycoside." **YAKUGAKU ZASSHI** 123, 7: 607-611.



35. Meenupriya, J., Sahaya A. Vinisha, and P. Priya. (2014). "*Cassia alata* and *Cassia auriculata* – Review of their bioactive potential." **World Journal of Pharmaceutical Sciences** 2, 12: 1760-1769.
36. Chatterjee, Saheli. et al. (2013). "Study of antioxidant activity and immune stimulating potency of the ethnomedicinal plant, *Cassia alata* (L.) Roxb." **Medicinal & Aromatic Plants** 2, 4: 1-6.
37. Lagarto, Parra A. et al. (2001). "Comparative study of the assay of *Artemia salina* L. and the estimate of the medium lethal dose (LD50 value) in mice, to determine oral acute toxicity of plant extracts." **Phytomedicine** 8, 5 (September): 395-400.
38. Pieme, Anatole Constant. et al. (2006). "Evaluation of acute and subacute toxicities of aqueous ethanolic extract of leaves of *Senna alata* (L.) Roxb (Ceasalpiniaceae)." **African Journal of Biotechnology** 5, 3: 283-289.
39. Sodipo, O. A., K. D. Effraim, and E. Emmagun. (1998). "Effect of aqueous leaf extract of *Cassia alata* (Linn.) on some haematological indices in albino rats." **Phytotherapy Research** 12, 6: 431-433.
40. Appiah-Opong, Regina. et al. (2008). "Interactions between cytochromes P450, glutathione S-transferases and Ghanaian medicinal plants." **Food and Chemical Toxicology** 46, 12 (December 1): 3598-3603.
41. Ogunwande, I. A. et al. (2010). "Aromatic plants growing in Nigeria: essential oil constituents of *Cassia alata* (Linn.) Roxb. and *Helianthus annuus* L." **Records of Natural Products** 4, 4: 211-217.
42. Liu, An. et al. (2009). "Studies on chemical constituents from leaves of *Cassia alata*." **Zhongguo Zhong Yao Za Zhi** 34, 7: 861-863.
43. Gupta, Dipti., and J. Singh. (1991). "Flavonoid glycosides from *Cassia alata*." **Phytochemistry** 30, 8: 2761-2763.
44. Hazni, Hazrina. et al. (2008). "Phytochemical Constituents from *Cassia alata* with Inhibition against Methicillin-Resistant *Staphylococcus aureus* (MRSA)." **Planta Medica** 74, 15 (December): 1802-1805.
45. Ramsay, Aina., and Irene Mueller-Harvey. (2016). "*Senna alata* leaves are a good source of propelargonidins." **Natural Product Research** 30, 13: 1548-1551.

46. Fernand, Vivian E. et al. (2008). "Determination of pharmacologically active compounds in root extracts of *Cassia alata* L. by use of high performance liquid chromatography." **Talanta** 74, 4 (January 15): 896-902.
47. Yang, You. et al. (2017). "Diosmetin exerts anti-oxidative, anti-inflammatory and anti-apoptotic effects to protect against endotoxin-induced acute hepatic failure in mice." **Oncotarget** 8, 19 (May): 30723-30733.
48. Pharkphoom Panichayupakaranant, Apirak Sakunpak, and Athip Sakunphueak. (2009). "Quantitative HPLC determination and extraction of anthraquinones in *Senna alata* leaves." **Journal of Chromatographic Science** 47, 3: 197-200.
49. Yadav, Satyender K., and Suraj B. Kalidhar. (1994). "Alquinone: An Anthraquinone from *Cassia alata*." **Planta Medica** 60, 06 (December): 601.
50. Hemlata, and Suraj B. Kalidhar. (1993). "Alatinone, an anthraquinone from *Cassia alata*." **Phytochemistry** 32, 6: 1616-1617.
51. Pharkphoom Panichayupakaranant, and Niwan Intaraksa. (2003). "Distribution of hydroxyanthracene derivatives in *Cassia alata* and the factors affecting the quality of the raw material." **Songklanakarinn Journal of Science and Technology** 25, 4: 497-502.
52. Moriyama, Hiroyoshi. et al. (2003). "Adenine, an inhibitor of platelet aggregation, from the leaves of *Cassia alata*." **Biological and Pharmaceutical Bulletin** 26, 9: 1361-1364.
53. Zhou, Yan-Xi. et al. (2015). "Rhein: A review of pharmacological activities." **Evidence-based Complementary and Alternative Medicine : eCAM** (June): 1-10.
54. Dave, Hemen., and Lalita. Ledwani. (2012). "A review on anthraquinones isolated from *Cassia* species and their applications." **Indian Journal of Natural Products and Resources** 3, 3: 291-319.
55. Guo, Mei-Zi. et al. (2003). "Effect of rhein on the development of hepatic fibrosis in rats." **Zhonghua ganzangbing zazhi** 11, 1: 26-29.
56. Sheng, Xiaoyan. et al. (2011). "Rhein ameliorates fatty liver disease through negative energy balance, hepatic lipogenic regulation, and immunomodulation in diet-induced obese mice." **American Journal of Physiology - Endocrinology And Metabolism** 300, 5 (May): E886-893.

57. He, Dongyuan. et al. (2011). "Preventive effects and mechanisms of rhein on renal interstitial fibrosis in obstructive nephropathy." **Biological and Pharmaceutical Bulletin** 34, 8: 1219-1226.
58. Su, J. et al. (2013). "Chronic allograft nephropathy in rats is improved by the intervention of rhein." **Transplantation Proceedings** 45, 6 (July 1): 2546-2552.
59. Sheng-Nan, Peng. et al. (2013). "Protection of rhein on IgA nephropathy mediated by inhibition of fibronectin expression in rats." **Indian Journal of Pharmacology** 45, 2: 174-179.
60. Ji, Ze-quan. et al. (2005). "Effects of rhein on activity of caspase-3 in kidney and cell apoptosis on the progression of renal injury in glomerulosclerosis." **Zhonghua Yi Xue Za Zhi** 85, 26: 1836-1841.
61. Yu, De-Qian. , Yuan Gao, and Xiao-Hong Liu. (2010). "Effects of rhein on the hypertrophy of renal proximal tubular epithelial cells induced by high glucose and angiotensin II in rats." **Zhong Yao Cai** 33, 4: 570-574.
62. Sanchez, Christelle. et al. (2003). "Effects of rhein on human articular chondrocytes in alginate beads." **Biochemical Pharmacology** 65, 3 (February): 377-388.
63. Borderie, D. et al. (2001). "Inhibition of the nitrosothiol production of cultured osteoarthritic chondrocytes by rhein, cortisol and diclofenac." **Osteoarthritis and Cartilage** 9, 1: 1-6.
64. Yaron, Michael., Idit Shirazi, and Ilana Yaron. (1999). "Anti-interleukin-1 effects of diacerein and rhein in human osteoarthritic synovial tissue and cartilage cultures." **Osteoarthritis Cartilage** 7, 3: 272-280.
65. Legendre, F. et al. (2009). "Rhein, the metabolite of diacerhein, reduces the proliferation of osteoarthritic chondrocytes and synoviocytes without inducing apoptosis." **Scandinavian Journal of Rheumatology** 38, 2: 104-111.
66. Martin, Grégoire. et al. (2003). "Rhein inhibits interleukin-1 $\beta$ -induced activation of MEK/ERK pathway and DNA binding of NF- $\kappa$ B and AP-1 in chondrocytes cultured in hypoxia: A potential mechanism for its disease-modifying effect in osteoarthritis." **Inflammation** 27, 4 (August): 233-246.

67. Mendes, Alexandrina Ferreira. et al. (2002). "Diacerhein and rhein prevent interleukin-1beta-induced nuclear factor-kappaB activation by inhibiting the degradation of inhibitor kappaB-alpha." **Pharmacology and Toxicology** 91, 1: 22-28.
68. Tamura, Tadafumi., and Kenji Ohmori. (2001). "Rhein, an active metabolite of diacerein, suppresses the interleukin-1&alpha-induced proteoglycan degradation in cultured rabbit articular chondrocytes." **The Japanese Journal of Pharmacology** 85, 1: 101-104.
69. Hu, Gang. et al. (2013). "Rhein inhibits the expression of vascular cell adhesion molecule 1 in human umbilical vein endothelial cells with or without lipopolysaccharide stimulation." **American Journal of Chinese Medicine** 41, 3: 473-485.
70. Cong, Xiao-Dong. et al. (2012). "ER Stress, P66shc, and P-Akt/Akt mediate adjuvant-induced inflammation, which is blunted by argirein, a supermolecule and rhein in rats." **Inflammation** 35, 3 (June): 1031-1040.
71. Heo, Sook-Kyoung. et al. (2010). "Emodin and rhein inhibit LIGHT-induced monocytes migration by blocking of ROS production." **Vascular Pharmacology** 53, 1 (July): 28-37.
72. Zhong, Xian-Feng. et al. (2012). "Protective effect of rhein against oxidative stress-related endothelial cell injury." **Molecular Medicine Reports** 5, 5: 1261-1266.
73. Zhao, Yan-Ling. et al. (2011). "Rhein protects against acetaminophen-induced hepatic and renal toxicity." **Food and Chemical Toxicology** 49, 8 (August 1): 1705-1710.
74. Lin, Meng-Liang. et al. (2009). "Rhein inhibits invasion and migration of human nasopharyngeal carcinoma cells in vitro by down-regulation of matrix metalloproteinases-9 and vascular endothelial growth factor." **Oral Oncology** 45, 6 (June): 531-537.
75. Shi, Ping., Zhiwei Huang, and Guichen Chen. (2008). "Rhein induces apoptosis and cell cycle arrest in human hepatocellular carcinoma BEL-7402 cells." **The American Journal of Chinese Medicine** 36, 04: 805-813.
76. Fernand, Vivian E. et al. (2011). "Rhein inhibits angiogenesis and the viability of hormone-dependent and -independent cancer cells under normoxic or hypoxic conditions in vitro." **Chemico-Biological Interactions** 192, 3 (July 15): 220-232.
77. Chen, Ya-Yin. et al. (2010). "Emodin, aloe-emodin and rhein inhibit migration and invasion in human tongue cancer SCC-4 cells through the inhibition of gene expression of matrix metalloproteinase-9." **International Journal of Oncology** 36, 5: 1113-1120.

78. Du, Hong. et al. (2010). "Effect of rhein treatment on first-phase insulin secretory function in db/db mice." **Zhongguo Zhong Yao Za Zhi** 35, 20: 2764-2767.
79. Liu, Jing. et al. (2013). "Rhein protects pancreatic  $\beta$ -cells from dynamin-related protein-1-mediated mitochondrial fission and cell apoptosis under hyperglycemia." **Diabetes** 62, 11: 3927-3935.
80. Du, H. et al. (2012). "Improvement of glucose tolerance by rhein with restored early-phase insulin secretion in db/db mice." **Journal of Endocrinological Investigation** 35, 6 (June 1): 607-612.
81. Du, H. et al. (2011). "Effect of early intervention with rhein on islet function in db/db mice." **Nan Fang Yi Ke Da Xue Xue Bao** 31, 9: 1526-1529.
82. Zhu, J., Z. Liu, and Y. Li. (2001). "Inhibition of glucose transporter 1 overexpression in mesangial cells by rhein." **Zhonghua Nei Ke Za Zhi** 40, 8: 537-542.
83. Bian, D. X. et al. (2013). "Protective effects of rhein on hepatic progression in HBV-transgenic mice with nonalcoholic steatohepatitis induced by a high-fat diet." **Zhonghua Shi Yan He Lin Chuang Bing Du Xue Za Zhi** 27, 5: 328-331.
84. Tang, Jing-cheng. et al. (2009). "Inhibition of cytochrome P450 enzymes by rhein in rat liver microsomes." **Phytotherapy Research** 23, 2: 159-164.
85. Wagener, Frank A. D. T. G., Carine E. Carels, and Ditte M. S. Lundvig. (2013). "Targeting the Redox Balance in Inflammatory Skin Conditions." **International Journal of Molecular Sciences** 14, 5 (May): 9126-9167.
86. Nathan, Carl., and Amy Cunningham-Bussel. (2013). "Beyond oxidative stress: an immunologist's guide to reactive oxygen species." **Nature reviews. Immunology** 13, 5: 349-361.
87. Bedard, Karen., and Karl-Heinz Krause. (2007). "The NOX family of ROS-generating NADPH oxidases: physiology and pathophysiology." **Physiological Reviews** 87, 1: 245-313.
88. Bhattacharyya, Asima. et al. (2014). "Oxidative stress: An essential factor in the pathogenesis of gastrointestinal mucosal diseases." **Physiological Reviews** 94, 2: 329-354.
89. Valko, Marian. et al. (2007). "Free radicals and antioxidants in normal physiological functions and human disease." **The International Journal of Biochemistry & Cell Biology** 39, 1: 44-84.

90. West, A. Phillip., Gerald S. Shadel, and Sankar Ghosh. (2011). "Mitochondria in innate immune responses." **Nature reviews. Immunology** 11, 6 (June): 389-402.
91. Bouayed, Jaouad., and Torsten Bohn. (2010). "Exogenous antioxidants—Double-edged swords in cellular redox state: Health beneficial effects at physiologic doses versus deleterious effects at high doses." **Oxidative Medicine and Cellular Longevity** 3, 4: 228-237.
92. Karlenius, Therese Christina., and Kathryn Fay Tonissen. (2010). "Thioredoxin and cancer: A role for thioredoxin in all states of tumor oxygenation." **Cancers** 2, 2 (June): 209-232.
93. Averhoff, Petra. (2006). "**Characterization of the specificity of human neutrophil elastase for *Shigella flexneri* virulence factors.**" Master degree Humboldt-Universität zu Berlin.
94. Dröge, Wulf. (2002). "Free radicals in the physiological control of cell function." **Physiological Reviews** 82, 1: 47-95.
95. Palm, Fredrik. et al. (2007). "Dimethylarginine dimethylaminohydrolase (DDAH): expression, regulation, and function in the cardiovascular and renal systems." **American Journal of Physiology - Heart and Circulatory Physiology** 293, 6: H3227-3245.
96. Vitale, Giovanni., Stefano Salvioli, and Claudio Franceschi. (2013). "Oxidative stress and the ageing endocrine system." **Nature Reviews Endocrinology** 9, 4 (February): 228-240.
97. Mittal, Manish. et al. (2014). "Reactive oxygen species in inflammation and tissue injury." **Antioxidants & Redox Signaling** 20, 7 (March): 1126-1167.
98. Evgenov, Oleg V. et al. (2006). "NO-independent stimulators and activators of soluble guanylate cyclase: discovery and therapeutic potential." **Nature reviews. Drug discovery** 5, 9: 755-768.
99. Suvara Kimnate Wattanapitayakul, and John Anthony Bauer. (2001). "Oxidative pathways in cardiovascular disease: roles, mechanisms, and therapeutic implications." **Pharmacology & Therapeutics** 89, 2 (February 1): 187-206.
100. Kaneto, Hideaki. et al. (2010). "Role of reactive oxygen species in the progression of type 2 diabetes and atherosclerosis." **Mediators of Inflammation** 2010, (February): 1-11.

101. Mirshafiey, Abbas., and Monireh Mohsenzadegan. (2008). "The role of reactive oxygen species in immunopathogenesis of rheumatoid arthritis." **Iranian Journal of Allergy, Asthma and Immunology** 7, 4: 195-202.
102. Portugal, Meital. et al. (2007). "Interplay among oxidants, antioxidants, and cytokines in skin disorders: Present status and future considerations." **Biomedicine & Pharmacotherapy** 61, 7 (August): 412-422.
103. Gomes, Ana., Eduarda Fernandes, and José L. F. C. Lima. (2005). "Fluorescence probes used for detection of reactive oxygen species." **Journal of Biochemical and Biophysical Methods** 65, 2 (December 31): 45-80.
104. Kalyanaraman, Balaraman. et al. (2012). "Measuring reactive oxygen and nitrogen species with fluorescent probes: challenges and limitations." **Free Radical Biology and Medicine** 52, 1 (January): 1-6.
105. Maghzal, Ghassan J. et al. (2012). "Detection of reactive oxygen species derived from the family of NOX NADPH oxidases." **Free Radical Biology and Medicine** 53, 10 (November): 1903-1918.
106. Bensouilah, Janetta., and Philippa Buck. (2006). **Aromadermatology: Aromatherapy in the treatment and care of common skin conditions**. Oxford: Radcliffe Publishing.
107. McLafferty, Ella., Charles Hendry, and Alistair Farley. (2012). "The integumentary system: anatomy, physiology and function of skin." **Nursing Standard** 27, 3: 35-42.
108. Benson, Heather A.E., and Adam C. Watkinson. (2012). **Transdermal and topical drug delivery**. Singapore: A John Wiley & Sons.
109. James, William D., Timothy Berger, and Dirk. Elston. (2006). **Andrews' Diseases of the Skin**. 10th ed. USA: Elsevier Health Sciences.
110. Bickers, David R., and Mohammad Athar. (2006). "Oxidative stress in the pathogenesis of Skin Disease." **Journal of Investigative Dermatology** 126, 12 (December): 2565-2575.
111. Turner, Mark D. et al. (2014). "Cytokines and chemokines: At the crossroads of cell signalling and inflammatory disease." **Biochimica et Biophysica Acta (BBA) - Molecular Cell Research** 1843, 11 (November 1): 2563-2582.
112. Müller, Kerstin., and Viktor Meineke. (2007). "Radiation-induced alterations in cytokine production by skin cells." **Experimental Hematology** 35, 4 supplement 1 (April): 96-104.

113. Ravi, Rethika., and Terrence J. Piva. (2013). **Highlights in Skin Cancer**. Croatia: InTech.
114. Barker, J. N. W. N. et al. (1991). "Keratinocytes as initiators of inflammation." **The Lancet** 337, 8735 (January 26): 211-214.
115. Twentyman, P. R., and M. Luscombe. (1987). "A study of some variables in a tetrazolium dye (MTT) based assay for cell growth and chemosensitivity." **British Journal of Cancer** 56, 3: 279-285.
116. Riss, T.L. et al. (2016). "Cell Viability Assays." In **Assay Guidance Manual**, 262-291. Edited by G.S. Sittampalam et al. Eli Lilly & Company and the National Center
117. Cox, K.L. et al. (2014). "Immunoassay Methods." In **Assay Guidance Manual**, 185-226. Edited by G.S. Sittampalam et al. Eli Lilly & Company and the National Center.
118. Sohn, Jong Hee. et al. (2005). "Protective effects of panduratin A against oxidative damage of *tert*-Butylhydroperoxide in human HepG2 cells." **Biological and Pharmaceutical Bulletin** 28, 6: 1083-1086.
119. Bito, Toshinori., and Chikako Nishigori. (2012). "Impact of reactive oxygen species on keratinocyte signaling pathways." **Journal of Dermatological Science** 68, 1 (October): 3-8.
120. Lans, Cheryl. (2007). "Comparison of plants used for skin and stomach problems in Trinidad and Tobago with Asian ethnomedicine." **Journal of Ethnobiology and Ethnomedicine** 3, 3: 1-12.
121. Sun, Hao. et al. (2016). "A comprehensive and system review for the pharmacological mechanism of action of rhein, an active anthraquinone ingredient." **Frontiers in Pharmacology** 7, 247: 1-16.



## APPENDIX

### Appendix A

#### Cell preparation

The HaCaT cells (the human keratinocyte cell line) was maintained in DMEM with 10% Fetal Bovine Serum (FBS), 10% Penicillin-Streptomycin, and 0.02% Amphotericin B. Passage number of cell was used in the experiments was less than 30, due to phenotypic changes concerning. Culture medium was removed from HaCaT cell 75 cm<sup>2</sup> culture flask and washed twice with PBS, then trypsinized with 1 mL of 0.05% trypsin-EDTA. After incubated at 37°C in 5% CO<sub>2</sub> incubator for 10 minutes, the reaction was stopped by adding culture medium. Cells were incubated at 37°C in 5% CO<sub>2</sub> incubator. The medium was replaced every 48 hours. Typically, cell were sub-cultured when it reached to subconfluence of plate surface.

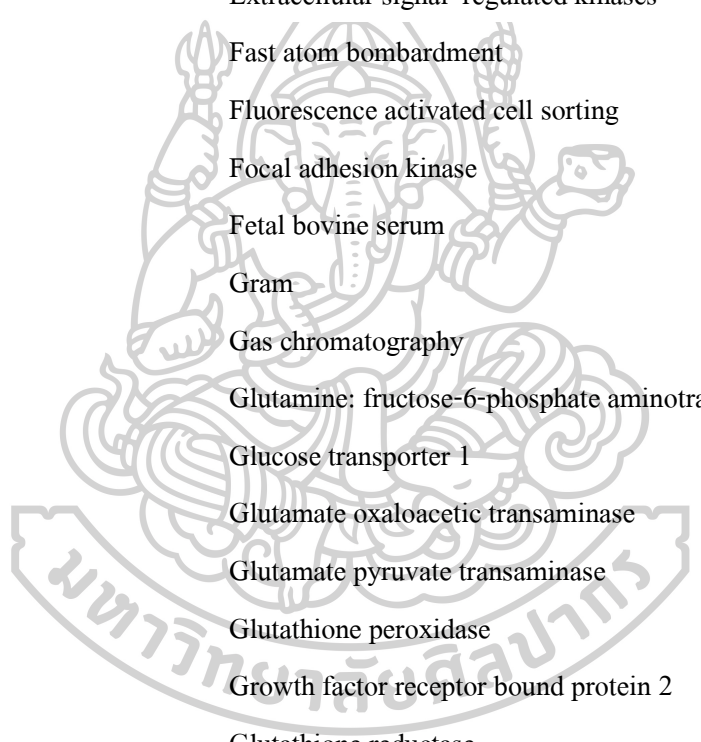
#### Reagent in ELISA test

1. Reagent diluent preparation  
4% Bovine serum albumin (BSA) in D-PBS
2. Blocking buffer preparation  
4% BSA, and 5% Sucrose in D-PBS
3. Washing buffer preparation  
0.05% tween 20 in D-PBS

## Appendix B

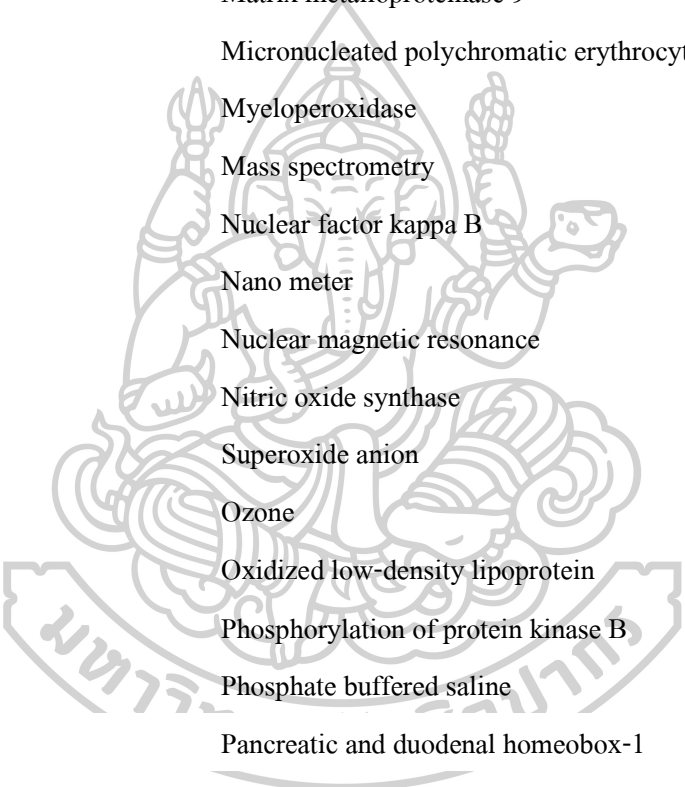
### List of abbreviations

<	Less than
>	More than
µg	Micro gram
µl	Micro liter
µm	Micro meter
µM	Micro molarity
<sup>1</sup> O <sub>2</sub>	Singlet oxygen
ADMA	Asymmetric dimethylarginine
ALA	Alpha lipoic acid
ALP	Alkaline phosphatase
ALT	Alanine aminotransferase
AngII	<i>Angiotensin II</i>
AP-1	Activator protein 1
Apaf-1	Apoptotic protease activating factor 1
Asc <sup>•-</sup>	Ascorbyl radical
AST	Aspartate aminotransferase
ATF6	Activating transcript factor 6
Bcl 2	B-cell lymphoma 2
BSA	Bovine serum albumin
Conc	Concentration
CoQ	Coenzyme Q
COX	Cyclooxygenase
CYP	Cytochromes P450
Cyt <i>c</i>	Cytochrome <i>c</i>
DDAH	Dimethylarginine dimethylaminohydrolase
DHLA	Dihydrolipoic acid
DIT	Diiodotyrosine
DMEM	Dulbecco's modified eagle medium

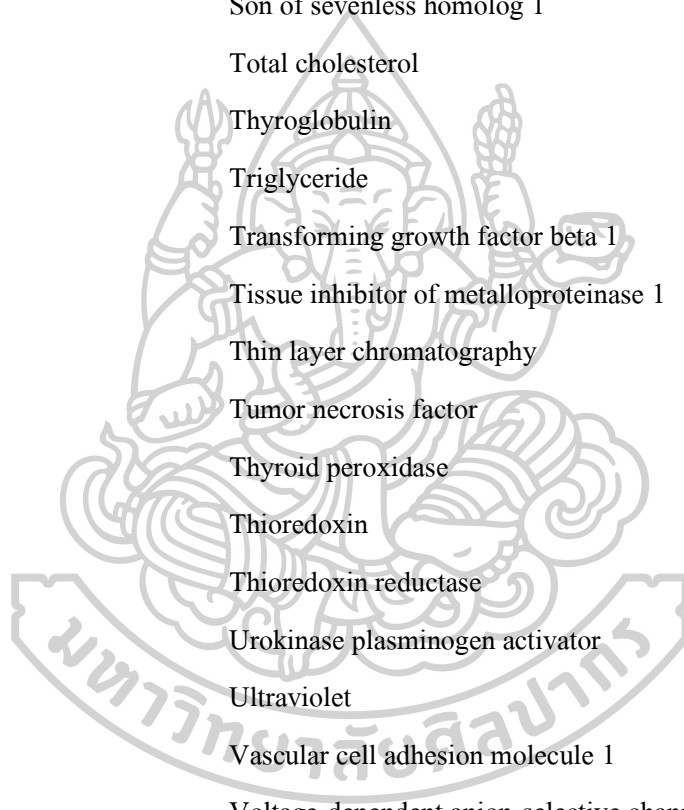


DMSO	Dimethyl sulfoxide
DNA	Deoxyribonucleic acid
DPPH	2,2-diphenyl-1-picrylhydrazyl
Drp1	Dynamin related protein 1
DUOX	NADPH dependent oxidase/oxidase
EGF	Endothelial growth factor
EI	Electron ionization
ELISA	Enzyme linked immunosorbent assay
ERK	Extracellular signal-regulated kinases
FAB	Fast atom bombardment
FACS	Fluorescence activated cell sorting
FAK	Focal adhesion kinase
FBS	Fetal bovine serum
g	Gram
GC	Gas chromatography
GFAT	Glutamine: fructose-6-phosphate aminotransferase
GLUT1	Glucose transporter 1
GOT	Glutamate oxaloacetic transaminase
GPT	Glutamate pyruvate transaminase
GPx	Glutathione peroxidase
GRB2	Growth factor receptor bound protein 2
Gred	Glutathione reductase
GSH	Glutathione
GSSG	Oxidised glutathione
GSTs	Glutathione S transferases
H <sub>2</sub> O <sub>2</sub>	Hydrogen peroxide
HBSS	Hank's balanced salt solution
HCL	Hydrochloric acid
HDL	High density cholesterol
HIF PH2	Hypoxia inducible factor prolyl hydroxylase 2

HIF1 $\alpha$	Hypoxia-inducible factor 1 alpha
HO•	Hydroxyl radical
HOCl	Hypochlorous
HPLC	High performance liquid chromatography
HRFAB	High resolution fast atom bombardment
I <sup>-</sup>	Iodine
IC50	Half maximal inhibitory concentration
ICAM-1	Intercellular adhesion molecule 1
I $\kappa$ B- $\alpha$	Inhibitor kappa B alpha protein
IL	Interleukin
iNOS	Inducible nitric oxide synthase
IR	Infrared
JNK	c-Jun N-terminal kinases
K <sub>i</sub>	Inhibition constant
KOH	Potassium hydroxide
L	Liter
L•	Lipid radical
LAT	Linker for T-cell activation
LD50	Lethal dose
LDH	Lactate dehydrogenase
LDL	Low density cholesterol
LO•	Lipid alkoxyl radicals
LOO•	Lipid peroxy radical
LPS	Lipopolysaccharide
m	Meter
MAPK	Mitogen activated protein kinases
MCP-1	Monocyte chemoattractant protein 1
mg	Milli gram
MICs	Minimum inhibitory concentrations
min	Minute



MIT	Monoiodotyrosine
ml	Milli liter
mm	Milli meter
mM	Milli molarity
MMP-1	Matrix metalloproteinase 1
MMP-2	Matrix metalloproteinase 2
MMP-3	Matrix metalloproteinase 3
MMP-9	Matrix metalloproteinase 9
MPE	Micronucleated polychromatic erythrocytes
MPO	Myeloperoxidase
MS	Mass spectrometry
NF-kB	Nuclear factor kappa B
nm	Nano meter
NMR	Nuclear magnetic resonance
NOS	Nitric oxide synthase
O <sub>2</sub> <sup>•-</sup>	Superoxide anion
O <sub>3</sub>	Ozone
oxLDL	Oxidized low-density lipoprotein
p-Akt	Phosphorylation of protein kinase B
PBS	Phosphate buffered saline
PDX-1	Pancreatic and duodenal homeobox-1
p-ERK	Phosphorylated extracellular signal regulated kinase
pg	Pico gram
PGE2	Prostaglandin E2
PI3K	Phosphatidylinositol 3 kinase
p-JNK	Phosphorylated c-Jun N terminal kinases
PKC	Protein kinase C
PPAR	Peroxisome proliferator activated receptor
ppm	Parts per million
Prx	Peroxiredoxin



PTP	Protein tyrosine phosphatase
ROS	Reactive oxygen species
RSD	Relative standard deviation
SAPK	Stress-activated protein kinases
SD	Standard deviation
sGC	Soluble guanylate cyclase
SOD	Superoxide dismutase
SOS-1	Son of sevenless homolog 1
TC	Total cholesterol
Tg	Thyroglobulin
TG	Triglyceride
TGF- $\beta$ 1	Transforming growth factor beta 1
TIMP-1	Tissue inhibitor of metalloproteinase 1
TLC	Thin layer chromatography
TNF	Tumor necrosis factor
TPO	Thyroid peroxidase
Trx	Thioredoxin
TrxR	Thioredoxin reductase
u-PA	Urokinase plasminogen activator
UV	Ultraviolet
VCAM-1	Vascular cell adhesion molecule 1
VDAC	Voltage-dependent anion-selective channel
VEGF	Vascular endothelial growth factor
VHL	Von Hippel–Lindau tumour-suppressor protein
VS	Versus
XO	Xanthine oxidase
$\alpha$ KG	Alpha ketoglutarate
$\alpha$ -SMA	Alpha smooth muscle actin

## VITA

**NAME** Kwanchanok Wadkhien

**DATE OF BIRTH** 13 January 1988

**PLACE OF BIRTH** Chiang Mai, Thailand

**INSTITUTIONS ATTENDED** 2006-2010 Silpakorn university: Bachelor of Pharmacy  
2013-2017 Silpakorn university: Master of Pharmacy (Pharmaceutical Science)

**PUBLICATION** Poster presentation: 2017, The 2 nd International Conference and Pre-symposium on Herbal and Traditional Medicine, Bangkok Thailand

